Electrical Impedance Spectroscopy Applied in Plant Physiology Studies

Xing Liu

Master of Engineering

2006

RMIT

Electrical Impedance Spectroscopy Applied in Plant Physiology Studies

A thesis submitted in fulfilment of the requirements
for the degrees of Master of Engineering

Xing Liu

B.Eng

School of Electrical and Computer Engineering
Science, Engineering and Technology Portfolio
RMIT University
August 2006

Electrical Impedance Spectroscopy Applied in Plant Physiology Studies

Xing Liu

Supervised by

Dr. John Q Fang

Prof. Irena Cosic

to my parents

Declaration

I certify that except where due acknowledgement has been made, the work is that of the author alone; the work has not been submitted previously, in whole or in part, to qualify for any other academic award; the content of the thesis is the result of work which has been carried out since the official commencement date of the approved research program; and, any editorial work, paid or unpaid, carried out by a third party is acknowledged.

Xing Liu

31st August, 2006

Acknowledgement

I would like to express the special thanks to my supervisors, Dr. John Q Fang and Prof. Irena Cosic for having provided me the opportunity as a member of the biomedical research group in RMIT University and their encouragements and suggestions for this research and the preparation of thesis.

I would like to take this opportunity to thank all the staff in the food science lab and the applied chemical lab for their kindly help.

I also would like to thank Prof. Ian Bates for arranging me a place in the AECM research centre. I wish to thank Lynda Gilbert for her assistance over the last two years. I can not thank my friends enough for their supporting during my time in Australia, they are Lu Miao, Li Zhong, Smitha Shankar, Vuk Vojisavljevic, Dedi Berlian, Manting Huang, Wei Fu. I will always cherish the friendships that have been formed and the time spent at RMIT.

I wish to address my appreciation to my family for their support and love.

Thank you all.

Table of Content

Declaration ..... **i**
Acknowledgement ..... **ii**
Table of Content ..... **iii**
List of Figures ..... **vi**
List of Tables ..... **viii**
List of Abbreviations ..... **ix**
Abstract **1**
Chapter 1 Introduction **4**
1.1 Overview 4
1.2 Motivation 5
1.3 Background of Quality Assessment Techniques 6
1.3.1 Quality Definition 6
1.3.2 Quality Evaluation Techniques 7
1.4 Objectives of Research 9
1.5 Contributions 10
1.6 Thesis Organisation 12
Chapter 2 Literature Review **13**
2.1 Overview 13
2.2 Impedance - Definition 14
2.3 Methods of Electrical Impedance Measurement 16
2.3.1 Single Frequency Impedance Measurement 16
2.3.2 Multiple Frequency Impedance Measurement 17
2.3.3 Electrical Impedance Spectroscopy 17
2.4 Electrodes Configurations 19
2.4.1 Two-terminal Measurement 19
2.4.2 Four-terminal Measurement 20
2.5 Data Representation 21

2.5.1 Nyquist Plot 21
2.5.2 Bode Plot 22
2.6 Electrical Modelling 23
2.6.1 Plant Cell Anatomy 23
2.6.2 Electrical Modelling Components 25
2.6.2.1 Cole Model 25
2.6.2.2 Hayden Model 26
2.6.2.3 Double-shell Model 27
2.7 Application of Impedance Measurement 28
2.7.1 Impedance Analysis on Human Body Composition 28
2.7.2 Impedance Analysis on Plants 30
2.7.3 Impedance Measurements on Food Quality Assessment 32
Chapter 3 Application of EIS for Evaluation of Apple Quality 35
3.1 Introduction 35
3.2 Methodology 36
3.2.1 Material 36
3.2.2 Experimental Setup 36
3.2.2.1 Electrical Impedance Measurement for Apples 37
3.2.2.2 Soluble Solid Measurement 38
3.2.2.3 Titratable Acidity Measurement 39
3.3 Results 40
3.3.1 Results from Instrumental and Chemical Measurements 40
3.3.2 Results from Electrical Impedance Measurement 42
3.3.3 Comparison of Impedance Measurement and Laboratory Measurement 45
3.4 Discussion & Conclusion 48
Chapter 4 Application of EIS for Evaluation of Banana Ripening 51
4.1 Introduction 51
4.2 Methodology 52
4.2.1 Material 52
4.2.2 Electrical Impedance Measurement for Bananas 52
4.3 Results and Discussion 53
4.3.1 Analysis of Impedance Parameters 53
4.3.2 Equivalent Electrical Model 58
4.4 Conclusion 66
Chapter 5 Application of EIS for Vegetable Dehydration 68

5.1 Introduction 68
5.2 Methodology 69
5.2.1 Materials 69
5.2.2 Drying Procedures 69
5.2.3 Electrical Impedance Measurement for Cucumbers 70
5.3 Results & Discussion 71
5.3.1 Moisture Content 71
5.3.2 Impedance Variations 73
5.3.2.1 Magnitude of Impedance 73
5.3.2.2 Diameter of Impedance Arc 76
5.3.3 Relationship between the Impedance Property and Moisture Content 78
5.3.4 Equivalent Electrical Modelling 79
5.4 Conclusion 81
Chapter 6 Conclusions and Future Research 83
6.1 Conclusions 83
6.2 Future Research 85
Reference 87
Appendix Raw Data and MATLAB Scripts 101

List of Figures

Figure 2-1 Impedance complex plane 15
Figure 2-2 Cylinder model for the relationship between impedance and human body geometry. A is the cross-sectional area; L is the height of human body. 16
Figure 2-3 Flow chart for the principle of EIS (Macdonald, 1987) 18
Figure 2-4 Two-terminal connection method 19
Figure 2-5 Four-terminal connection method 21
Figure 2-6 Nyquist Plot with impedance vector 22
Figure 2-7 Bode Plot of one experiment from bananas investigation 22
Figure 2-8 Plant cell anatomy 23
Figure 2-9 A line drawing of a single plant cell 24
Figure 2-10 Cole Model (Cole, 1940). $\boldsymbol{R}_1$ is the extracellular space resistance, $\boldsymbol{R}_2$ is the intracellular space resistance, C is the cell membrane capacitance 25
Figure 2-11 Low and high frequency current paths in tissue (Grimnes et al., 2000). The dashed line represents current path of high frequency, the solid line represents current path of low frequency. 26
Figure 2-12 Hayden model (Hayden et al., 1969) 26
Figure 2-13 Double-shell model (Zhang et al., 1991) 28
Figure 2-14 Electrical model proposed by Zhang et al. (1990) 28
Figure 3-1 Electrical impedance measurement setup. 38
Figure 3-2 Snapshot of soluble solid content measurement 39
Figure 3-3 Schematic of experiment setup for titration 40
Figure 3-4 Nyquist Plot of the calculated resistance against reactance for one of the sample of Pink Lady. The sweeping frequency is from 1 Hz to 1 MHz. f_c is the characteristic frequency (maximum reactance frequency), f_o is the transitional frequency where EPI occurs. 43

Figure 3-5 Correlations between impedance and chemical compositions for four varieties ..48
Figure 4-1 The standard colour chart of bananas (Jackson, 2001).....52
Figure 4-2 Experiment setup for impedance measurement of banana ripening investigation.53
Figure 4-3 Nyquist plot of one sample each from two banana varieties. The sweeping frequency is from 1 Hz to 1 MHz. f_c is the characteristic frequency (maximum reactance frequency), f_o is the transitional frequency where EPI occurs. 54
Figure 4-4 Relationships between the diameters of fitted semicircular arcs and peel colour grade. Error bars represent the standard deviation. Different letters in the figures denote significant differences among means ($p<0.05$). 57
Figure 4-5 The equivalent circuit components as functions of peel colour grade for the Cavendish Bananas. The observed frequency range is from 100 Hz to 1 MHz.....61
Figure 4-6 The equivalent circuit components as functions of peel colour grade for the Lady Finger Bananas. The observed frequency range is from 100 Hz to 1 MHz. 62
Figure 5-1 Dehydrator 70
Figure 5-2 Impedance measurement setup. 71
Figure 5-3 Moisture content percent variation during drying. 73
Figure 5-4 An example of the circular fitting of one typical sample. The red line is the raw data and the green line is the fitted circle. The sweeping frequency range is from 100 Hz to 1 MHz. 74
Figure 5-5 Individual Nyquist Plots of the other 8 samples before drying. The sweeping frequency range is from 100 Hz to 1 MHz. 74
Figure 5-6 Impedance variations during the 270 minutes drying for 9 samples at the selected frequencies. 76
Figure 5-7 Diameter of impedance arc changes with moisture content for 9 samples. The two falling stages are detailed in Sample 1. 78
Figure 5-8 Impedance changes during the 270 minutes dehydration progress (Sample 1).....78
Figure 5-9 The distributed element consists of a resistor R_o in parallel with a DCE.....80

List of Tables

Table 2-1 Passive element impedance 16
Table 3-1 Milliequivalent factors of common fruit acids (Garner et al., 2005) 41
Table 3-2 Summary of chemical and physical parameters among four apple varieties 41
Table 3-3 Summary of the Nyquist Plot parameters for the four apple varieties 44
Table 3-4 Correlations between impedance square root and chemical compositions of fruit juice at the selected frequencies. Frequencies were chosen based on the smallest R^2 value. .. 46
Table 3-5 Differences in the degree of association between impedance and biochemical predictors 49
Table 4-1 Summary of the Nyquist Plot parameters for the CBs and LFBs 55
Table 4-2 Comparisons of the fitting results between the Hayden Model and the double-Shell Model 59
Table 4-3 The changes of resistance of the cell wall, cytoplasm and vacuole as well as capacitances of the plasma membrane and tonoplast of the Cavendish bananas and the Lady Finger bananas during ripening. 63
Table 5-1 Cucumber slices mass and moisture content percent changes during drying 72
Table 5-2 Summary of the goodness-of-fit values for the fitting of the Hayden model and the double-shell model 80

List of Abbreviations

- μHz Micro-Hertz $=10^{-6}$ Hertz
- AC alternating current
- ANOVA analysis of variation
- AVE average value
- BCM body cell mass
- BIA bioelectrical impedance analysis
- BSR best subsets regression
- CB Cavendish banana
- CD coefficient of determination
- CNLS complex nonlinear least squares
- CPE constant phase element
- CV coefficient of variation
- DC direct current
- DCE distributed element
- ECW extracellular water
- EIS electrical impedance spectroscopy
- EIT electrical impedance tomography
- EPI electrode polarization impedance
- FFM fat free mass
- FJ Fuji
- GC gas chromatography
- GS Granny Smith
- Hz hertz
- ICW intracellular water
- IED inter-electrode distances

- IR infrared
- ISR impedance square root
- kHz Kilo-Hertz = 10^3Hertz
- LFB Lady Finger banana
- M mole concentration
- MC moisture content
- MHz Mega-Hertz = 10^6 Hertz
- ml Milli Litre
- MRI magnetic resonance imaging
- mV Milli-Volt = 10^{-3} Volt
- nF Nano-Farad = 10^{-9} Farad
- NIR near infrared
- NMR nuclear magnetic resonance
- PL Pink Lady
- RD Red Delicious
- rpm revolutions per minute
- SD standard deviation
- SEE standard error of the estimate
- SS sum of squares
- TA titratable acidity
- TBW total body water

Abstract

Electrical impedance spectroscopy (EIS) is a relatively new method applied to food quality assessment. It has been demonstrated that impedance measurement is capable of reflecting rapid changes when the food has any physical damage, such as chilling and bruising. Additionally, impedance variations can be measured from the physiological changes of food, such as wooliness or mealiness. Nowadays, superior qualities of fruits and vegetables contribute towards preventing of chronic diseases such as cancers, cardiovascular diseases, stroke etc. Numerous studies have been made to devise accurate food quality measuring techniques. However, the drawbacks of some of new techniques such as nuclear magnetic resonance, acoustic response approach etc. are: expensive equipment and strict experimental environment requirements. In contrast, EIS allows relatively inexpensive assessment, is fast, easy to operate and non-invasive. It has been adopted for investigation of fundamental electrical properties of plant tissues. Although the applications of EIS for food quality determination have been reported previously, the analytical relationships between electrical impedance properties and quality criteria have not yet been fully developed. Further exploration is thus important in acquiring more data on electrical impedance characteristics of fruits and vegetables and researching new approaches for determination of their quality.

This dissertation aims to investigate the electrical impedance properties of fruits and vegetables, and explore the relationship between impedance and quality criteria. In particular, the present dissertation outlines experimental research conducted on relationships between impedance properties and fruit tastes as well as the impedance changes observed during ripening process. Impedance measurement to monitor moisture content changes in the progress of drying is also included in this research.

Experiments were performed on fruit and vegetables such as apples, bananas and cucumbers. EIS is used to examine the electrical characteristics of fruit and vegetables, and reveals their

electrical properties variations during the ripening and drying processes. It may assist future research in fruit quality classifications and explore the potential applications in this field. The summary below outlines the extent of this research.

1. It was found that the relationships between impedance and soluble solid content and/or acid percent could be used to divide the four apple varieties examined into low-acid variety (Fuji, Red Delicious), high-acid variety (Granny Smith), and medium acid variety (Pink Lady).

2. Linear relationships between impedance square root and the corresponding predictors (i.e. total soluble solid content, acid percent) were observed from the four apple varieties at different frequencies using multiple regression analysis method.

3. The pH value of apples does not show any correlation with fruit impedance parameters in this investigation. In addition, another predictor the sugar-to-acid ratio does not correlate with fruit impedance. It is suggested that impedance is not a good taste indicator.

4. It was found that electrical impedance measurements could be used to monitor ripening changes in bananas. From colour grade 3.5 to 7, a positive linear relationship between impedance and banana colour was observed in the Cavendish bananas and a fourth polynomial relationship was observed in the Lady Finger bananas. However, impedance varied differently after colour grade 7 for these two varieties. Therefore, the banana ripening process is divided into three stages based on this finding, namely physiological self-development, eating-ripe stage, and overripe stage.

5. It was observed that the typical electrical model (the double-shell model) fits the data about bananas better than the Hayden model. The double-shell model allows the analysis of EIS data conducted at the cellular level. The variations of the resistances of cell wall, cytoplasm and vacuole, the capacitors of plasma membrane and tonoplast were studied based on the Complex Nonlinear Least Squares data fitting approach. It was found that the cell wall resistance and the vacuole resistance increase linearly during ripening period.

6. The magnitude of impedance was used to monitor the drying progress in cucumbers.

The impedance arc of pure cucumber pulp had a tendency to fall when the moisture content was reduced from the initial 95% to 65%. Then, it jumped to a relatively high value when moisture content further declined to 25.83% (coefficient of variation is 48.82%). In addition, the diameter of the impedance arc displayed in the Nyquist Plot decreased with the loss of moisture. It disappeared at the end stage of dehydration (270 minutes).

7. It was also observed that a distributed model contains a distributed element in series with a resistor fits cucumbers better than the Hayden model and the double-shell model. However, the distributed model can not be linked to a specific cellular structure.

In summary, the impedance properties have merits in fruits and vegetables quality assessment. The currently used subjective visual inspection and assessment could be replaced by the EIS based approach as it is a more precise measure of food quality. This methodology could also be used by the wine industry. Further study is required to give this method practical value.

Chapter 1 Introduction

1.1 Overview

This chapter outlines the reasons for conducting this research, research problem raised from the existing knowledge and the contributions of this thesis.

Section 1.2 describes the motivation of this investigation.

Section 1.3 elaborates the definition of food quality and the main quality criteria. Quality assessment techniques are also reviewed here.

Section 1.4 raises the research problems and objectives of this investigation.

Section 1.5 describes the contributions which have been achieved from this investigation.

Section 1.6 explains the outline for this thesis.

1.2 Motivation

Fruits and vegetables are one of the four major groups of food humans need to ingest daily and play an increasingly important role in human health and well-being. The other three groups are grains and breads, dairy and meats. Cancer has become the second leading cause of death worldwide. Conventional treatments through drugs, chemotherapy radiation may cause serious side effects. Therefore, it is very necessary to develop new strategies to prevent cancers. It is estimated that at least 35% of cancers are attributed to poor dietary habits (Reddy et al., 2003). Fruits and vegetables are good sources of micronutrients, fibres, water, proteins etc. Their consumption has been shown to help prevent chronic diseases such as cancers, cardiovascular diseases, stroke, obesity, diabetes, diverticulosis and cataracts (Steinmetz et al., 1996; WHO, 2002). Furthermore, fruits and the corresponding processing of this food group can bring huge economic profits for developing countries such as Africa, Asia, and Latin America. Fruit and vegetable intake requires high quality products. Furthermore, consumers' expectations of higher food quality have risen along with improved standard of living. Therefore, it is of great importance to develop effective food quality assessment techniques.

Conventional quality determination approaches include: sorting and grading by human visual evaluation, firmness measurement by penetrometer, sensory evaluation by trained human sensory panels, sugar content measurement by refractometer etc. Continuous efforts have been made to explore quick, handy and accurate approaches to assist quality determinations. Recently, electrical impedance measurement has gained popularity for plant tissue investigation (Bauchot et al., 2000; DeBaerdemaeker et al., 1997; Harker et al., 1997). Electrical impedance technology has been applied in biological systems since the late 1800s (Ackmann et al., 1984). With the development of devices and analytical approaches, Electrical Impedance Spectroscopy (EIS) has become widely used to investigate the fundamental electrical properties of plant tissues and to detect tissue changes under different physiological conditions since the beginning of the 1990s (Repo, 2004). It has been reported that impedance parameters are sensitive to fruit and vegetables being damaged by bruising or chilling (Cox et al., 1993; Harker et al., 1997).

Impedance measurements have also been applied in food quality determination. Cox et al. (1993) assessed apple bruises through electrical impedance measurements, and suggested that impedance measurement, together with a bruise index, could be an alternative option for

assessing fruit bruises. Varlan et al. (1996) tried to classified apples according to their natural ripening process, but found it difficult owing to the large parameter dispersion amongst samples. A more promising ripening classification was obtained for tomato evaluation (Varlan et al., 1996). It is suggested that more work needs to be done to study the relationship between the impedance parameters and fruit mealiness (Lammertyn et al., 2002). Mealiness is an internal quality parameter, which is characterised by texture deterioration of the fruits during inappropriate storage, resulting in soft, dry and mealy fruits (Lammertyn et al., 2002). Since the applications of electrical impedance techniques on food quality assessment have not been fully researched, this thesis will demonstrate impedance measurements on fresh fruit and vegetables, and propose new approaches for quality determinations. If the process of plant growing and ripening can be monitored in a predictable manner, then the quality classification by impedance measurement can be demonstrated.

1.3 Background of Quality Assessment Techniques

In order to better understand quality assessment, this section provides a brief review.

1.3.1 Quality Definition

Quality is defined as meeting the expectations of consumers (Robert et al., 2000). Generally, the quality criteria for fresh products are appearance, texture and flavour (Aked, 2002; Wang, 1994).

- Appearance comprises colour, shape, size etc. and is a key factor when consumers in purchasing fruits. Many fruits undergo colour changes during ripening, for example in bananas, the chlorophyll content of the peels of bananas reduces with ripening which contributes to peel colour changes (Li et al., 1997). Thus the fruit colour is considered to be a strong indicator of ripening.

- Texture is one of the key factors in determining harvest date, and it has also been used as an indicator for the consistency of products in manufactured foods (Hung et al., 1999). Texture is a complex term which has not been given an entirely satisfactory definition (Aked, 2002; Malcolm, 1982). Malcolm (1982) states: “Texture is the response if the tactile senses to physical stimuli that result from contact between some

part of the body and the food." "Texture" is preferred to be termed "textural properties", because it is a concept which consists of group properties.

- Flavour consists of taste and aroma. Sweetness, acidity, astringency, and bitterness are the four key taste components. Sugar level is measured on the Brix scale (Harker et al., 2002a), which is a hydrometer scale for measuring the concentration of sugar content of a solution at a given temperature. The sugar level is usually measured to determine the best time for fruit to go to market. Additionally, the ratio of sugar to acid is very critical for fruit taste, especially in the fruit juice and wine-making industry (Fellers, 1991). Fruit ripening is always associated with ethylene evolution. Ethylene as a classical plant hormone plays an important role in the ripening of fruits and vegetables (Kende et al., 1997). Its presence in the storage environment decreases the storage life of fruits and vegetables (Bower et al., 2003).

1.3.2 Quality Evaluation Techniques

Consumers' preferences drive fresh food industry to provide good quality fruit and vegetables (Peneau et al., 2006). Moreover, efforts have been made to enhance their quality using genetic engineering. Quality evaluation techniques have been around for several decades. These techniques started from single parameter measurement, such as weight, size, firmness measurements etc. Then more complex biochemical and biophysical analysis were applied to observe internal quality changes, such as titratable acidity measurement, nutritional analysis, and enzymes degrade analysis etc. With the development of information technology, quality assessment is in the state of evolution. Computer aided imaging techniques can identify precise internal quality deterioration, and even show the deterioration location.

Colour

Human visual evaluation has been the primary empirical method for the grading and sorting of fruit and vegetables. Another option is to use Near-Infrared (NIR) spectroscopy to analyse colour variations (Gunasekaran, 2001).

Firmness

Firmness is also a term for hardness (Szczesniak, 1963). It is a very good indicator concerning eating quality of products, and it has also been used as a measure of maturity and ripeness of fruits (Hoehn et al., 2003). It is usually measured by a penetrometer. The disadvantage of this

method is that the samples examined are destroyed and can not be sold. A non-destructive measurement is therefore very much more desirable. Over the past two decades, resonant frequencies, acoustic response, and ultrasonic approaches have been used to investigate the firmness of food (Gunasekaran, 2001).

Sweetness & Sourness

Sweetness is normally referred as the total soluble content in °Brix (Harker et al., 2002a). It is measured with a refractometer. Generally, the refractive index increases with the rise of soluble solids concentration. Additionally, infrared (IR) and NIR methods also have the capabilities to determine total sugar content directly from fruit juice (Rodriguez-Saona et al., 2001). Acidity is generally determined by a titration approach. Titratable acidity measures total available hydrogen ion in solution.

Sensory Evaluation

Human sensory panels are trained to assess the overall quality of fruits and vegetables. However, there is a growing demand for trained sensory panels to be standardised for quality assessment.

Aroma

The headspace Gas Chromatography (GC) is one of the popular methods currently used to conduct measurement of odour properties (Poll et al., 1984). The concentration of ethylene can be detected using this method. Another technique known as “Electronic Nose” which simulates the function of human nose is used and is more sensitive to the total headspace volatiles (Pathange et al., 2006).

Apart from the above approaches, there are several new techniques which have emerged for the applications of food quality assessment. These include nuclear magnetic resonance (NMR), used to determine the internal bruising and ripeness of fruit and vegetables (Ruan et al., 2001). Moreover, electrical impedance has being used in fruit quality investigations (Cox et al., 1993; DeBaerdemaeker et al., 1997). It has been reported that the decreasing of cell wall resistance was closely related to changes in nectarine fruit texture during ripening (Harker et al., 1994a).

1.4 Objectives of Research

The objective of this research is to investigate fruits and vegetables quality variations by using electrical impedance measurement, and to propose new methods for quality assessment.

It has been noticed that both conventional and novel techniques have advantages and disadvantages. Some techniques require expensive devices, such as NMR, which will affect product cost, whilst some have not been adapted to manufacturing requirements and can only be performed in laboratory conditions, such as an acoustic response approach. Therefore, the development of effective techniques on quality assessment is becoming more popular.

Fruit and vegetables are good electrical conductors owing to their high water content. It is estimated that about 80% of fruit is water (Jayaraman et al., 1992). Moreover, the rich metal ions inside fruit and vegetables make them good electrical conductors. Thus it is possible to perform impedance measurements on them. Since the equivalent models proposed through electrical impedance spectroscopy measurement allow cellular analysis towards plant tissues, it is expected that impedance measurement can be used to monitor plant physiological changes. Hence, one of the aims of this thesis is to investigate impedance parameters changes during fruit normal ripening process.

Most literature focus on monitoring the impedance of plants under different physiological conditions. Few papers have reported the associations between impedance and the plant's internal organic elements, for example, sugar content, organic components, etc. Therefore, this thesis examines whether there is any relationship between plant impedance and the properties of its organic elements. The total amount of sugar present and sugar to acid ratio are considered good indicators for determining the maturity of most fruit. It is also an important criteria for flavour (Hoehn et al., 2003).

Electrical conductivity is the ability of a material to carry electrical current. Generally, the conductivity of a certain solution increases with the increasing hydrogen ions concentration at a given temperature (Clarkson, 1974). Resistivity is the reciprocal of conductivity. Fruits are rich of organic acids (malic acid, citric acid, tartaric acid etc.), which accumulate or degrade

during ripening process. Thus the concentration of hydrogen ions inside fruits varies accordingly. Thus, this ions variation forms the basis for conducting this research.

This research is on fruit and vegetables post-harvest quality assessment. More specifically, the present research has following objectives:

1. To determine the relationship between electrical impedance and other biochemical parameters, such as the total amount of sugar present, acid content, sugar to acid ratio and hydrogen ions concentration.

2. To observe electrical impedance spectroscopy in the application of fruit ripening monitoring.

3. To analyse plant cellular changes via building up the equivalent electrical model.

4. To explore the feasibility of electrical impedance spectroscopy in monitoring the moisture content changes during drying progress.

1.5 Contributions

The research covers the electrical properties of fruits and vegetables, and the applications of EIS in the relevant quality assessment. Experiments were performed on apples, bananas and cucumbers. Results have shown that EIS has merit in fruit and vegetables quality assessment. The EIS can help future research in fruit quality classifications, and help explore potential applications in this field. The EIS studies have revealed that:

1. The relationships between impedance and soluble solid content and/or acid percent can be used to divide the four apple varieties into low-acid variety (Fuji, Red Delicious), high-acid variety (Granny Smith), and medium acid variety (Pink Lady).

2. Linear relationships between impedance square root and the corresponding predictors (i.e. total soluble solid content, acid percent) were observed from the four apple varieties at different frequency ranges using multiple regression

analysis method. The analysis of correlations between impedance and internal chemical parameters of fruits has not yet been reported.

3. The pH value of apples does not show any correlation with fruit impedance parameters in this investigation. In addition, another predictor, the sugar-to-acid ratio, does not correlate with impedance, although it is suggested this is a good indicator of taste.

4. The electrical impedance measurements could be used to monitor ripening changes in bananas. A positive linear relationship between impedance and banana colour grade was observed in the Cavendish bananas from colour grade 3.5 to 7 and a fourth polynomial relationship was observed in the Lady Finger bananas. However, impedance varied after colour grade 7 for the two varieties. The banana ripening process can be divided into three stages, namely physiological self-development, eating-ripe stage, and overripe stage.

5. The typical electrical model which is the double-shell model fits the data from the investigation of banana ripening much better than the Hayden model. The double-shell model is used to analyse EIS data conducted at the cellular level. The variations of resistance of cell wall, cytoplasm, and vacuole, the capacitors of plasma membrane and tonoplast were studied based on the Complex Nonlinear Least Squares data fitting approach. It was found that the cell wall resistance and the vacuole resistance also increase linearly during ripening period.

6. The magnitude of impedance was useful to monitor the drying progress in cucumbers. The impedance arc of pure cucumber pulp had a tendency to fall when the moisture content reduced from the initial 95% to 65%. However, it jumped to a relatively high value when the moisture content further declined to 25.83% (coefficient of variation is 48.82%). In addition, the diameter of impedance arc displayed in the Nyquist Plot decreased with the loss of moisture. It disappeared at the end stage of dehydration (270 minutes).

7. A distributed model containing a distributed element in series with a resistor fits cucumbers better than the Hayden model and the double-shell model. However, the distributed model cannot be linked to a specific cellular structure.

1.6 Thesis Organisation

Chapter 2 provides background knowledge for electrical impedance analysis. Details include basic knowledge about electrical circuit components, the principle of electrical impedance spectroscopy, measurement methods, electrical modelling etc. Also the applications of electrical impedance measurement on human and plant are reviewed in this chapter.

Chapter 3 investigates on apples. Impedance measurement was performed on four apple varieties to detect associations between impedance parameters and biochemical parameters of fruit, such as the total soluble solid content and acid content.

Chapter 4 investigates bananas. The banana ripening process was monitored by impedance measurement. Impedance and phase displacement were used to perform data fitting by the Z-view program. The results were used to verify two equivalent models of electrical circuits, namely the Hayden model and the double-shell model.

Chapter 5 investigates the electrical impedance on the dehydration of cucumbers. Results from these experiments were used to analyse how the electrical impedance changes with the loss of moisture content. An electrical model is proposed for cucumbers.

Chapter 6 concludes the overall study, and recommends future research.

Chapter 2 Literature Review

2.1 Overview

This chapter summarises the literature to date on impedance measurement.

Section 2.2 reviews the basic knowledge about electrical impedance, and the relevant mathematical representations.

Section 2.3 introduces impedance measurement basics, including single frequency measurement, multiple frequency measurement and electrical impedance spectroscopy.

Section 2.4 introduces two common electrodes configurations used in electrical impedance spectroscopy measurement.

Section 2.5 describes the Nyquist and Bode plane plotting used in data representation.

Section 2.6 elaborates the anatomical structure of plant cell, and reviews several electrical models used in analysing the electrical properties of plant in the cellular level.

Section 2.7 reviews the applications of electrical impedance measurement, including the analysis on human body composition and plant tissues, and its feasibility on food quality assessment.

2.2 Impedance - Definition

"*Ohm's law states that the voltage across a resistance is directly proportional to the current flowing through it*" (Alexander et al., 2004). The mathematical relationship of Ohm's law is illustrated by the following:

$$v(t) = \mathrm{R} \times i(t), \text{ where } \mathrm{R} \geq 0 \qquad \text{Eq. 2-1}$$

where R is the resistance, measured in ohms, which is defined as the constant of proportionality between the voltage and current. $v(t)$ is the potential difference between the two points of a resistance. $i(t)$ is the current flows through the resistance. Eq.2-1 is applicable when direct current (DC) applied. Whereas, Ohm's law is rewritten as Eq.2-2 when alternating current (AC) is applied.

$$\mathbf{V} = \mathbf{I} \times \mathbf{Z} \qquad \text{Eq. 2-2}$$

where **Z** is a frequency-dependent quantity known as impedance, measured in ohms. "*The impedance* **Z** *of a circuit is the ratio of the phasor voltage* **V** *to the phasor current* **I**" (Alexander et al., 2004). Therefore, impedance in an AC circuit is analogous to resistance in a DC circuit. Since impedance is a complex quantity, it can be expressed in rectangular form as

$$\mathbf{Z} = \mathrm{R} + j\mathrm{X} \qquad \text{Eq. 2-3}$$

where R is the real component (resistance), and X is the imaginary component (reactance). The reactance may be positive or negative. The impedance is shown graphically on a vector plane (Figure 2-1).

The impedance can also be expressed in polar form as

$$\mathbf{Z} = |\mathbf{Z}| \angle \theta \qquad \text{Eq. 2-4}$$

Therefore,

$$\mathbf{Z} = \mathrm{R} + j\mathrm{X} = |\mathbf{Z}| \angle \theta \qquad \text{Eq. 2-5}$$

where

$$j = \sqrt{-1}\,, |\mathrm{Z}| = \sqrt{\mathrm{R}^2 + \mathrm{X}^2}\,, \theta = \tan^{-1}\frac{\mathrm{X}}{\mathrm{R}} \qquad \text{Eq. 2-6}$$

and

$$\mathrm{R} = |\mathrm{Z}| \cos\theta$$

$$X = |Z| \sin\theta \qquad \text{Eq. 2-7}$$

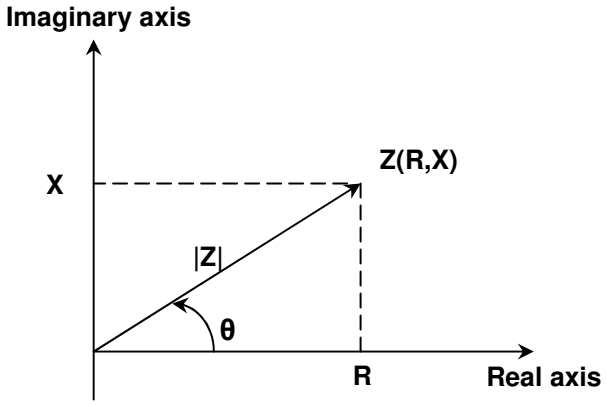

Figure 2-1 Impedance complex plane

As well as resistors, there are another two passive elements - capacitors and inductors, which store energy, which can be retrieved at a later time. "*Capacitance is the ratio of the charge on one plate of a capacitor to the voltage difference between the two plates, measured in farads*" (Alexander et al., 2004). A capacitor is an open circuit to DC. The voltage-current relation for capacitors is given by:

$$\mathbf{V} = \frac{\mathbf{I}}{\mathbf{j}\omega\mathbf{C}} \qquad \text{Eq. 2-8}$$

where ω is the radian or angular frequency of applied signal. C is the capacitance.

"*Inductance is the property where by an inductor exhibits opposition to the change of current flowing through it, measured in henrys*" (Alexander et al., 2004). An inductor acts a short circuit to DC. The voltage-current relation for inductors is given by:

$$\mathbf{V} = j\omega L\mathbf{I} \qquad \text{Eq. 2-9}$$

where ω is the radian or angular frequency of applied signal. L is the inductance.

The equivalent impedance of resistors, inductors, and capacitors in AC circuits can be obtained from Eq.2-2, Eq.2-8, and Eq.2-9. The details are illustrated in Table 2-1.

Table 2-1 Passive element impedance

Passive Element	Impedance
R	$\mathbf{Z} = \mathrm{R}$
L	$\mathbf{Z} = j\omega L$
C	$\mathbf{Z} = \frac{1}{j\omega C}$

2.3 Methods of Electrical Impedance Measurement

This section will review impedance measurement methods and the principle of electrical impedance spectroscopy which is the main method employed in this research.

2.3.1 Single Frequency Impedance Measurement

Bio-impedance analysis is applied in human body composition evaluation because it is a rapid, non-invasive, easy to operate approach. The geometric shape of human body is assumed as a cylinder with one uniform cross section (Figure 2-2). Therefore, bioelectrical impedance is expressed as a function of conductor length and conductor volume for a given frequency.

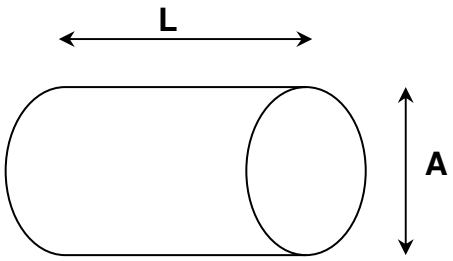

Figure 2-2 Cylinder model for the relationship between impedance and human body geometry. A is the cross-sectional area; L is the height of human body.

$$Z = \rho \frac{L}{A} \qquad \text{Eq. 2-10}$$

where ρ is the resistivity of the conductor, L is the length of the conductor, and A is the cross-sectional area. Eq. 2-10 can be rewritten as:

$$Z = \rho \frac{L}{A} = \rho \frac{L^2}{V} \qquad \text{Eq. 2-11}$$

where V is the volume of the conductor. In general, V represents the observed body water volume, and L refers to the body height.

Single frequency measurement usually chooses 50 kHz as the working frequency to estimate total body water (TBW) and fat free mass (FFM) (Matthie et al., 1998). Surface electrodes are placed on hand and foot (De Lorenzo et al., 2003; Patterson, 1989). Cell membrane which acts as an insulator at low frequency separates cell into intracellular space and extracelluar space (Kyle et al., 2004a). 50 kHz is the frequently employed frequency in several body composition analysers as it is in this frequency range where extracellular fluid contributes to conduction and intracellular fluid starts to contribute (Thompson et al., 1993). Consequently, the observed body water is the TBW, which can be used to indicate any abnormal symptoms of diseases.

2.3.2 Multiple Frequency Impedance Measurement

Although single frequency measurement can be efficient in assessing TBW, it is limited when the distribution between extracellular and intracellular fluids is to be observed, such as in cirrhosis (Hills et al., 1998; Lehnert et al., 2001; Schoeller, 2000). It is suggested that multiple frequency measurement can improve prediction of body composition. Such a technique is frequency sweeping (Lehnert et al., 2001). The prediction of extracellular water (ECW) is measured by low frequency impedance measurement (i.e. 1-5 kHz) (Deurenberg et al., 1996; Lehnert et al., 2001). Whilst, the prediction of TBW is measured by high frequency impedance measurement (i.e. 100-500 kHz) (Deurenberg et al., 1996; Lehnert et al., 2001). Reactance against resistance is plotted in a complex plane, the frequency at the peak of the plot is the so-called characteristic frequency. Current flows through both ECW and intracellular water (ICW) at the characteristic frequency. Impedance measured at the characteristic frequency is related to the estimation of TBW. Frequencies of 1, 5, 50,100, 200 to 500 kHz are generally employed in several evaluations (Kyle et al., 2004a; Kyle et al., 2004b).

2.3.3 Electrical Impedance Spectroscopy

Electrical impedance spectroscopy (EIS) is used for studying the structures of organic and inorganic materials with wide and continuous frequency impedance measurement (Repo et al., 2000). It deals with complex quantities. It analyses the subsequent electrical response of a subject when small AC signals are applied and characterizes the physicochemical properties of the system (Macdonald, 1992). The span of frequency used in EIS ranges from about 10^{-5} Hz to about 10^{7} Hz (Macdonald et al., 1987). EIS generally makes use of equivalent circuits to characterise experimental frequency response. Figure 2-3 elaborates the flow diagram of a complete EIS study which aims to evaluate the behaviour of a material-electrode system from its electrical response.

Once there are suitable mathematical models available for the specific physicochemical process, they should be used to fit the data from the EIS experiments. Otherwise, built up equivalent electrical circuits could be used to analyse the various changes take place during physical process of the particular system. The major applications of EIS are on the investigations of fuel cells, rechargeable batteries, and corrosion (Macdonald, 1992). It has also been used in the biological area, such as the studies of human body fluid as well as animal and plant tissues (Bauchot et al., 2000; Cox et al., 1993; Goovaerts et al., 1998; Kyle et al., 2004a) etc.

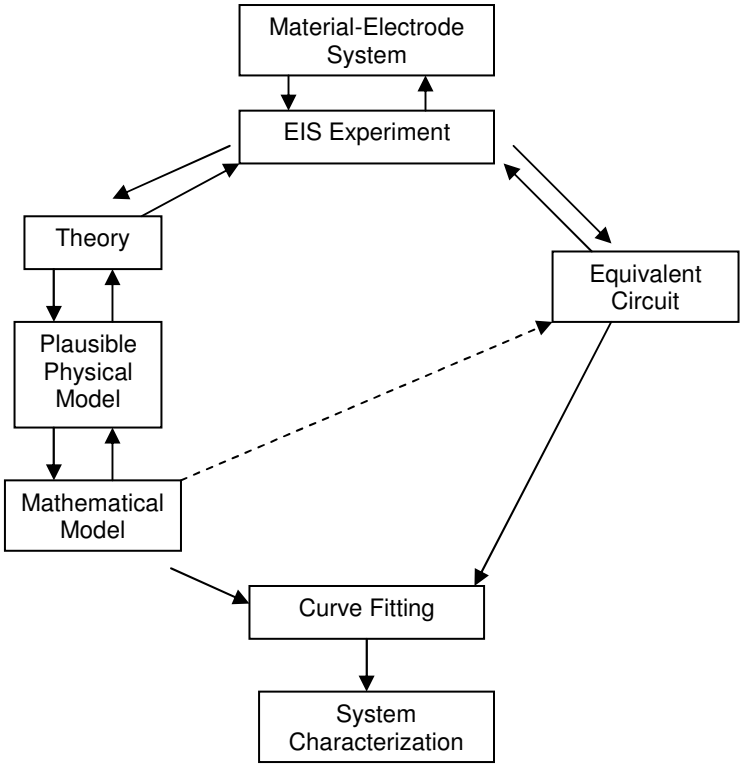

Figure 2-3 Flow chart for the principle of EIS (Macdonald, 1987)

2.4 Electrodes Configurations

EIS measurement is complicated in practice, due to the influences of electrode-tissue interface and electrode polarization impedance. Two of the common measurement methods are introduced, namely two-terminal system and four-terminal system.

2.4.1 Two-terminal Measurement

The most commonly employed approach in biological tissue investigations is the two-terminal measurement technique. The electrodes connection can be seen from Figure 2-4. The two electrodes are connected with a sample in series, therefore, the measured impedance contains the electrode polarization impedance (EPI). When polarisable electrodes (steel, copper) are used, the electrode and tissue contact impedance has to be considered. The EPI is caused by the electrochemical reaction which occurs in the contact interface between electrodes and tissue when polarisable needle electrodes impale plant tissue. It has been postulated that the impedance of an electrode-electrolyte interface depends on electrode material, electrolyte concentration, and temperature (Ackmann et al., 1984). Harker et al. (1994b) had reported that EPI can be very large and many times larger than the sample impedance at low frequencies, which can lead to inaccuracies in the measurement. EPI is mainly apparent at frequencies below 1 kHz, and is a severe problem below 20 Hz (Ferris, 1974). Therefore, it is important to eliminate the effect of EPI from tissue impedance while analysing data.

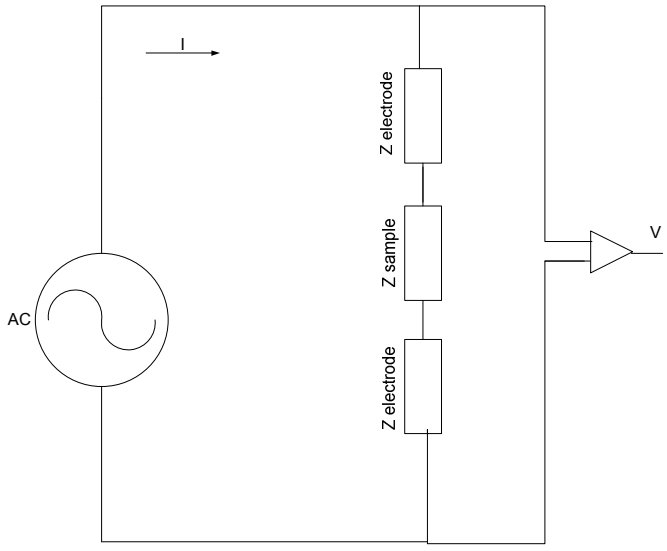

Figure 2-4 Two-terminal connection method

Various methods have been proposed to reduce the effects of AC polarization impedance. Surface treatment of electrodes can be used to reduce the polarization impedance significantly, for instance, electrolytic deposition of colloidal platinum on platinum (Ferris, 1974; Schwan, 1963). The inter-electrode distances (IED) method has been widely used to correct EPI in several experiments (Shedlovsky, 1930; Zhang et al., 1991). The principle of the IED method can be summarised as impedance measurements are performed at three different inter-electrode distances at each frequency. The three sets of measured resistances and reactances against different inter-electrode spacing are plotted separately. The linear least squares regression is used to calculate the corresponding slope and intercept. As a result, the slope represents the value of resistance and reactance of tissue, whilst the intercept represents the value of resistance and reactance of electrode. Consequently, the impedance of tissue sample and electrode are separated. Sufficiently high frequencies can reduce the EPI. Glerum (1973) and Repo (1992) introduced frequencies higher than 500 Hz to minimise the EPI. Freywald et al. (1995) used a frequency spectrum starting at 4 kHz to reduce the EPI.

2.4.2 Four-terminal Measurement

In contrast to the two-terminal configuration, the four-terminal configuration uses one pair of electrodes for voltage or current excitation, and another pair of electrodes for potential measurement (Figure 2-5). When the four-terminal measurement is employed, there is no current flow through the voltage measurement electrodes, thus there is no voltage drop across these electrodes, and the problem of electrode polarization can be largely eliminated.

The two-terminal measurement is the most accurate at high frequencies, but the measurement is time consuming. In addition, the EPI affects the measurement very much especially at low frequencies, and the influences of EPI increase with frequency decrease. The four-terminal technique is a highly efficient method and largely minimises the EPI problem. It can be useful when the sample is undergoing rapid changes within a short time, such as bruising and chilling. Therefore, the four-terminal configuration was carried out in these experiments.

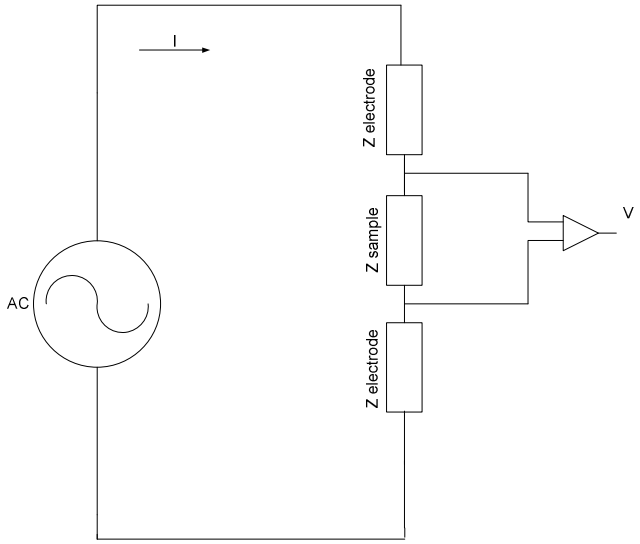

Figure 2-5 Four-terminal connection method

2.5 Data Representation

Once the raw data of experiment have been obtained, it is important to extract characteristic parameters to analyse the system properties. There are a few ways the data can be plotted, such as the Nyquist and Bode plane plotting. This section describes the several methods used to present data graphically.

2.5.1 Nyquist Plot

The Nyquist Plot is named after Harry Nyquist. It is also known as the complex plane, which generally plots the negative of the imaginary part of impedance against the real part of impedance. Impedance measurements were only conducted in the high frequency range initially where the electrode-electrolyte interface exhibits only a capacitive behaviour. Thus, the imaginary part of impedance is negative. In order to plot data in the first quadrant, the sign convention has been adopted in the Nyquist Plot (Gabrielli, 1993). Figure 2-6 gives an example of the Nyquist Plane. In practice, there are no intercepts of real axis at relative low and high frequencies, owing to the existing equipment not being able to measure such frequencies. Therefore, the values of $\boldsymbol{R}_{\infty}$ and $\boldsymbol{R}_{0}$ are calculated by extrapolation and interpolation respectively from the values obtained over frequency range (Cornish et al., 1993). The disadvantage of this data presentation is that it cannot directly indicate frequency response.

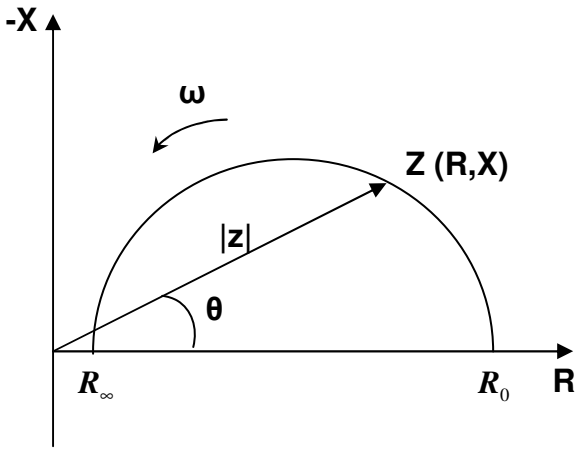

Figure 2-6 Nyquist Plot with impedance vector

2.5.2 Bode Plot

The Bode plot is named after Hendrik Wade Bode. This consists of two subplots, the Bode magnitude plot and the Bode phase plot respectively. A Bode magnitude plot is a graph of log magnitude against log frequency. A Bode phase plot is a graph of phase against log frequency, which usually used in conjunction with the magnitude plot. An example of the Bode plot is given in Figure 2-7. The data presented in this figure were obtained from one of the experiments in this study, the curves were drawn by Z-view software. Figure 2-7(A) is the Bode magnitude plot, and Figure 2-7(B) is the Bode phase plot.

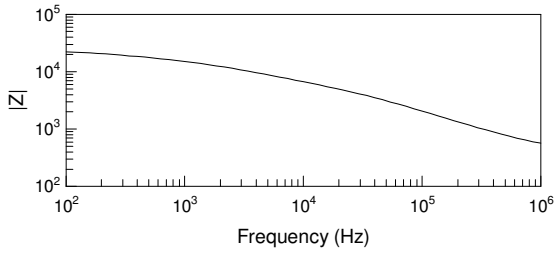

(A) Bode magnitude plot

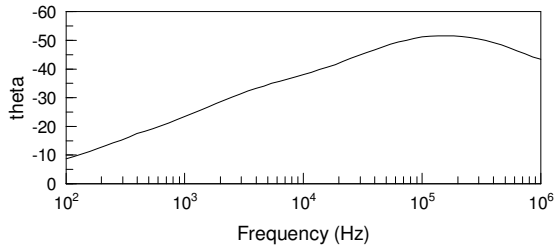

(B) Bode phase plot

Figure 2-7 Bode Plot of one experiment from bananas investigation

2.6 Electrical Modelling

A complete EIS analysis usually requires an equivalent circuit to fit the measured data and to characterize the behaviour of the electrode-electrolyte system. It is desirable that the equivalent circuit should include as few frequency-dependent elements as possible (Macdonald et al., 1977; Varlan et al., 1996). There are several electrical models regarding the electrical properties of biological tissues that have been proposed by researchers, such as the Cole model, the Hayden model and the double-shell model etc.

2.6.1 Plant Cell Anatomy

Before building any electrical model, it is necessary to be familiar with the investigated sample structure. The cell is the basic structural and functional unit of living things, and can exist independently (Hall et al., 1974). Animal cells and plant cells are different in their structures. The complete anatomical structure of a plant cell is illustrated in Figure 2-8 (Alters et al., 2006). A simplified cell structure is represented in Figure 2-9 (Labavitch et al., 1998).

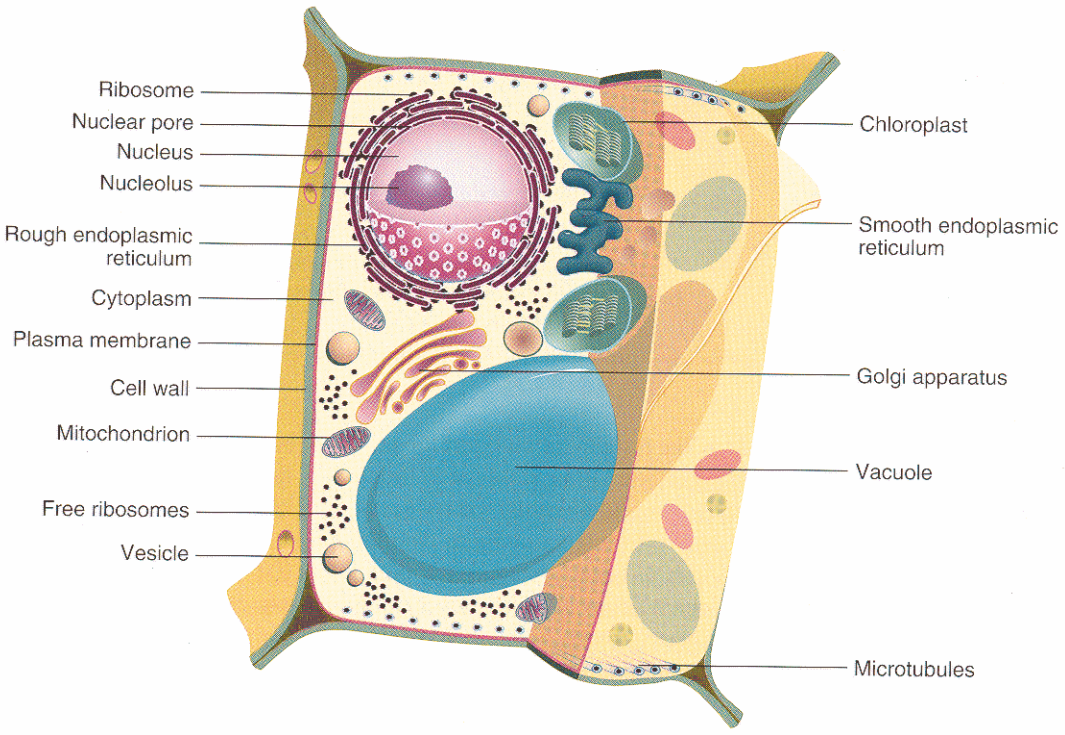

Figure 2-8 Plant cell anatomy

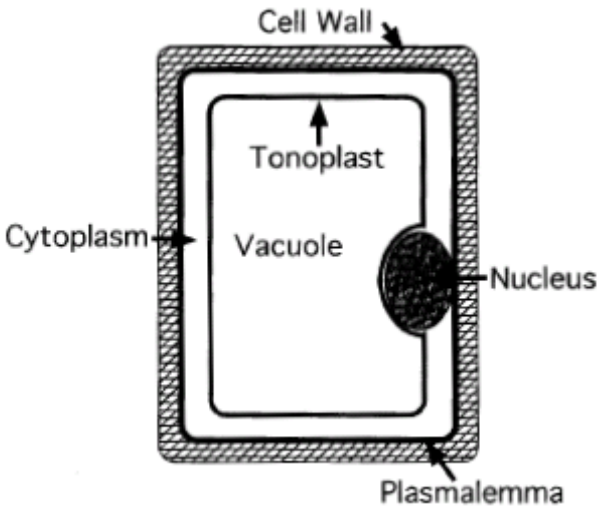

Figure 2-9 A line drawing of a single plant cell

The cell membrane (*plasmalemma*) is a phospholipid bilayer with embedded proteins surrounded by cell wall. It is a semipermeable barrier, water can pass through freely, whereas some selectivity is shown to the passage of solutes (Hall et al., 1974). The cell membrane defines the cell boundary, and regulates the molecules passing into and out of cells.

Outside the *plasmalemma*, a plant cell has a rigid and thick structure which is known as the cell wall. It has always been regarded as one of the features of plant cells which distinguish them from animals. The cell wall limits the size and shape of the cell. It plays an important role in plant metabolic processes, because of specific enzymes contained in the cell wall (Hall et al., 1974).

The nucleus is the largest of the cellular organelles, which consists of a number of distinct components. The contents are separated from the cytoplasm by a nuclear envelop or a membrane which surrounds the nuclear sap (Hall et al., 1974). It is the control centre of a cell.

Cytoplasm is the viscous fluid between the plasma membrane and all the cell organelles except the nucleus. The vacuole inside each plant cell stores substances and has diverse functions in reproduction, growth, and development of the plant (Clarkson, 1974). The inner boundary of the cytoplasm is marked by a membrane, known as the tonoplast, which surrounds the vacuole (Clarkson, 1974).

2.6.2 Electrical Modelling Components

In order to study the electrical properties of plants, the cell structure has been simulated by equivalent electrical circuits. The values of circuit components determine the electrical response. A single cell isolated from a tissue was simulated by an equivalent circuit consisting of resistors and capacitors arranged in series and parallel. Thus, a tissue block can be presumed to be a network of cells, which contain numerous arrays of mini-circuits (Varlan et al., 1996; Zhang et al., 1991). Below is a review of a few popular electrical circuit based models for representing tissue blocks. All these models were constructed for the ideal case, which assumes that the tissue structure, dimension, shape, and orientation are uniform.

2.6.2.1 Cole Model

The Cole model, which is the simplest electrical model for a biological body, is shown in Figure 2-10. The Cole model simplified biological tissue into a two-branch parallel circuit. $\boldsymbol{R}_1$ represents the extracellular space resistance, $\boldsymbol{R}_2$ represents the intracellular space resistance, and C represents the cell membrane capacitance. The current paths of different frequencies are illustrated in Figure 2-11. Tissue impedance at low frequencies is almost independent of cell membrane and internal resistivity (Cole et al., 1950; Otto, 1950), which is due to the cell membrane acting as a capacitor. The cell membrane is open-circuit at very low frequencies, thus impedance is given by a purely resistive path: $\boldsymbol{R}_1$. The cell membrane is short-circuit at high frequencies (characteristic frequency), which is the maximum value of reactance. The measured impedance is $\boldsymbol{R}_1 \| \boldsymbol{R}_2$. Impedance characteristic is represented by $\boldsymbol{R}_1 \| \boldsymbol{R}_2$ -j**X** at the intermediate frequencies, where $\boldsymbol{X} = \frac{1}{\omega \boldsymbol{C}}$, $\mathbf{j} = \sqrt{-1}$, $\omega = 2\pi f$.

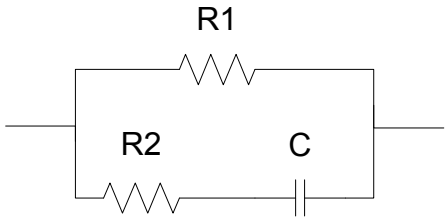

Figure 2-10 Cole Model (Cole, 1940). $\boldsymbol{R}_1$ is the extracellular space resistance, $\boldsymbol{R}_2$ is the intracellular space resistance, C is the cell membrane capacitance

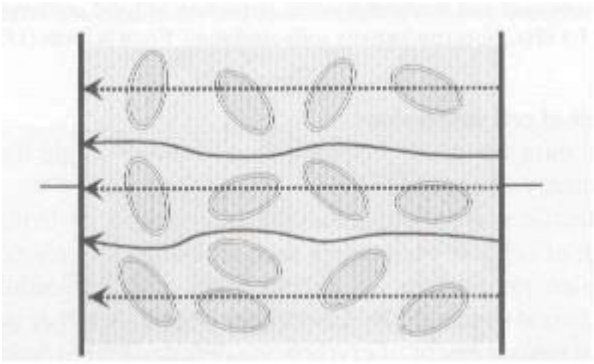

High Frequency ..... Low Frequency ——

Figure 2-11 Low and high frequency current paths in tissue (Grimnes et al., 2000). The dashed line represents current path of high frequency, the solid line represents current path of low frequency.

2.6.2.2 Hayden Model

The Hayden model was proposed by Hayden and his co-workers (Hayden et al., 1969) when they explored the quantitative relationships between plant impedance and temperature and humidity. The cells of potato tuber were examined under a microscope and they were found roughly isodiametric. Therefore, according to plant cell structure, the cells are equivalent to many small capacitor-resistors connected in parallel with their cell walls. The current path through a potato tuber tissue is represented in Figure 2-12. $\boldsymbol{R}_1$ represents the resistance of all cell walls, $\boldsymbol{R}_2$ represents the resistance of all membranes of all actual cells, $\boldsymbol{R}_3$ represents the resistance of cytoplasm of actual cells, and C represents the capacitance of all membranes of actual cells.

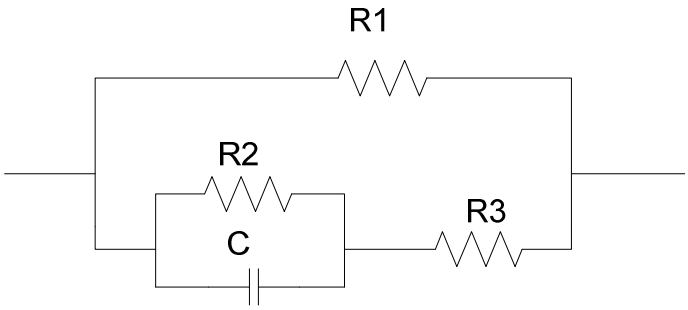

Figure 2-12 Hayden model (Hayden et al., 1969)

The impedance of this circuit is expressed as:

$$\boldsymbol{Z} = \frac{\boldsymbol{R}_1\boldsymbol{R}_2\boldsymbol{R}_3 - \boldsymbol{jXR}_1(\boldsymbol{R}_2 + \boldsymbol{R}_3)}{\boldsymbol{R}_2(\boldsymbol{R}_1 + \boldsymbol{R}_3) - \boldsymbol{jX}(\boldsymbol{R}_1 + \boldsymbol{R}_2 + \boldsymbol{R}_3)} \qquad \text{Eq. 2-12}$$

where $\mathbf{X} = \frac{1}{\omega \mathbf{C}}$, $\mathbf{j} = \sqrt{-1}$, $\omega = 2\pi f$

Eq.2-12 is simplified to $Z = \frac{\boldsymbol{R}_1^{\,2}\boldsymbol{R}_3 + \boldsymbol{X}^2\boldsymbol{R}_1 - \boldsymbol{jXR}_1(\boldsymbol{R}_1 - \boldsymbol{R}_3)}{\boldsymbol{R}_1^{\,2} + \boldsymbol{X}^2}$, whenever $\boldsymbol{R}_2 \geq \boldsymbol{R}_1 > \boldsymbol{R}_3$ at any frequency

At zero frequency, $\omega = 0$, $Z = \boldsymbol{R}_1$

At infinite frequency, $\omega = \infty$, $Z = \boldsymbol{R}_3$

2.6.2.3 Double-shell Model

In contrast to the Hayden model, the double-shell model adds one more branch, which is the resistance of vacuole and capacitance of tonoplast in series (Figure 2-13). The various components in the circuit include the cell wall resistance ($\boldsymbol{R}_1$), cytoplasm resistance ($\boldsymbol{R}_2$), vacuole resistance ($\boldsymbol{R}_3$), plasma membrane capacitance ($\boldsymbol{C}_1$), and tonoplast capacitance ($\boldsymbol{C}_2$). The double-shell model has been validated in several plant investigations, such as the impedance measurements conducted on nectarine fruit (Harker et al., 1994a), persimmon fruit (Harker et al., 1997), kiwifruit (Bauchot et al., 2000), and leaves of *Peperomia obtusifolia* L. and *Brassica oleracea* L. (Zhang et al., 1993). Figure 2-14 is an electrical model proposed by Zhang et al. (Zhang et al., 1990), where $\boldsymbol{R}_4$ and $\boldsymbol{R}_5$ are the resistances of plasma membrane and tonoplast. However, the second model does not improve the accuracy of curve fitting, and it is more complex than the double-shell model. Thus it is not usually employed in practical investigations.

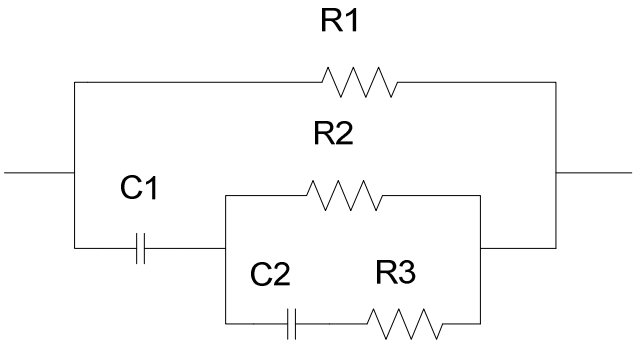

Figure 2-13 Double-shell model (Zhang et al., 1991)

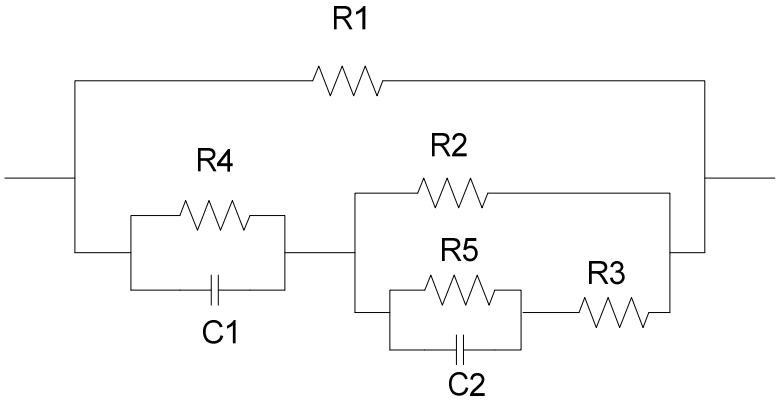

Figure 2-14 Electrical model proposed by Zhang et al. (1990)

2.7 Application of Impedance Measurement

2.7.1 Impedance Analysis on Human Body Composition

Bioelectrical impedance has been used as an important index for clinical diagnosis and prognosis. The most prominent applications are human body composition research (Schoeller et al., 1989), cardiac performance monitoring (Palko, 2004), tumour identification(Hua et al., 1993), and imaging of organs and tissues and so on (Cherepenin et al., 2002).

Adiposity

Hypertension, diabetes, cardiovascular diseases and psychosocial problems are some of the severe outcomes associated with obesity (WHO/FAO, 2003). The ratio of childhood obesity is increasing in most developed countries. Pure body weight index is insufficient to evaluate fat

mass. Bioelectrical impedance analysis (BIA) has become the dominant technique owing to its powerful capability to analyse body composition. Pecoraro et al. (2003) have shown that BIA is more accurate than body mass index in measuring percentage of fat mass. And this method has shown its superiority over the tricep skinfold thickness approach as well (Pecoraro et al., 2003). However, large dispersion among subjects is still an issue for researchers. Further refinement of BIA method is very much desirable for individual body composition estimation.

Body Water Distribution

How to improve the precision of BIA is the issue in recent research. It has been suggested that the one cylinder with a uniform cross-sectional area assumption about the geometrical shape of the human body causes a large error. The trunk has large cross-sectional area and short length. Therefore, according to $Z = \rho L/A$, the impedance of the trunk is quite small compared to the limbs, which contributes just 10% of whole body impedance but is as much as 50% of whole body mass (Kyle et al., 2004a). Thus the whole body impedance change is influenced largely by the changes of FFM or the body cell mass (BCM) in the limbs to this extent. Hence, segmental BIA is based on another hypothesis that human body consists five cylinders (arms, legs, trunk) (Cornish et al., 1999). The segmental BIA has shown its advantage in diagnosing diseases with fluid distribution, such as determining fluid volume in liver disease (Schloerb et al., 1996). Liver disease is often characterized by an accumulation of excess body water as ascites, oedema, or both. The ratio of reactance to resistance also has been used to distinguish healthy subjects from critically ill patients (Woodrow et al., 1996). A number of research groups have showed that tetrapolar (hand-foot) BIA is not a suitable method for nutrition evaluation in cirrhotic patients with ascites (Cabre et al., 1995; Zillikens et al., 1992). Therefore, using BIA as an approach to detect body fluid is still a challenge for physicians.

Malnutrition is a prognostic feature in several chronic diseases or the complications in dialysis patients. Modern nutrition includes macronutrients and micronutrients. Water, energy, proteins, carbohydrates, and lipids are the examples of macronutrients, while vitamins, minerals and other organic nutrients are included in micronutrients (Berdanier, 1994; Berdanier, 2000). Pencharz et al. (1996) conducted a pioneering determination on the body changes during malnutrition by BIA. BCM, ECW, and TBW were investigated. The segmental BIA has improved the assessment of BCM in malnourished and acromegaly patients. But this method does not show any improvement in assessing BCM in patients with severe fluid overload or acute fluid changes (Pirlich et al., 2003). Moreover, Mushnick et al.

(2003) reported the phase angle is a strong index to show the survival in peritoneal dialysis patients than reactance and serum prealbumin is directly related to phase angle.

EIT

Electrical impedance tomography (EIT) is a new application of BIA. It is a safe and simple diagnosing approach. EIT has a high potential for significant correlation between electrical impedances of biological tissues and their physiological states (Cherepenin et al., 2002). It estimates the resistivity distribution inside a medium from boundary measurement (Hua et al., 1993). The measured stimulating voltage is reconstructed to provide anatomic and functional images. Cherepenin et al. (2002) investigated the state of mammary glands among women with different hormonal status through EIT. It has been found that EIT can be used to detect and localise tumors, especially malignant tumors of the mammary gland. However, the spatial resolution provided by this method is still very low. It is a major barrier of this new technique. The imaging reconstruction technique needs to be improved.

2.7.2 Impedance Analysis on Plants

Impedance characterization of plants is mainly based on the electrical impedance spectroscopy method. This method is widely employed in several biological tissues studies, for instance, apples, persimmons, nectarines, plant leaves and scots pine shoots. This section provides review on impedance investigations on plants.

Apples & Tomatoes

Impedance measurements were carried on apples and tomatoes by Varlan et al. (1996). It has been found that as low-frequency resistance increased, constant phase angle increased, characteristic frequency decreased, and high-frequency resistance slightly increased in normal ripening process. Apart from these observed trends, fruit classification was considered to be very difficult using EIS, owing to the large individual parameter dispersion over the whole population. In contrast, tomato classifications were more promising, due to the thinner skin and juicier flesh (Varlan et al., 1996). The variations of impedance parameters confirmed the tendencies observed from apple measurements. Green colour and red colour tomatoes were delimited well by the low frequency resistance and the constant phase angle. The Hayden Model was used to interpret data. It was observed that signal mainly comes from peel with the increase in low frequency resistance. In addition, skin extracellular resistance increases with

ripening, and cell uniformity also increases in ripening (Varlan et al., 1995; Varlan et al., 1996).

Nectarines

Impedance measurements were used to characterize changes between extracellular and intracellular resistance during cool storage and normal fruit ripening in nectarines (Harker et al., 1994a; Harker et al., 1994b). It is demonstrated that tissue resistance at 50 Hz has strong linear correlations with fruit texture, which is assessed by flesh firmness. The low frequency resistance was also closely related to the apparent juice content. Electrical models allow analysis performed at the cellular level. Nectarine fruit tissues conform to the double-shell model. The magnitude of tissue block impedance was greater than the whole fruit, which indicates that each mini-circuit inside whole tissue connects in parallel, and that the current travels indirectly between two electrodes (Harker et al., 1994a; Harker et al., 1994b). Low frequency resistance of nectarine increased with the time stored in cool condition, and decreased during normal ripening. A similar change pattern has been observed from the previous peach study (Furmanski et al., 1979).

Persimmons & Kiwifruit

Electrical impedance spectroscopy has been applied in persimmons (Harker et al., 1997). The arc represented in the Nyquist Plot displayed a semicircular shape. They dilated gradually for the first 21 days, but contracted with further ripening. Resistance at 50 Hz in this study reflects the electrical properties of extracellular space, and resistance at 300 kHz reflects the properties of all tissue compartments (Harker et al., 1997). In addition, the double-shell model fits data very well compared with the Hayden model and the model proposed by Zhang et al. (1990). Cytoplasm resistance of persimmon fruit was significantly lower when undergoing chilling conditions, but it showed a rapid increasing trend when fruits were transferred to room temperature for ripening (Harker et al., 1997).

Impedance investigation on kiwifruit did not indicate good relationships between impedance changes and physiological events (Bauchot et al., 2000). There was little change in the impedance characteristics of the fruit during ripening, although firmness decreased by 10-fold. Apoplast resistance and total tissue resistance varied from one year to the other. It is suggested that the mobility of electrolytes inside the cell wall did not change during kiwifruit ripening through electrolyte leakage analysis. The physicochemical interactions taking place within the cell wall may have a major impact on the tissue impedance (Bauchot et al., 2000).

Woody Plants

The impedance spectra of fruit, vegetable and plant leaves contain a typical single semicircular circle with its centre depressed below the x-axis (Repo, 2004; Varlan et al., 1996; Zhang et al., 1993). However, the shapes of impedance spectra of woody samples vary. For instance, the spectrum function of shoots and wood of the Scot pine is composed of two arcs, whilst the spectrum for the bark has only one arc, which shows a strongly depressed centre (Repo, 1994). The three organs of Scot pine have different characteristics, it is suggested different models should be applied to them.

2.7.3 Impedance Measurements on Food Quality Assessment

The value of electrical impedance analysis depends on being able to relate the electrical impedance correctly to physical or physiological properties of the observed sample (Zhang et al., 1990). Various environmental factors such as temperature and humidity will strongly affect the physiological status of fruits and vegetables. It has been demonstrated that impedance measurement is capable of reflecting rapid changes when the objective has any physical damage, such as that caused by chilling and bruising. Furthermore, impedance observations can be connected to the physiological changes of food. This section reviews the relevant applications of impedance measurement to food quality assessment.

Bruising Damage

Bruising can be caused anywhere during harvest, transportation and uploading. It is defined as damage to plant tissue by external forces which results in physical changes in texture and/or eventual chemical alteration of colour and flavour (Cox et al., 1993). It is not only a cosmetic problem, but also it alters the functioning of plant cells (Labavitch et al., 1998). Cell wall-digesting enzymes are free to digest the complex molecules of the cell wall when they are outside of the plasmalemma. As a result, the cell wall is weakened and fruit becomes soft. Bruising can lead to uncontrolled action of cell wall-digesting enzymes, so that the quality can be largely affected (Labavitch et al., 1998).

There are a few indirect methods to assess the bruising in agricultural products, such as X-ray and gamma ray transmission (Cox et al., 1993), nuclear clear magnetic resonance (Gunasekaran, 2001), and electrical impedance characteristics (Cox et al., 1993; Jackson et al.,

2000; Vozary et al., 1999). Impedance measurement provides a rapid method to detect the internal bruising of fruit without waiting for tissue browning as evidence of this. The magnitude of bruised tissue impedance is significantly lower than normal tissue, and the impedance spectra of bruised tissue displays two or more overlapped peaks compared with a single peak in the unbruised tissue. Therefore, a bruised index is defined according to these phenomena (Cox et al., 1993). Jackson et al.(2000) found that the impedance difference before and after bruising at 50 Hz has good correlation with bruise weight. All the measurements and the calculations of the volume fraction of intact cells were significantly affected by cultivar. It is further found that the ratio of the extracellular resistance to the intracellular resistance has been reported to depend on the degree of the bruise only (Vozary et al., 1999).

Chilling Damage

Chilling damage is primarily a disorder of crops of tropical and subtropical origin. The injured fruit becomes dry, mealy, woolly, or like leather. There is flesh or pit cavity browning and flesh bleeding or internal reddening (Lurie et al., 2005). Flesh tissue separation and cavity formation are accompanied with the advanced stage of chilling damage. These symptoms are frequently observed from peach cultivars (Lurie et al., 2005). Chilling damage manifests in increased ion leakage (Saltveit, 2002), and rigidified cell wall (Fukushima et al., 1978). Therefore, chilling damage limits the marketing and consumption of agricultural products.

Low frequency resistance exhibits a clear decreasing for tomato due to solute leakage cause by injury (Varlan et al., 1996). Resistance of cytoplasm is the only parameter tends to significantly lower in chilling damaged persimmons in one out of the five components of the double-shell model (Harker et al., 1997). But it increases rapidly when fruit is transferred to room temperature for ripening. The cytoplasm resistance follows the same trend in nectarines with that of in persimmons. However, there is a further reduction when fruit is removed from cool storage (Harker et al., 1994a).

Other Applications

Electrical impedance spectroscopy challenges traditional sensory method, bacteriological assessment and the relevant chemical component analysis to determine fish freshness (Niu et al., 2000). It was reported that the phase angle change with frequency is dependent on the storage time after kill. Rapid liquefaction of fish tissue due to deterioration increases the conductivity (Niu et al., 2000). Therefore, impedance can also be employed as an indicator of

freshness. Moreover, it is referred changes in impedance have been used as indicators of shrimp freshness (Marshall et al., 1997).

Apart from the application on seafood products, the impedance method has also been tried for meat quality assessment (Freywald et al., 1995). Freywald et al. (1995) introduced a parameter $\boldsymbol{P}_y$, defined as the relationship between the conductivity of the extracellular and the intracellular pathway, should be in good agreement with the quality of fresh meat.

Electrical impedance is sensitive towards physiological changes derived from the physical events. The extracted impedance parameters such as phase angle, phase angle shift, low-frequency resistance and the cytoplasm resistance etc. reflect food quality changes to some extent. However, there are still some physiological changes which cannot be fully explained by their electrical behaviours. For instance, the explanation for the failure to observe any impedance difference in kiwifruit could have been based on the investigators' faulty hypothesis. The available literature lacks information about the electrical properties of food and their chemical compositions. Therefore, the following chapters attempt to determine the parameters of electrical model of food products and to explore any potential correlations between impedance parameters and food quality determination criteria. The experiments were carried on different fruit and vegetable cultivars - apples, bananas and cucumbers respectively.

Chapter 3 Application of EIS for Evaluation of Apple Quality

3.1 Introduction

An apple a day to keep the doctor away.

Apple is a common fruit variety, its moisture content is more than 80% of the fruit weight. It is a rich source of fibre. One medium apple contains 5 grams of fibre (Johnson, 2004). New research has shown the apple is one of the fruits containing rich antioxidants. Antioxidants are the substances found in food that are capable of preventing chronic and degenerative diseases (Wu et al., 2004). Moreover, it has been shown that apple juice may prevent oxidative stress and impaired cognitive performance (Rogers et al., 2003). Marchand et al. (2000) show that the apple, together with onion and white grapefruit, are important dietary sources of quercetin, which has a significant inverse association with the risk of lung cancer.

As a general statement that a high intake of apples can help strengthen the immune system of the human body against many diseases including cancer, heart disease, Alzheimer's and Parkinson's diseases (Wu et al., 2004). Many people do not include a high level of fruit in their diet. The World Health Organization and Food and Agriculture Organization of the United Nations stated that the overall daily consumption of fruits and vegetables is 100 g below the recommended intake level (WHO/FAO, 2003).

In choosing to eat fruit, people do not place the health benefit as a major factor. Taste, aroma, and freshness are ranked as the top three criteria from consumers' perceptions as the factors which attract consumers to purchase fruit (Peneau et al., 2006). According to the conventional quality assessment method introduced in Chapter 1, the taste test mainly relies on the use of a human test panel. Flavour quantification is still a complicated problem.

Electrical Impedance Spectroscopy (EIS) has been used extensively to characterize electrical properties of plant tissue. This research explores the potential connections between impedance and any parameters can contribute to fruit taste. If fruit quality can be described as a predictable function, then the relationship can be treated as a new quality specification criterion.

3.2 Methodology

3.2.1 Material

Four popular apple varieties sold in Australian market are that of the Granny Smith (GS), Fuji (FJ), Pink Lady (PL), and Red Delicious (RD) were used in the experiment. Granny Smiths were first grown in Australia. They are accepted as extremely tart, crisp, juicy and versatile features. Fuji is a super sweet and low acid apple. Pink Lady is a variety with firm, crisp flesh and a unique sweet-tart flavour. Red Delicious is considered as a mildly sweet apple without a distinguishable tartness. The quality of each apple was set as the similar grade based on visual assessment. Fresh apples were kept at a room temperature of 20℃, and all the experiments were carried out at the room temperature. Apples weighing approximately 205 grams were chosen in experiments. There were six samples for each variety. The weight of each apple was recorded with a digital scale with a 0.01g graduation.

3.2.2 Experimental Setup

The experiments consisted of three sub-experiments, the electrical impedance measurement, the soluble solids measurement and the titratable acidity measurement.

3.2.2.1 Electrical Impedance Measurement for Apples

Impedance measurement was carried out using a Solartron 1260A Impedance/Gain-Phase Analyzer (Solartron Analytical, England, UK). The impedance analyser employed here uses digital correlation techniques for measurement in the frequency range of 10 μHz to 32 MHz. The basic accuracy is 0.1% for magnitude and 0.1° for phase measurements. This instrument allows both the two-terminal and four-terminal measurements. The combination of the impedance analyser and the Solartron 1294 Impedance Interface offers high accuracy, repeatability and versatility, has been extensively used for bio-impedance measurements on live subjects, electro-analytical systems, characterization of thin films and coatings, biotechnology research and food freshness investigations etc. (Bao et al., 1992; Hinton et al., 1998; Jorcin et al., 2006). The 1294 impedance interface makes use of a driven shield technique to minimise the measurement error introduced by input and cable capacitance that especially takes place at high frequency. Furthermore, a balanced generator is used to reduce the error caused by electrode impedance (Hinton et al., 1998).

The impedance measurements used a 100 mV generator voltage and scanned 91 spot frequencies between 1 Hz and 1 MHz. A four-electrode measurement method was used. Two tin-plated copper cylindrical electrodes with diameter of 0.7 mm and length of 12 mm were inserted into apple flesh symmetrically along the radial direction as shown in Figure 3-1. The AC signal was injected into the sample through two current stimulus terminals from the 1294 impedance interface (GenHi and GenLo), and the voltage measurement was achieved from another pair of terminals from the interface (VHi and VLo). Magnitude and phase angle were measured directly from the readings, while resistance and reactance were computed according to the Eq. 2-7 (Chapter 2). All the experiments were performed inside a Faraday cage to isolate samples from the electrical noise particularly the line frequency of 50 Hz.

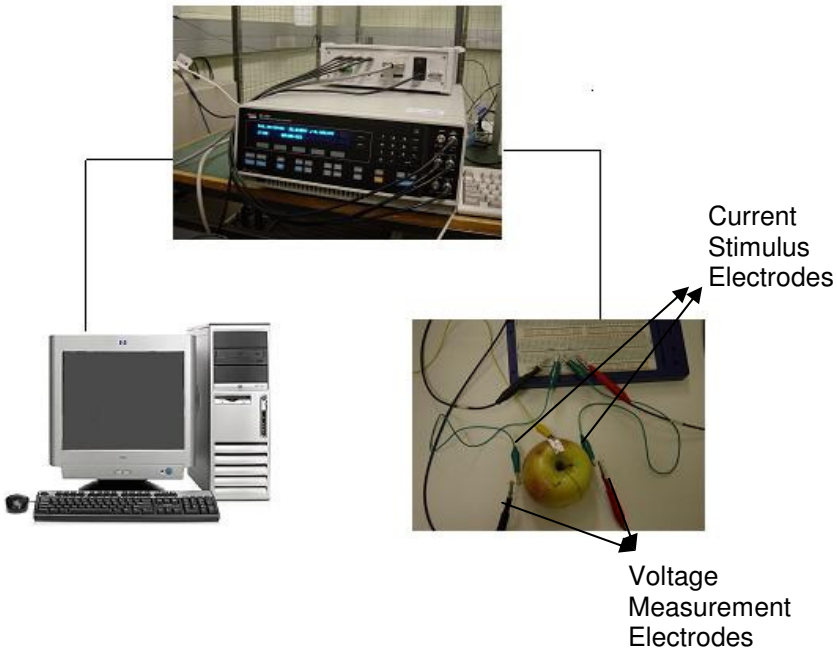

Figure 3-1 Electrical impedance measurement setup.
A four-electrode measurement method was used.

3.2.2.2 Soluble Solid Measurement

Fruit flavour is fundamentally the balance between sugar and acid (Whiting, 1970). Sugar content increases steadily as apples mature. Apple soluble solids, a factor highly correlated with sugar content, is an important tasting quality feature which indicates apple sweetness.

Each apple was used to extract fruit juice right after the electrical impedance measurement. $^{0}Brix$ was measured by a hand held 0-32% Brix refractometer. Brix scale is a hydrometer scale for measuring the concentration of sugar content of a solution at a given temperature. A few drops of juice were placed on top of the prism assembly, and data were read from the graduations. The snapshot of the experiment setup is shown in Figure 3-2.

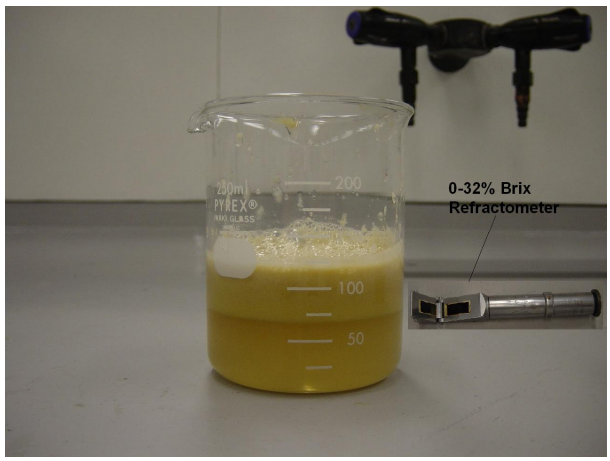

Figure 3-2 Snapshot of soluble solid content measurement

3.2.2.3 Titratable Acidity Measurement

The titration measurement is used to determine the acid of a solution. Sample of fruit juice takes reaction with alkaline solution such as sodium hydroxide (NaOH). The total volume of titrated NaOH is recorded when the pH value of the mixed solutions reaches an endpoint of 8.1~8.3 (Greco et al., 2002). The acid percentage can then be calculated.

Sample Preparation

It is well known that the sugar level of fruit decreases from the stem-end to the calyx-end. Hence, apples were cut into longitudinal slices. Then apple slices were put into a blender to extract juice. Fruit juice was centrifuged at 3000 rpm for 3 minutes, and filtered through filter paper to get clear juice. The experiments were conducted at a constant temperature of 21ºC, as pH meter calibration and titratable acidity measurement are subject to temperature variation.

Titration Procedure

The schematic of experiment setup for titration is shown in Figure 3-3.

- The pH value was measured by a Metrohm 744 pH meter (Metrohm, Switzerland)
- 6 grams of clean juice was put into a 100 mls beaker, and 50 mls of distilled water was added
- The buret was rinsed with 0.0978M NaOH twice, and the microburet was filled to the 0.00 ml mark with the solution

- A magnetic capsule and a magnetic stirrer were used to fully mix the solution in the beaker
- The pH value of the solution was measured, the reading was recorded
- Three drops phenolphthalein indicator were added to the beaker as a reference, and pH changes were monitored for titratable acidity
- The sample was titrated with 0.0978M NaOH to an end point pH value of 8.2, and repeated two or three times to ensure the calculated acid percentages are within 1% relative average deviation for each sample. The mean value is used in data analysis.

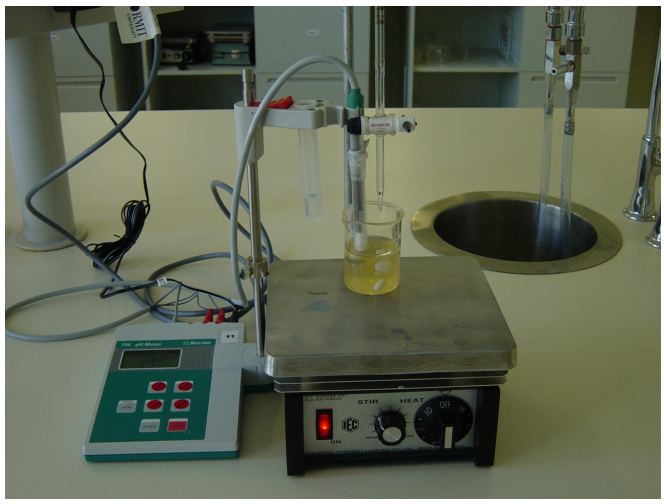

Figure 3-3 Schematic of experiment setup for titration

3.3 Results

3.3.1 Results from Instrumental and Chemical Measurements

The titratable acidity percentage is calculated by the following formula (Garner et al., 2005):

$$\%\ \text{acid} = \frac{[\boldsymbol{mls\_NaOH\_used}]\times[0.0978\boldsymbol{M\_NaOH}]\times[\boldsymbol{milliequivalent\_factor}]\times 100}{\boldsymbol{grams\_of\_sample}}$$

Eq. 3-1

Table 3-1 displays the milliequivalent factors of common fruit acids. As malic acid is the predominant acid in apple fruit, then the malic acid percentage is computed by

$$\%\ \text{malic acid} = \frac{[\boldsymbol{mls\_NaOH\_used}]\times[0.0978\boldsymbol{M\_NaOH}]\times 0.067\times 100}{\boldsymbol{grams\_of\_sample}} \qquad \text{Eq. 3-2}$$

Table 3-1 Milliequivalent factors of common fruit acids (Garner et al., 2005)

Commodity	Predominant Acid	Milliequivalent Factor
Stone fruit, apples, kiwifruit	Malic Acid	0.067
Citrus	Citric Acid	0.064
Grapes	Tartaric Acid	0.075

Objective taste predictors such as the ${}^{0}Brix$, Titratable Acidity (TA), ${}^{0}Brix$/TA ratio, and the physical parameters that of pH value, as well as the mass of the four apple varieties are displayed in Table 3-2. The results are expressed as mean versus CV%. CV stands for the coefficient of variation, which is a relative measure of dispersion. CV is calculated as the following equation:

$$\text{CV}= 100\times\left(\frac{\boldsymbol{s}}{\bar{\boldsymbol{x}}}\right) \qquad \text{Eq. 3-3}$$

where s is the standard deviation (SD), and $\bar{\boldsymbol{x}}$ is the mean value

Table 3-2 Summary of chemical and physical parameters among four apple varieties

Variety	${}^{0}Brix\,(\%)$ Mean/CV(%)	TA(%) Mean/CV(%)	${}^{0}Brix$/TA Mean/CV(%)	pH value Mean/CV(%)	Mass(gram) Mean/CV(%)
Granny Smith (GS)	11.25/11.50	0.65/20.77	18.14/29.90	3.51/2.52	182.01/13.90
Fuji (FJ)	13.30/6.98	0.27/14.2	50.88/18.30	4.16/2.75	206.07/11.19
Red Delicious (RD)	12.67/23.77	0.23/8.58	56.47/25.54	4.14/2.50	204.89/3.13
Pink Lady (PL)	15.75/9.99	0.47/25.13	34.77/19.66	3.75/3.61	205.30/12.58

It can be seen from Table 3-2, the ${}^0Brix$, TA, ${}^0Brix$/TA and pH values vary among different varieties. The GS has the highest malic acid percentage average value of 0.65% among the four varieties, followed by the PL of 0.47%, the FJ of 0.27%, and the RD of 0.23%. Their acid percentage values are statistically significant ($p<0.05$). Good relationships have been found between the ratio of ${}^0Brix$ to TA and fruit maturity, palatability, and consumer acceptability (Fellers, 1991; Harker et al., 2002a). It was found that the four apple cultivars cannot be classified on the basis of their soluble solid content. However, the four apple cultivars can be divided into three groups according to the ratio of ${}^0Brix$ to TA ($p<0.05$), namely low-acid variety (FJ, RD), high-acid variety (GS) and medium-acid variety (PL). The GS has the lowest value of 18.14, which corresponds to its strong tart taste. The FJ and RD have higher ratios amongst the four varieties. They can be divided into the same group ($p=0.444$), due to both of them being very sweet apple cultivars. The ratio of the PL is 34.77, which is between low-acid variety and high-acid variety. The pH values for the four varieties also follow the same tendency: pH values of the RD and the FJ do not differ very much ($p=0.857$), whilst the pH values of the three apple groups are significantly different ($p<0.05$).

3.3.2 Results from Electrical Impedance Measurement

Resistance and reactance were calculated from the measured impedance and phase angle. Resistance and the absolute value of reactance were plotted in the Nyquist Plot (Figure 3-4). It is apparent that the curve displays a semicircular arc with its centre below X-axis. Data used in this figure is generated from a sample of the PL. It is observed that the curved shape of all the other three apple varieties are consistent with the one found in the PL. There is a tail at low frequencies (112.2 Hz in Figure 3-4), due to the electrode polarization. The details of parameters which determine the semicircle are summarised in Table 3-3. Z-view software was used to perform curve fitting. The fitted curve can be determined by five parameters, namely resistance at zero frequency ($\boldsymbol{R_H}$), resistance at infinite frequency ($\boldsymbol{R_L}$), diameter of impedance arc ($\boldsymbol{D}$), characteristic frequency ($\boldsymbol{f_c}$) and transitional frequency ($\boldsymbol{f_o}$). The diameter of impedance arc is the distance between the maximum reactance and the circle centre. $\boldsymbol{R_H}$ and $\boldsymbol{R_L}$ are calculated by the extrapolation method. As a result, $\boldsymbol{R_H}$ is the low intersection of the semicircle with X-axis, and $\boldsymbol{R_L}$ is the high intersection. $\boldsymbol{D}$ is the distance between the maximum reactance and the circle centre. $\boldsymbol{f_c}$ corresponds to the maximum

reactance frequency. f_o is the frequency where the electrode polarization occurs. AVE is the average value, STD is the standard deviation, CV is the coefficient of variation.

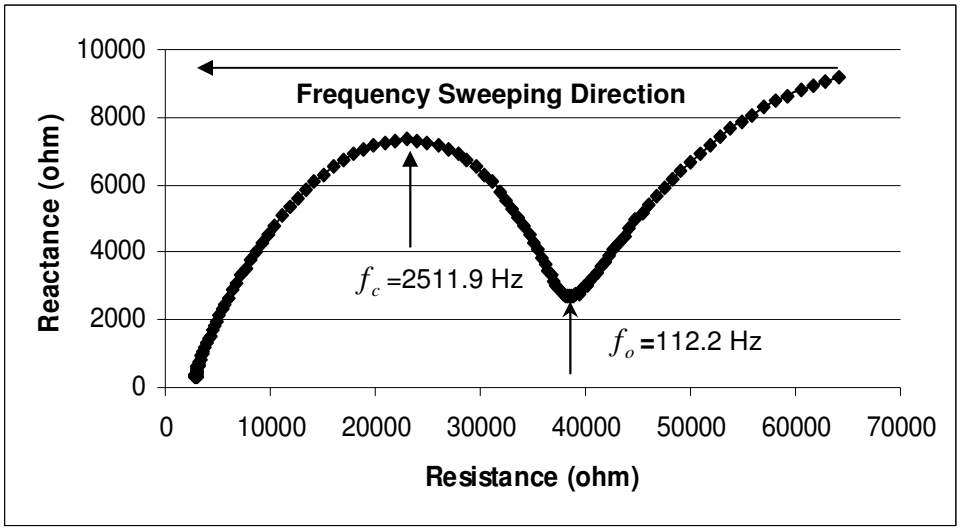

Figure 3-4 Nyquist Plot of the calculated resistance against reactance for one of the sample of Pink Lady. The sweeping frequency is from 1 Hz to 1 MHz. f_c is the characteristic frequency (maximum reactance frequency), f_o is the transitional frequency where EPI occurs.

Analysis of Variation (ANOVA) was used to observe the difference between the means of impedance arc diameter for the four apple varieties (Bethea et al., 1995). It was found that their impedance arc diameters are significant different ($p>0.05$). In other words, the three apple groups divided by the ratio of ${}^0Brix$ to TA cannot be observed from the diameters of impedance arc.

It can be seen from Table 3-3 that the transitional frequency varies among different varieties, but mainly distributes at frequencies below 1 kHz. This is of good agreement with the phenomenon introduced in the literatures (Ferris, 1974). Because the influence of Electrode Polarization Impedance (EPI) only plays a major role below 1 kHz for both resistance and reactance, it is suggested that the influence of EPI can be deemed negligible while frequency exceeds 1 kHz. As a result, data measured over frequency range between 1 kHz and 1 MHz were used for the following analysis.

Table 3-3 Summary of the Nyquist Plot parameters for the four apple varieties

Variety	No.	R_H (ohm)	R_L (ohm)	D (ohm)	f_c (Hz)	f_o (Hz)
FJ	1	2578.9	31836	29976	2511.9	112.2
	2	2401.3	24652	23738	2818.4	112.2
	3	2135.9	26808	26381	2818.4	125.89
	4	2274.5	28347	26242	2818.4	125.89
	5	2010.4	28940	28810	2511.9	125.89
	6	2072.2	27076	26013	2511.9	112.2
	AVE	2245.53	27943.2	26860	2665.15	119.05
	STD	216.14	2415.92	2217.55	167.88	7.50
	CV	9.63	8.65	8.26	6.30	6.30
GS	1	1753.8	26714	26389	2818.4	125.89
	2	1897.4	21127	20685	3548.1	158.49
	3	2338.8	24420	23503	3548.1	158.49
	4	2234.6	25198	25892	2818.4	125.89
	5	1957.5	21059	21179	3162.3	141.25
	6	1844	24807	24683	3548.1	141.25
	AVE	2004.35	23887.50	23721.83	3240.57	141.88
	STD	231.08	2300.27	2386.78	359.53	14.59
	CV	11.53	9.63	10.06	11.09	10.28
PL	1	3950.3	37300	35699	2818.4	112.2
	2	3972.2	42014	41066	2511.9	112.2
	3	3403.4	37998	37363	2511.9	112.2
	4	3088.1	41622	42950	2238.7	125.89
	5	3259.9	34968	34578	2511.9	112.2
	6	3343.3	35987	35508	2511.9	125.89
	AVE	3502.87	38314.80	37860.70	2517.45	116.76
	STD	370.65	2911.07	3388.42	183.519	7.07
	CV	10.58	7.60	8.95	7.29	6.05
RD	1	2611.2	37267	37362	2238.7	112.2
	2	2578	35232	35725	2818.4	112.2
	3	2562.4	36357	38446	2818.4	112.2
	4	3195.4	44815	43155	2238.7	112.2
	5	3068.8	45143	44719	2395.3	125.89
	6	2876.8	37538	46003	2818.4	125.89
	AVE	2815.43	39392.00	40901.67	2554.65	116.76
	STD	273.66	4403.47	4266.86	294.53	7.07
	CV	9.72	11.18	10.43	11.53	6.05

R_H is the high-frequency resistance, R_L is the low-frequency resistance, D is the diameter of the semicircle in the Nyquist Plot, f_c is the maximum reactance frequency (characteristic frequency), f_o is the transitional frequency where the electrode polarization occurs. AVE is the average value, STD is the standard deviation, CV is the coefficient of variation.

3.3.3 Comparison of Impedance Measurement and Laboratory Measurement

In order to detect any potential association between impedance and other measured parameters, the data were first analysed using the Best Subsets Regression (BSR) by MINITAB 14. BSR is a method used to identify which predictor variables should be included in multiple regression models. The adjusted R_square (Adj. $\boldsymbol{R}^2$) together with the standard deviation (s) are the main criteria when determining which model is the best. Additionally, C-p is the measure of the difference of a fitted regression model from a true model; p is the number of independent variables. The C-p value for the best model should equal to p+1 or less. An example is given here to illustrate how to choose the suitable parameters. Data are from the RD.

Best Subsets Regression: impedance_300k versus Brix, TA, pH, ratio

```
Response is impedance_300k

                                                    r
                                                B   a
                                                r   t
                                 Mallows        i T p i
Vars  R-Sq  R-Sq(adj)      C-p         S        x A H o
   1  66.6       58.2      0.1  555.32        X
   1  65.2       56.4      0.2  566.94              X
   2  70.4       50.7      1.8  603.34        X X
   2  70.4       50.7      1.8  603.46        X   X
   3  81.1       52.7      3.2  590.73        X X   X
   3  71.0       27.5      3.8  731.38        X X X
   4  84.0       19.8      5.0  769.28        X X X X
```

Each model appears on a different line in the output. Vars is the number of predictor variables used in the model. The R_square ($\boldsymbol{R}^2$), adjusted R_square (Adj. $\boldsymbol{R}^2$), C-p and s are displayed in the above Best Subsets Regression output. We look for the model gives the highest Adj. $\boldsymbol{R}^2$, taking the standard deviation (S) into account. In this example, the model with one predictor of Brix has the highest Adj. $\boldsymbol{R}^2$ value (58.2) and the lowest S value (555.32). In addition, we look at C-p value. When a regression model with p independent variables contains only random differences from a true model, the average value of C-p is (p+1), where p is the number of parameters. As a result, the goal is to find a model with a C-p of (p+1) or less. Accordingly, the model with one predictor of Brix has the value of C-p (0.1) which is less than 2. As a result, the model with $^0\boldsymbol{Brix}$ only is the best model. The adding of other predictors does not improve the fit of the model. Similar procedures were performed on other apple varieties to reduce the number of variables. As a result, $^0 Brix$ was chosen as the best predictor variable for the RD

and FJ. Malic acid percentage was the best predictor for the GS. Whilst, both $^{0}Brix$ and malic acid percentage was suitable for the PL variety. Impedance Square Root (ISR) was used instead of impedance (Z) itself when the standard error of the estimated was taken into account. The chosen predictor variables were used for multiple regression afterwards.

Multiple regression was used to detect correlations between ISR and the corresponding predictors. MATLAB software was used to scan the frequency range from 1 kHz to 1 MHz to select the best frequency that represents the relationship between ISR and the biochemical parameters based on the smallest CD value. Table 3-4 shows the equations generated by the applied regression. For the GS, a strong correlation between ISR and its malic acid percent in juice takes place at 224 kHz, p_value is 0.011. FJ's good correlation between its ISR and sugar concentration in juice is detected at 1 kHz, p_value is 0.034. The relationship between the ISR and sugar content for the RD is detected at 1 MHz, p_value is 0.004. 224 kHz is the best frequency represents the relationship between the ISR of PL and the corresponding sugar concentration and malic acid percent, p_value is 0.001. The relationships between ISR and other predictor variables are illustrated in Figure 3-5.

Table 3-4 Correlations between impedance square root and chemical compositions of fruit juice at the selected frequencies. Frequencies were chosen based on the smallest R^2 value.

Variety	Frequency (Hz)	Equation	R^2*	SEE*
GS	224 k	$\sqrt{Z} = 74.7 - 38.2 \times TA$	0.8361	2.55
FJ	1 k	$\sqrt{Z} = 77.6 + 5.46 \times Brix$	0.7129	3.61
RD	1 M	$\sqrt{Z} = -0.62 + 4.2 \times Brix$	0.8962	4.82
PL	224 k	$\sqrt{\boldsymbol{Z}} = 100 + 3.71 \times \boldsymbol{Brix} + 2.79 \times \boldsymbol{TA}$	0.9926	0.62

* R^2 - coefficient of determination, SEE- standard error of the estimate

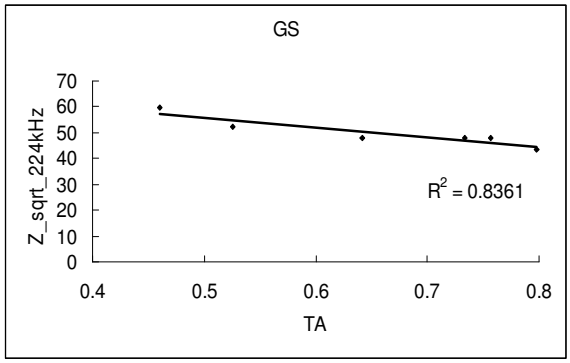

(A) Linear correlation between impedance and titratable acidity of the GS at 224 kHz

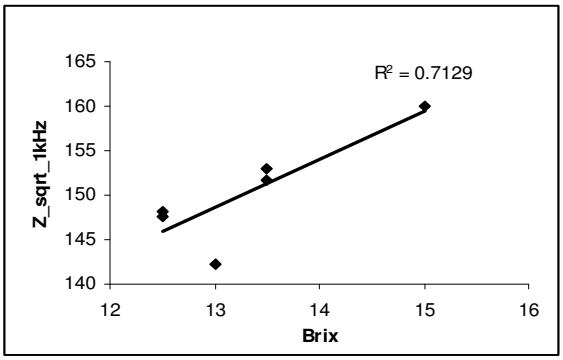

(B) Linear correlation between impedance and Brix of the FJ at 1 kHz

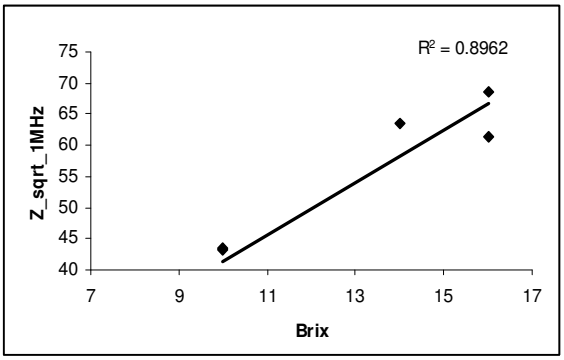

(C) Linear correlation between impedance and Brix of the RD at 1 MHz

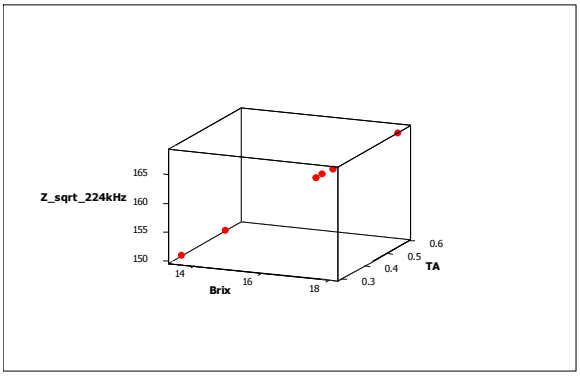

(D) Correlations amongst impedance, $^{0}Brix$, and titratable acidity of the PL at 224 kHz

Figure 3-5 Correlations between impedance and chemical compositions for four varieties

pH is a measure of the activity of hydrogen ion in a solution. It has been known that the electrical conductivity of a solution has correlation with its hydrogen ion concentration. However, pH does not show any correlation with fruit impedance in this study and the adding of pH does not improve data fitting. Moreover, the ratio of ${}^{0}Brix$ to acid percentage which is suggested as a good indicator of fruit taste does not correlate with impedance.

3.4 Discussion & Conclusion

Electrical impedance measurement and chemical composition analysis have been conducted on four apple varieties. It is noticed that the four varieties can be divided into three groups by the ratio of soluble solid content to malic acid percentage. The three groups can also be exhibited from the correlations between impedance and soluble solid content and/or acid percent. Soluble solid content correlates with impedance for low-acid variety (FJ & RD), titratable acidity has linear relationship with impedance for high-acid variety (GS), and both soluble solid content and acid percent contribute to the linear association with impedance for medium-acid variety (PL).

Hotelling's transformation was used to transform the correlation coefficients for the analysis of variance (Hotelling 1953). By using this transformation, it can be observed how close the ISR correlates with the different biochemical measurements. The details of the transformation are presented in the following formulas (Harker et al., 2002b).

$$z^* = z - \frac{(3z + r)}{4(n - 1)} \qquad \text{Eq. 3-4}$$

where

$$z = \log\left(\frac{1 + r}{1 - r}\right) \qquad \text{Eq. 3-5}$$

r is the coefficient of correlation. n is the number of sample for each apple variety, n equals to 6 in this example. Analysis of variance was conducted on the value of z*, which was defined as "degree of association" by Harker et al (2002a; 2002b). Electrical impedance measurement is able to precisely correlate with the biochemical responses if they have higher degree of

association. It can be seen from Table 3-5 that the degree of association depends on frequencies. However, impedance does show the correlations with biochemical predictors at various presented frequencies for different variety. For example, ºBrix is the best predictor connected to impedance for the RD, TA is a parameter which correlates to impedance very well for the GS.

Table 3-5 Differences in the degree of association between impedance and biochemical predictors

Variety	Frequency	Brix	TA	pH	Brix/TA
RD	1MHz	1.30	0.08	0.30	1.02
PL	224 kHz	2.25	1.18	0.96	0.87
GS	224 kHz	0.18	1.10	0.35	0.81
FJ	1kHz	0.87	0.24	0.40	0.50

Harker et al. (2002a) had performed experiments to investigate the relationship between objective and sensory measurements of apple taste and flavour. It has been found that TA is currently one of the best predictors of sensory attributes compared with acid taste, overall flavour, and apple flavour. Titration analysis is a relatively complex measurement procedure, and with a high temperature requirement. Thus, the determination of titratable acidity is mainly performed in a lab environment. In comparison, impedance measurement is a fast and portable approach can contribute to the acid taste measurement. According to the found correlations, it is deemed acid percentage has significant influence on these correlations. Acid percentage starts to be involved in the relationship with electrical impedance as its concentration increases. We suggest that the threshold value for TA is 0.47% to be linked to these relationships. Research has revealed that the eating quality acceptability of Golden Delicious should obtain the threshold value of 12 ºBrix for soluble solids content, and 3.2 g/l for acidity (Hoehn et al., 2003). ºBrix value should exceed 12 ºBrix for the acceptable consumption level for the Elstar apple (Hoehn et al., 2003). This principle may also be used in this research finding. Thus all the data relating to ºBrix and acidity may be replaced by the electrical impedance. It will make measurement easier and quicker.

In conclusion, electrical impedance method provides a new concept for apple quality assessment, focusing on distinguishing sweet tasting apples from sour tasting apples. The correlations between impedance and biochemical predictors depend on frequencies, different

varieties display their own characteristic frequencies. Impedance method can be used to replace soluble solids content and acidity measurements to quantify customers' requirements if the acceptable levels of Brix and TA from the observed varieties are given.

Chapter 4 Application of EIS for Evaluation of Banana Ripening

4.1 Introduction

Bananas are one of the most popular commercial fruits in the tropical and subtropical regions. Bananas are grown in more than 85 countries, and around 65 million tones per year is produced mainly in developing regions, such as Africa, Asia, the Caribbean and Latin America (Jackson, 2001). Not only do bananas bring commercial benefits for developing countries, but also they are consumed as a rich and cheap nutritional source of vitamin C, potassium and dietary fibre, etc. It has been reported that per 100 g banana, there is 11.6 mg of vitamin C, 178.8 mg of potassium, 90.3 mg of magnesium and 2.7 g of total dietary fibre (Lin, 1980).

Banana is an extremely perishable fruit, its post-harvest quality changes very quickly. Bananas start to ripen seven days after harvest and are fully ripe in two days if they are stored at room temperature (Mortan, 1987). The storage period of bananas is critical for retailers. Therefore, it is important to assess banana quality through an inexpensive and quick approach. Peel colour is considered a good indicator of banana ripeness as the chlorophyll content in the peel reduces with banana ripening (Li et al., 1997). However, this method is based on human visual determination. It can be imprecise and insufficient to assess the internal quality changes. In order to improve banana quality determination, this study analysed the electrical impedance spectra of samples from two banana varieties, and compared the difference in impedance changes during ripening.

4.2 Methodology

4.2.1 Material

Cavendish bananas (CBs) and Lady Finger bananas (LFBs), two of the most common banana varieties sold in Australia, were chosen for this study. Good quality bananas without visible bruises were purchased from the local market. Samples of each variety were obtained from the same bunch. The weights for the CBs and LFBs were 181 ± 11.26 grams and 154.86 ± 11.36 grams respectively. The ripeness of bananas was assessed by comparing the colour of the peel with the standard banana colour chart (Figure 4-1), which defines banana peel colour of 7 grades, namely: 1 is hard green, 2 is light green, 3 is more green than yellow, 4 is turning 50% green and 50% yellow, 5 is yellow with green tips, 6 is full yellow, 7 is yellow with black sugar spots (Jackson, 2001; Omoaka et al., 1997). Readings were recorded in 0.5 peel colour grade values. Bananas are ready to deliver to retailers at grade 3.5, bananas with grade 5 have firm texture, bananas with grade 6 are ready for eating, and grade 7 onwards mean fully ripe. Seven CBs with starting colour of 3.5 and seven LFBs with starting colour of 4 were kept at a room temperature of 18°C, and 55% relative humidity. The weight of each banana was recorded by a kitchen scale (1g graduation) over the course of the continuous seven days monitoring.

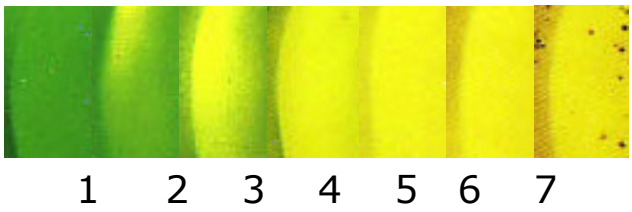

Figure 4-1 The standard colour chart of bananas (Jackson, 2001)

4.2.2 Electrical Impedance Measurement for Bananas

The impedance measurement setup for bananas is very similar to the one performed on the apple investigation. Impedance parameters were measured by a Solartron 1260A Impedance/Gain-phase Analyser™. Two tin-plated copper cylindrical electrodes with diameter of 0.7 mm and length of 12 mm were inserted into the flesh along the banana's

longitude direction. Magnitude and phase angle of impedance were measured at the frequency range of 1 Hz to 1 MHz. The impedance measurements were monitored once a day for seven days. All the experiments were carried out within the Faraday Cage to shield from the external noise, especially at the 50 Hz. The experiment setup is illustrated in Figure 4-2.

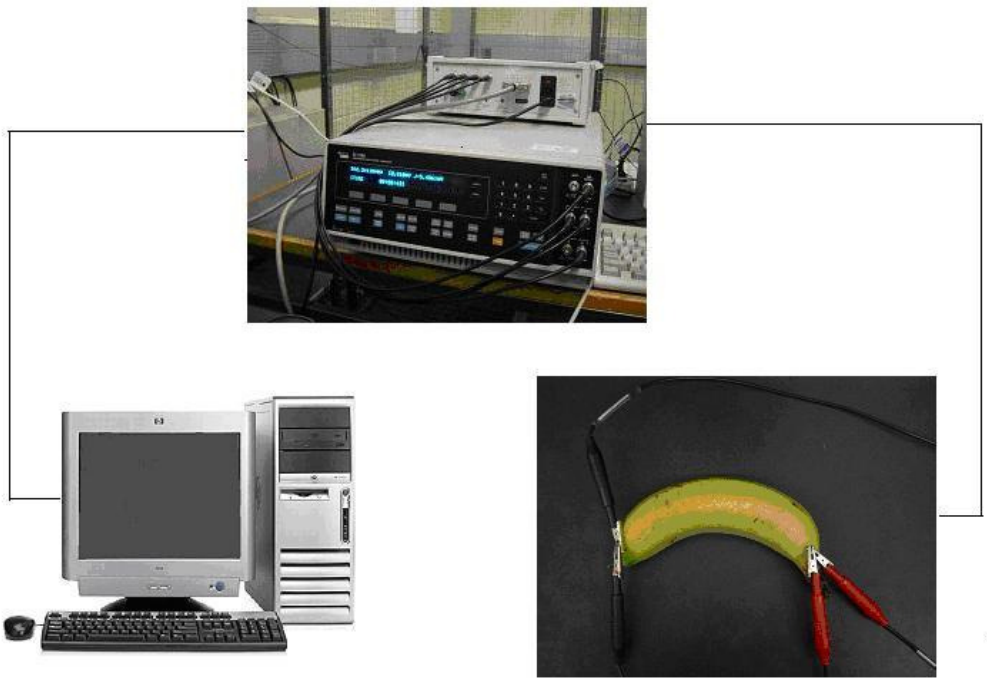

Figure 4-2 Experiment setup for impedance measurement of banana ripening investigation. A four-electrodes connection was used.

4.3 Results and Discussion

At the end of the seven days monitoring, the average weight loss percentages for each banana per day were 1.47% (CV=11.58%) for the CBs, and 2.25% (CV=2.37%) for the LFBs.

4.3.1 Analysis of Impedance Parameters

Resistance and reactance were calculated from the measured impedance and phase angle. Nyquist Plot of one sample each from the two banana varieties are illustrated in Figure 4-3. The Nyquist Plot of impedance parameters displays a semicircular arc with its centre below

the X-axis. The other bananas from the test groups have a consistent curve shape. The other samples also display the consistent curve shape.

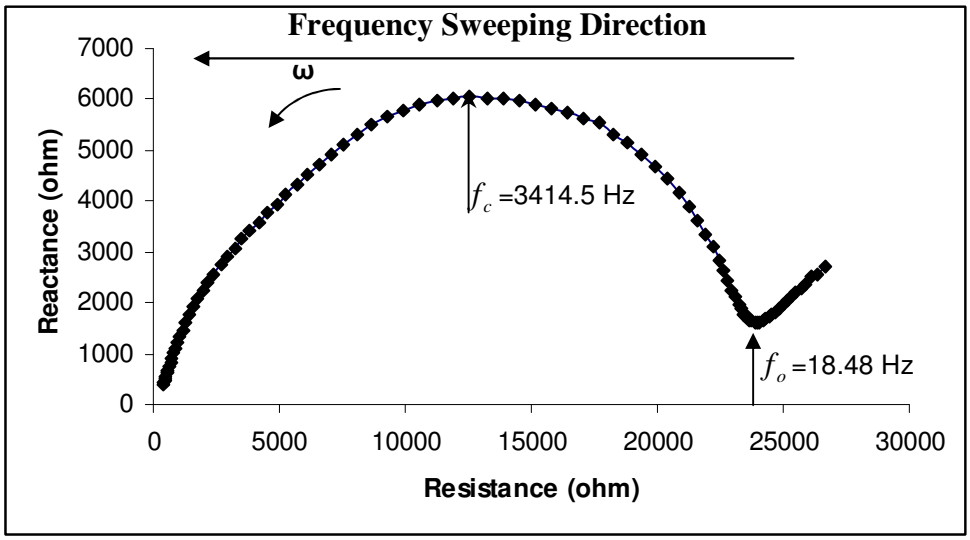

(a) Cavendish Banana

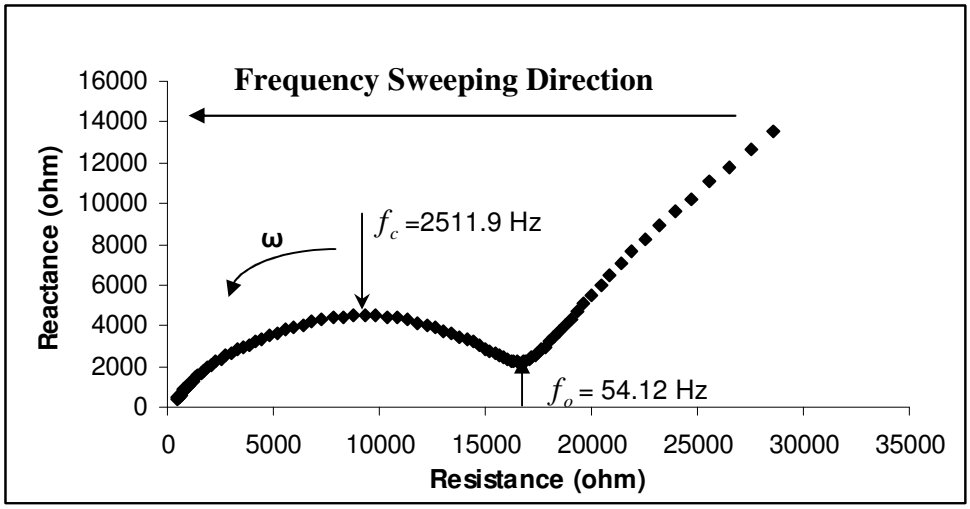

(b) Lady Finger Banana

Figure 4-3 Nyquist plot of one sample each from two banana varieties. The sweeping frequency is from 1 Hz to 1 MHz. f_c is the characteristic frequency (maximum reactance frequency), f_o is the transitional frequency where EPI occurs.

Z-view software (Scribner Associates Inc. 2005) was used to fit the semicircle mathematically. The fitted curve is determined by five parameters, namely resistance of low frequency, resistance of high frequency, impedance arc diameter, characteristics frequency and

transitional frequency. The contraction or expansion of the diameter indicates the decrease or increase in the electrical impedance of the sample. The details of the fitted curves for the two banana varieties are summarised in Table 4-1. The interaction of the Electrical Polarization Impedance (EPI) for the CBs occurred at 21.25 Hz on average (CV= 14%). Whilst, 42.28 Hz on average (CV= 20.04%) for the LFBs. Since EPI only plays a major role below 100 Hz for both the resistance and the reactance in the two banana varieties, it is suggested that the effect of EPI can be deemed negligible while frequencies exceed 100 Hz. As a result, data measured over frequency range between 100 Hz and 1 MHz were used for the following analysis.

Table 4-1 Summary of the Nyquist Plot parameters for the CBs and LFBs

Variety	No.	R_H (ohm)	R_L (ohm)	D(ohm)	f_c (Hz)	f_0 (Hz)
Cavendish Banana	no.1	-68.12	20165	26440	3414.50	18.48
	no.2	-59.32	22100	29042	2928.60	18.48
	no.3	-65.63	18752	24574	2928.60	18.48
	no.4	-73.80	20229	26676	2928.60	25.12
	no.5	-55.59	18070	24056	2928.60	21.54
	no.6	-77.95	21936	28803	3414.50	21.54
	no.7	-75.45	22142	29895	2928.60	25.12
	AVE	-67.98	20484.86	27069.43	3067.43	21.25
	STD	8.40	1656.44	2263.44	237.09	2.98
	CV	12.36	8.09	8.36	7.73	14.00
Lady Finger Banana	no.1	37.44	18447.00	23517.00	2511.90	54.12
	no.2	32.75	19054.00	24738.00	2511.90	54.12
	no.3	45.76	18299.00	22693.00	2928.60	39.81
	no.4	43.61	17399.00	21632.00	2511.90	34.15
	no.5	40.29	17767.00	22256.00	2928.60	39.81
	no.6	35.66	15521.00	19371.00	2511.60	39.81
	no.7	32.54	18522.00	23123.00	2928.60	34.15
	AVE	38.29	17858.43	22475.71	2690.44	42.28
	STD	5.16	1161.41	1686.60	222.78	8.47
	CV	13.47	6.50	7.50	8.28	20.04

$\boldsymbol{R_H}$ is the high-frequency resistance, $\boldsymbol{R_L}$ is the low-frequency resistance, D is the diameter of the semicircle in the Nyquist Plot, $\boldsymbol{f_c}$ is the maximum reactance frequency (characteristic frequency), $\boldsymbol{f_o}$ is the transitional frequency where the electrode polarization occurs. AVE is the average value, STD is the standard deviation, CV is the coefficient of variation.

The changes of the arc diameters and banana peel colours during ripening process for the two varieties are shown in Figure 4-4. Peel colour grade of 7.5 and 8 were added to represent the

continuous ripening. Sample size was seven for each variety. Error bar in the figure represents SD. We used different letters (A, B, C, D) in each figure to denote significant changes among means ($p<0.05$). For example, the change from A to B represents the diameter of impedance arc between peel colour grade 3.5 and 4 is highly significant (Figure 4-4 A). While there is no any significant change from peel colour grade 4 to 5. Thus, they are denoted by the same letter B and so forth. The Coefficient of Determination (CD), also known as $\boldsymbol{R}^2$ is used to determine the fit of the regression line (Bethea et al., 1995). The mathematical equation for the CD is given in Eq.4-1 (Bethea et al., 1995).

$$\boldsymbol{R}^2 = 1 - \frac{\boldsymbol{SS}_{Res}}{\boldsymbol{SS}_{Total}} = \frac{\sum_{i=1}^{n}(\hat{y}_i - \bar{y})^2}{\sum_{i=1}^{n}(y_i - \bar{y})^2} \qquad \text{Eq. 4-1}$$

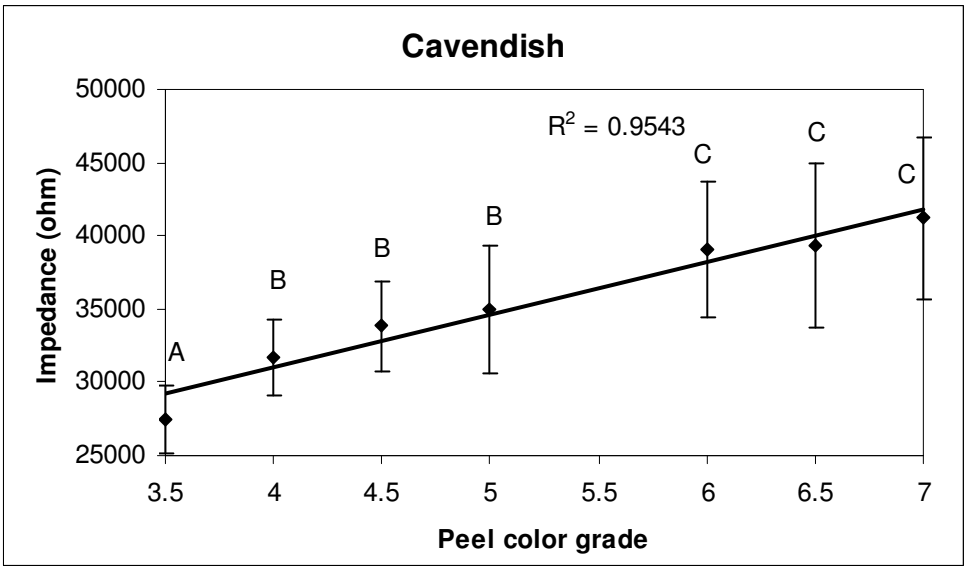

A

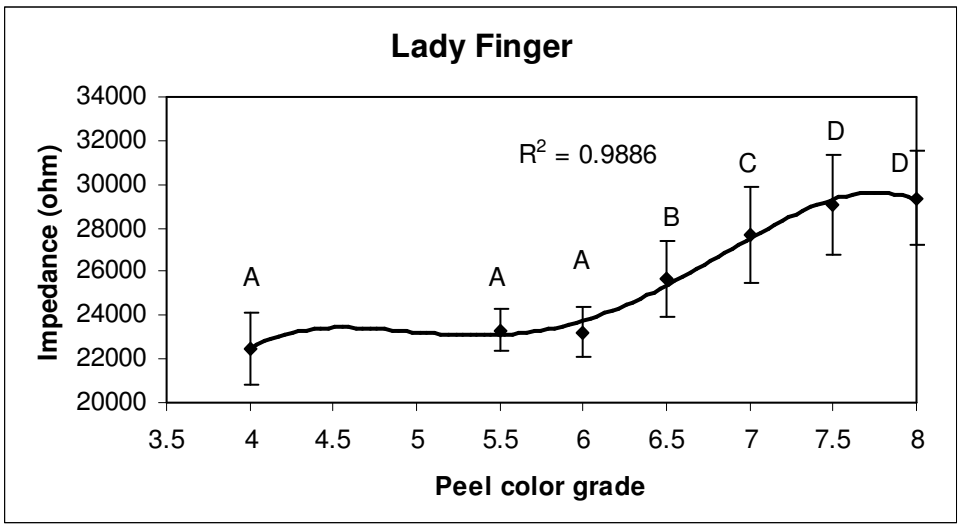

B

Figure 4-4 Relationships between the diameters of fitted semicircular arcs and peel colour grade. Error bars represent the standard deviation. Different letters in the figures denote significant differences among means ($p<0.05$).

As can be seen from Figure 4-4A, the impedance of the CBs increased from 27417 ohms to 41210 ohms over the seven days ripening. Their peel colour grade changed from 3.5 to 7 over the period. It is noted that there is a strong linear relationship between impedance of the CBs and their colours. The CD for the fitted line is 0.9543. The relationship between impedance of the LFBs and peel colour grade is illustrated in Figure 4-4B. Impedance increased as a fourth polynomial function with peel colour grade, the CD for the polynomial increasing is 0.9886. Impedance of the Day 7 was 29361 ohms, increased by 30.6% from the Day 1. For the CBs, significant changes took place at the beginning of the ripening period (colour 3.5-4) and between colour 5 and colour 6 ($p<0.05$). In comparison, rapid changes for the LFBs started from colour 6 to 7.5 ($p<0.05$).

Ion migration during ripening could be the reason for the expansion of the impedance arc diameter. Banana peel contains a huge amount of magnesium ions and potassium ions at the preclimacteric stage (John et al., 1995; Lin, 1980). Magnesium ions migrate from peel to pulp according to the degradation of chlorophyll during the ripening process. Moreover, the increased sugar content in the pulp brings about transformation of potassium ions to the pulp. Water loss of the whole fruit also contributes to mobile ions concentration increasing when ripening. In general, the increasing of ions concentration in the electrolyte of the banana leads to the decreasing of resistance (Toyoda et al., 2001; Zywica et al., 2005). However, highly concentrated solutions do not follow this pattern, they reveal the opposite trend instead.

Therefore, based on these experiments, it is believed that the concentration of ions in banana pulp becomes very high during ripening.

4.3.2 Equivalent Electrical Model

Graphical examination of EIS data can only be used in rough estimations of the simplest material-electrode system. More comprehensive analysis needs to be done to further understand the complex material-electrode systems such as biological tissues. Equivalent electrical circuit analysis is one approach to study the electrical behaviour of a certain system. The other approach is to build up a mathematical model according to the plausible physical model. Once the mathematical model is determined, it can be used to perform curve fitting. Complex nonlinear least squares (CNLS) data fitting, which was developed by J Ross Macdonald, is one of the useful techniques available in the applications of data fitting for EIS investigation (Macdonald, 1992; Macdonald et al., 1987).

Z-view software was used to perform the electrical circuit fitting. Both the Hayden model and the double-shell model were applied to the fitting. The fitting processes in Z-view are based on the principle of CNLS. The aim of least squares fitting is to find a set of parameters P which will minimize the sum (Macdonald et al., 1987):

$$S(P) = \sum \boldsymbol{w}_j [\boldsymbol{Y}_j - \boldsymbol{YC}_j(\boldsymbol{P})]^2 \qquad \text{Eq. 4-2}$$

The sum is taken over 1...M, where M is the total number of data points. $\boldsymbol{w}_j$ is the weight associated with the jth point, $\boldsymbol{Y}_j$ is the jth data point value to be fitted, and $\boldsymbol{YC}_j(P)$ is the corresponding value of the calculated fitting function involving the set of parameters P (Macdonald et al., 1987).

Impedance data is expressed as:

$$Z(\omega) = R(\omega) + jX(\omega) = u(\omega) + jv(\omega) \qquad \text{Eq. 4-3}$$

It is clear that u(ω) and v(ω) follow different functions of ω, and both of them involve some or all of the same parameters. When least squares fitting is applied, u(ω) and v(ω) will be fitted separately. As a result, the two independent fittings generate two separate sets of

different parameter value estimates. Apparently, this fitting is not a simultaneous least squares fitting of all the data. In contrast, the CNLS adjusts all parameters simultaneously, and yields very high resolution and can resolve process with strongly overlapping time constants (Macdonald et al., 1987). Furthermore, the CNLS program provides the estimations of standard deviations of parameters, which are measures of how well the data fits.

The goodness of fitting is usually determined by Chi-squared value (Bethea et al., 1995). Chi-square method calculates the standard deviation between the original data and the calculated spectrum. An alternative approach is to use the weighted sum of squares (SS). The sum of squares is the sum of the square of the vertical distances of the points from the curve. It is proportional to the average percentage error between an original data value at a given frequency and the corresponding value calculated from the model (Macdonald, 1992). The Chi-squared values and the weighted SS values are summarised in Table 4-2.

Table 4-2 Comparisons of the fitting results between the Hayden Model and the double-Shell Model

Variety		Hayden Model		Double-Shell Model	
		Chi-Squared	Weighted Sum of Squares	Chi-Squared	Weighted Sum of Squares
Cavendish Bananas	AVE	0.32	51.56	0.11	3.49
	STD	0.01	5.41	0.14	0.26
Lady Finger Bananas	AVE	0.31	42.4	0.03	3.29
	STD	0.12	4.77	0.001	0.25

By comparing the features of Chi-square and the weighted sum of squares (SS), it is noticed that Chi-square is often a poor estimation of the goodness of fit. For example, if there is a high frequency data point of 1 ohm and a low frequency data point of 10^5 ohms. If there was an error of 1 ohm in the fit of both points, the 10^5 ohms point would be a very good fit (10^{-3} %), but the 1 ohm point would have a 100% error. This will produce a much smaller Chi-square value than if both points had a 1% error (10^3 ohms error in the 10^5 ohms point and 10^{-2} ohm error in the 1 ohm value). In contrast, the weighted SS sums the percent error in each data point instead of summing to raw errors. It is particularly useful when comparing the goodness of fit of two different models to a single data set. Thus, the weighted SS is used, derived from these two models. This determines which model gives a better description of the electrical properties of bananas.

The weighted SS of the double-shell model for the CBs and LFBs were 3.49 ± 0.26, 3.29 ± 0.25 respectively, while, the weighted SS of the Hayden model for the CBs and LFBs were 51.56 ± 5.41, 42.40 ± 4.77 respectively. Since the weighted SSs from Hayden model is 15.7 and 11.9 times bigger than those of double-shell model for CBs and LFBs respectively, it is apparent that the Hayden model has higher average percentage error. In contrast, the double-shell model precisely fits the data. Therefore, the subsequent discussion about banana cellular changes is based on the double-shell model. Relationships between the equivalent circuit components as functions of peel colour grade are displayed in Figure 4-5 & 4-6. The values of the equivalent circuit components are displayed in Table 4-3.

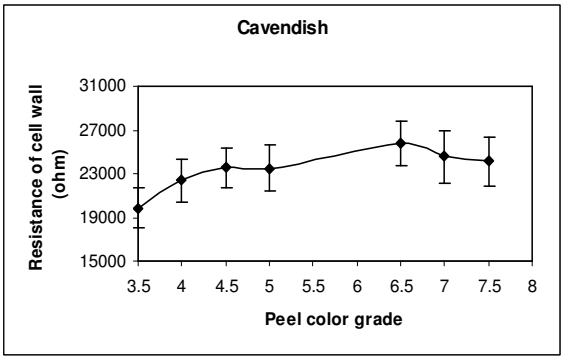

A

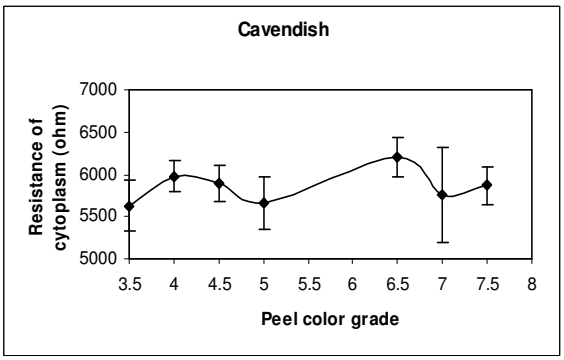

B

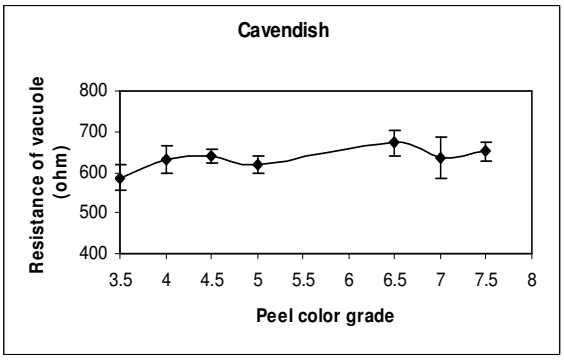

C

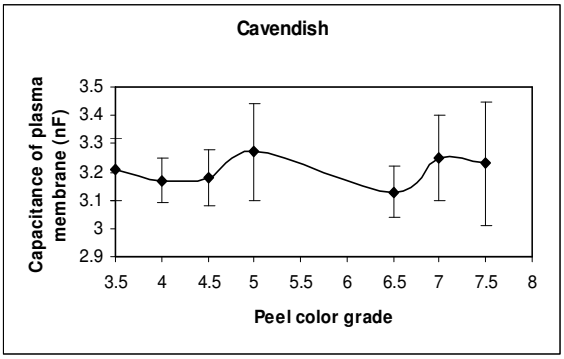

D

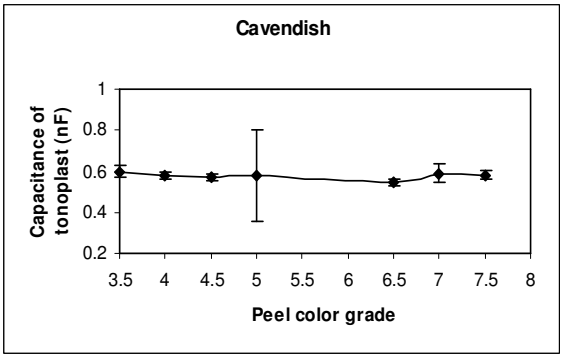

E

Figure 4-5 The equivalent circuit components as functions of peel colour grade for the Cavendish Bananas. Error bars represent the standard deviation. The observed frequency range is from 100 Hz to 1 MHz.

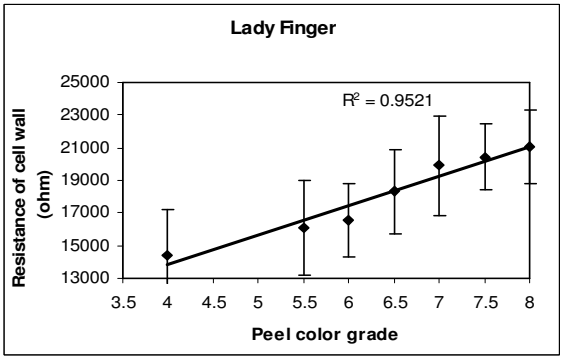

A

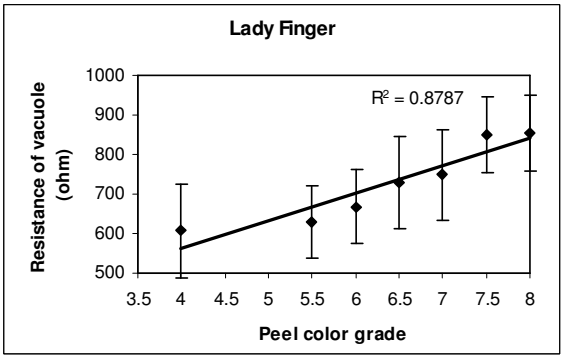

B

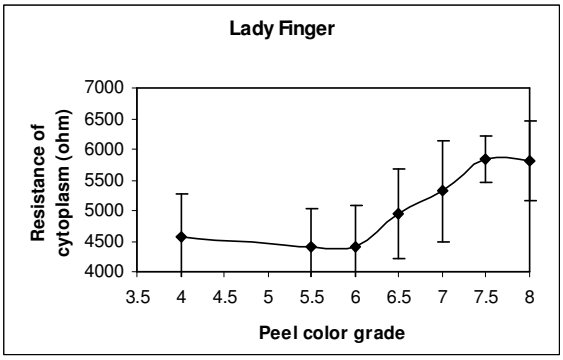

C

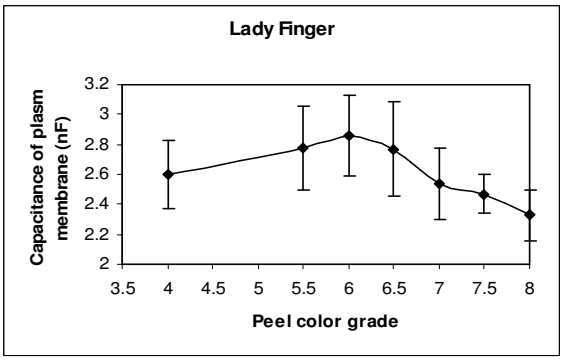

D

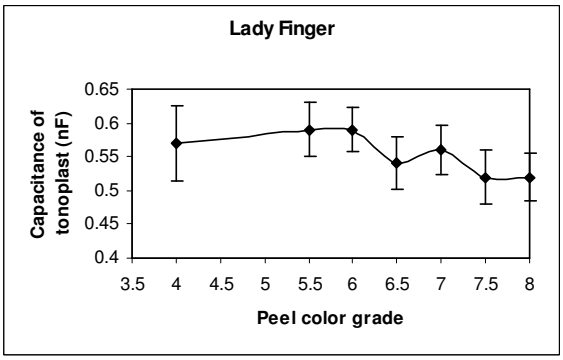

E

Figure 4-6 The equivalent circuit components as functions of peel colour grade for the Lady Finger Bananas. Error bars represent the standard deviation. The observed frequency range is from 100 Hz to 1 MHz.

Table 4-3 The changes of resistance of the cell wall, cytoplasm and vacuole as well as capacitances of the plasma membrane and tonoplast of the Cavendish bananas and the Lady Finger bananas during ripening.

Banana Variety	Peel Color Grade	Resistance (ohm) Mean/CV%			Capacitance (nF) Mean/CV%	
		Cell Wall	Cytoplasm	Vacuole	Plasma Membrane	Tonoplast
Cavendish Banana	3.5	16427/8.0	6263/8.4	843/7.3	2.22/9.4	0.5/11.1
	4	19072/7.7	6672/9.3	899/8.7	2.06/8.0	0.47/11.5
	4.5	21425/12.0	6634/5.2	922/6.2	2.08/5.2	0.46/7.0
	5	23753/16.4	6078/6.4	903/6.8	2.25/7.4	0.5/8.3
	6	27146/15.7	6365/6.7	970/7.8	2.29/5.2	0.49/8.3
	6.5	27249/16.5	6652/12.2	970/9.3	2.21/9.0	0.45/11.7
	7	28451/16.7	7053/9.7	1034/6.4	2.23/6.9	0.45/6.7
Lady Finger Banana	4	14423/5.8	4567/6.7	607/7.9	2.6/8.7	0.57/10.8
	5.5	16112/4.5	4399/5.0	630/4.8	2.78/6.3	0.59/7.9
	6	16597/5.2	4394/5.9	668/8.7	2.86/13.0	0.59/11.0
	6.5	18303/6.4	4950/6.3	730/5.9	2.77/5.8	0.54/8.7
	7	19931/6.2	5321/9.1	748/7.5	2.54/6.7	0.56/8.3
	7.5	20448/5.8	5844/10.3	850/9.8	2.47/8.4	0.52/14.1
	8	21065/7.6	5804/7.3	854/3.4	2.33/8.6	0.52/6.1

※The coefficient of variation (CV) is a relative measure of dispersion. $CV=100\times\left(\frac{s}{\bar{x}}\right)$ SD is denoted by symbol s, the mean value is denoted by symbol $\bar{x}$.

Figure 4-5A&C reflected the relationship between resistance of cell wall, vacuole and peel colour grade for the CBs. The value of resistance of cell wall rose by 73.2% from 16427 ohms to 28451 ohms. Whilst, resistance of vacuole increased by 22.7% from 843 ohms to 1034 ohms. By using the regression approach, it was observed that both the resistances of the cell wall and the vacuole had positive linear relationships with peel colour grades, which can be expressed as:

$$y = 5633 + 3340 \times x \quad (r^2 = 0.9588) \qquad \text{Eq. 4-4}$$

and

$$y = 700 + 45 \times x \quad (r^2 = 0.9000) \qquad \text{Eq. 4-5}$$

Eq.4-4 is for cell wall resistance and the r_square is 0.9588, Eq.4-5 is for vacuole resistance and the r_square is 0.9000.

In contrast, the variations of the resistances of cytoplasm followed an irregular pattern over time (Figure 4-5B). In addition, the capacitances of plasma membrane and tonoplast displayed a similar pattern with colour (Figure 4-5D&E). Plasma membrane varied between 2.06 nF and 2.29 nF, and the variation range for tonoplast is from 0.45 nF to 0.5 nF.

Similarly, both cell wall resistance and vacuole resistance for LFBs increased with time according to Figure 4-6 A&C. Cell wall resistance increased by 46.1% and vacuole resistance increased by 40.7%.

$$y = 6609 + 1812 \times x (r^2 = 0.9521) \qquad \text{Eq. 4-6}$$

and

$$y = 287 + 69 \times x (r^2 = 0.8787) \qquad \text{Eq. 4-7}$$

Eq.4-6 is for cell wall resistance and r_square is 0.9521, Eq.4-7 is for vacuole resistance and r_square is 0.8787.

As can be seen from Figure 4-6B, resistance of cytoplasm decreased from 4567 ohms of the Day 1 to 4394 ohms of the Day 3, then rose gradually to 5844 ohms on the Day 6, and then a slight drop to 5804 ohms on the Day 7. The capacitance of plasma membrane increased in the first three days, and reached a maximum value of 2.86 nF at peel color grade 6, and then followed by a reduction at the rest of days, the minimum value was 2.33 nF (Figure 4-6D). The tonoplast capacitance fluctuated within a small range from 0.52 nF to 0.59 nF (Figure 4-6E).

Redgwell et al. (1997) performed a series of experiments on the *in vivo* and *in vitro* of cell wall swelling on temperate fruit. Cell wall swelling takes place in fruit which ripens to a soft melting texture. In the case of bananas, the texture firmness declines with time. Therefore, the banana's cell wall swells or shrinks. Upon investigation, an increase in cell wall resistance has been found, which was opposite to the trend observed in the nectarine (Harker et al., 1994a), but was similar to the persimmon study (Harker et al., 1994a; Harker et al., 1994b; Harker et al., 1997; Varlan et al., 1996). It is suggested that the increase is due to the shrinkage of the cell wall, and a reduction of the cell wall cross-sectional area. The polysaccarides inside banana degrades and transforms into more soluble constituents such as oligosaccharides, disaccharides, and monosaccharides with the ripening process. Therefore, the cell wall becomes thinner. Low frequencies mainly measure the resistance of extracellular space, and the cell wall is the dominant component of the extracellular space. Therefore, the measured resistances mainly relate to the cell wall resistance at low frequencies. This finding is confirmed by this research as well as other investigations by Bauchot et al. (2000) and Harker et al. (1994a).

Observations show the resistance of the vacuole increased over the seven days. During this time, the CBs increased by 10.9% and the LFBs by 40.7%. It has been found that the resistances measured at high frequencies were very close to the magnitudes of the vacuole resistances. This is because plant vacuole accounts for more than 90% of the cell volume and contains the highest ion concentration (Clarkson, 1974; King et al., 1989). The penetrability of the cell membrane increases with ripening and the breakdown of the cell membrane makes the cell structure homogeneous when fruit is fully ripe. The extracellular space has a lower concentration of ions than the intracellular space, thus the mobile ions transfer from high concentration solution to low concentration solution. Subsequently, the mobile ions concentration in the vacuole declines and this may be the reason for the resistance increased

in vacuole. Cytoplasm is a fluid surrounding the contents of a cell and this forms the vacuole. It is a very thin layer adjacent to the cell wall, and its resistance changes within a very limited range.

Based on this observation, bananas ripening processing can be divided into three stages, namely physiological self-development (peel colour grade 3-5), eating-ripe stage (peel colour grade 6-7), and overripe stage (peel colour grade 7 onwards). Barnell (1940) reported that the total sugar of bananas increased as they ripened, and reached a peak at the eating stage. The accumulation of sugar leads to the whole fruit impedance and cell wall resistance increasing continuously from peel colour grade 3.5 to 6. The CBs revealed a declining impedance from colour 7 onwards (Figure 4-5C). Madamba et al. (1977) suggested the sugars formed from starch hydrolysis experienced further conversion to organic acids. As a result, the hydrogen ion concentration increases and tissue conductivity increases accordingly. Thus, impedance reduces at the last stage, which is the overripe stage. Alternatively, tissue conductivity may be affected by cell deterioration caused by over ripening. Thus, when decreases, bananas are overripe and they are no longer suitable for longer storage. Therefore, the best period for bananas to be eaten is between colour 6 and colour 7. The LFBs did not show a clear trend between colour 6 and colour 7, which could be explained by the fact that LFBs may have a longer storage period than CBs.

4.4 Conclusion

This study demonstrates the physiological changes of bananas through the use of impedance measurement during the ripening process. The impedance data has been used to verify two popular plant cell electrical models, namely, the Hayden model and the double-shell model. It has been found that the double-shell model fits this data much better than the Hayden model. A positive linear relationship between impedance and peel colour was observed for the Cavendish Bananas, and a fourth polynomial relationship between impedance and peel colour was observed for the Lady Finger Bananas. It was found that cell wall resistance and vacuole resistance also increase linearly with time. By combining the banana's physiological changes with impedance changes, it is suggested that the ripening time consists of three stages, physiological self-development, eating-ripe stage, and overripe stage respectively, as described above.

This investigation indicates that the electrical impedance measurement has a great potential in assessing fruit ripening and forecasting the length of fruit storage. The relationships between fruit impedance and peel colour grade presented in this study can be further developed into an algorithm for practical use and as a cheap, quick and easy approach.

Chapter 5 Application of EIS for Vegetable Dehydration

5.1 Introduction

Dehydration techniques are one of the oldest methods for food preservation and were improved during the Second World War (Barbosa-Canovas et al., 1996). Fruits and vegetables are perishable due to their high moisture content. "*Drying is a process in which water is removed to halt or slow down the growth of spoilage microorganisms as well as the occurrence of chemical reactions"*. (Barbosa-Canovas et al., 1996) The primary purpose of food dehydration is to extend the shelf life of products. It is typically suitable to process food used for military purposes.

Apart from preventing the growth and reproduction of microorganisms, dehydration reduces the volume of packing, storage and therefore the costs of transportation (Jayaraman et al., 1992). Dehydration techniques are mainly classified into spray drying, freeze dehydration, osmotic dehydration, sun drying and vacuum drying (Barbosa-Canovas et al., 1996). The choice of suitable dehydration techniques depends on the characteristics of the food to be dried.

Thermal dehydration is the most popular and efficient way in industrial process regarding food preservation (Torrey, 1974). The basic configuration of thermal dehydration is to place sample in a drying chamber equipped with hot air flow and an atmospheric air blower (Barbosa-Canovas et al., 1996).The quality of dried products can be assessed from the colour, aroma, flavour, nutrients etc. (Barbosa-Canovas et al., 1996; Barringer, 2004).

Moisture content is of great importance to the quality and stability of food products. Magnetic Resonance Imaging (MRI) is an ideal method for assessing water distribution through food products (Gunasekaran, 2001). However, the separation of signals of water proton from that of fat proton is still a challenging task. It is due to the fact that protons in both the water and fat molecules contribute to nuclear magnetic resonance signal in the imaging sequence (Gunasekaran, 2001). In addition, the high cost of MRI equipment makes this method less competitive. Therefore, it is necessary to expand moisture determination method from different aspects.

The large moisture content and metal ions inside fruit and vegetables allow them to be good electrical conductors. The loss of water in drying process leads to changes in electrical conductivity and electrical impedance changes. Electrical impedance measurement is fast and non-invasive, easy-to-operate and inexpensive which makes it a cheap for the investigation of moisture content variations during the drying process.

EIS is a relatively new method used for food processing and has shown its capabilities in detecting sugar and acidity contents of fruit and in classifying ripening stages of bananas outlined in previous chapters. In this chapter, EIS is applied to understand impedance characteristics caused by thermal dehydration of cucumber slices and to explore its potential as a method to monitor moisture changes during food dehydration.

5.2 Methodology

5.2.1 Materials

Fresh continental cucumbers were purchased from local market. Cucumbers were sliced into 9 pieces with thickness of 20 mm and diameter of 30 mm. The cucumber skin was peeled off. The weight of samples was measured by a lab scale (UWE Geniweigher, 0.2g graduation). The average value is 19.27 g with a CV value of 5.9%.

5.2.2 Drying Procedures

Drying procedures were performed by using a Lindner & May Dehydrator (Australia). The drying chamber is equipped with a heating and ventilation system. The ventilation system ensures each sample is dried evenly. Cucumber slices were spread on dehydration tray and loaded into the frame of the drying chamber. The drying temperature was set at 70ºC. The air flow speed was adjusted to 20 feet per minute by the control dial on the fan control box. The set up of the dehydrator is illustrated in Figure 5-1.

Drying experiments lasted 270 minutes. The drying procedure was divided into six stages based on the intervals of drying time, namely 30 minutes, 60 minutes, 90 minutes, 150 minutes, 210 minutes, and 270 minutes.

Figure 5-1 Dehydrator

5.2.3 Electrical Impedance Measurement for Cucumbers

The impedance of fresh cucumber slices was measured before drying. Cucumber slices were allowed 30 minutes to cool down at room temperature after each drying. Impedance was then measured on each slice to observe impedance characteristics changes caused by moisture content changes.

The configuration of electrical impedance measurement was different from the previous two measurements on apples and bananas. A non-destructive electrode setup, namely surface adhesive gel electrodes (3M, Red Dot) were attached symmetrically along the circumferential direction of samples. Current injective and potential detective electrodes were connected with the two surface electrodes. The frequency range used in this study was from 100 Hz to 1MHz. The details of experimental setup are shown in Figure 5-2.

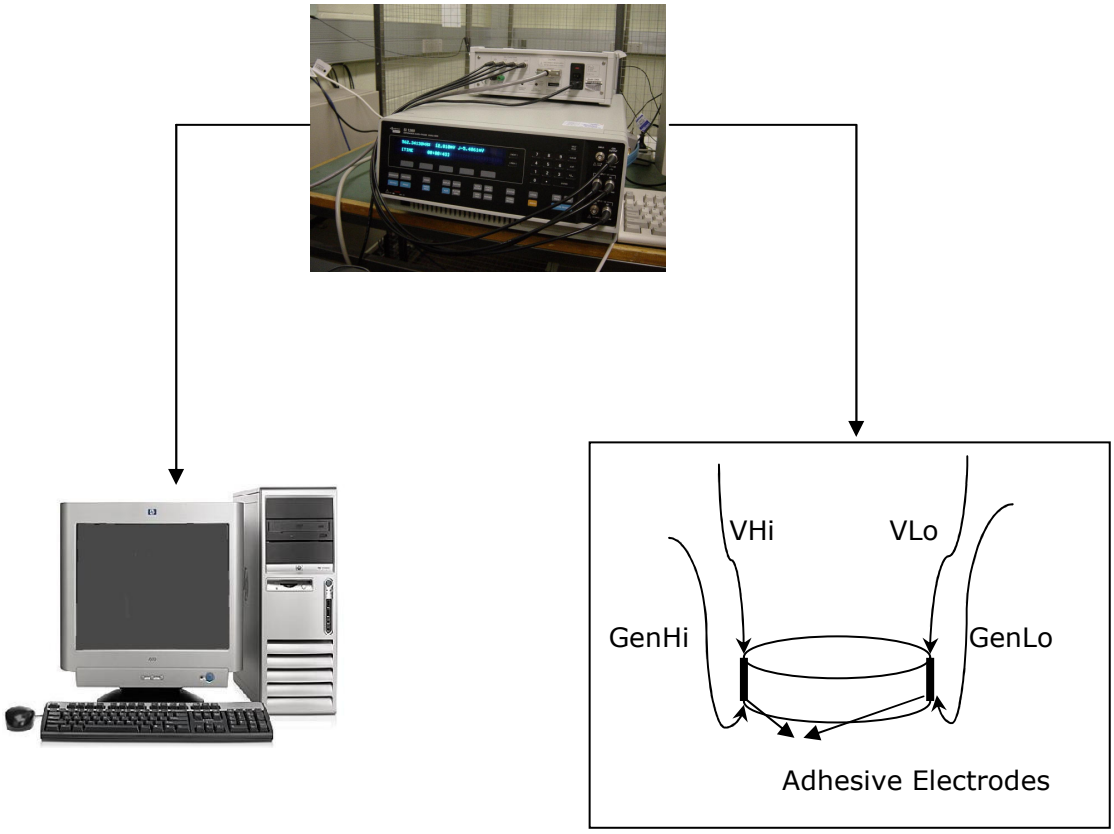

Figure 5-2 Impedance measurement setup.
A four-electrode configuration was used.

5.3 Results & Discussion

5.3.1 Moisture Content

The moisture content of a product is conventionally defined as the ratio of water mass to the total product mass in industry (Driscoll, 2004). Therefore, moisture content percent (MC) is calculated in the following formula:

$$MC\% = \frac{0.95 \times m_0 - (m_0 - m)}{m} \times 100\% \quad \text{Eq. 5-1}$$

where m_0 is the weight measured at the beginning of the drying

m is the weight measured before the impedance measurements

Fresh cucumber contains a moisture content of 95% (DeLong, 1979).

The average weight loss and moisture content percent during the dehydration was displayed in Table 5-1 & Figure 5-3. The weight of samples changed from 19.27g at the beginning of dehydration to 1.33g (CV=18.37%) at the end of dehydration. The drying process of the cucumber was composed of two stages. The first stage occurred from 0 minute to 90 minutes, the second stage occurred from 90 minutes to 270 minutes. The drying rate of the first stage was slower than the second stage according to the slopes of fitted lines, -0.0394 and -0.1954 respectively. MC decreased from 95% to 25.83% (CV=48.82%) during the 270 minutes drying. The vertical bar in Figure 5-3 represents the standard deviation. It is noticed that the MC of two typical samples achieved very low level after 270 minutes drying, 4% and 7% respectively. Their low MC values lead to a large dispersion of the average values. Therefore, the average value of MC at 270 minutes is meaningless owing to the large error percentage, so samples were observed individually.

Table 5-1 Cucumber slices mass and moisture content percent changes during drying

Drying Time (min)	Mass (g) Mean/CV%	Moisture Content% Mean/CV%
0	19.27/5.9	95.00/0.00
30	17.24/6.13	94.41/0.08
60	14.00/7.07	93.11/0.20
90	11.36/8.25	91.50/0.36
150	5.29/16.17	81.47/2.83
210	3.13/22.34	68.05/9.37
270	1.33/18.37	25.83/48.82

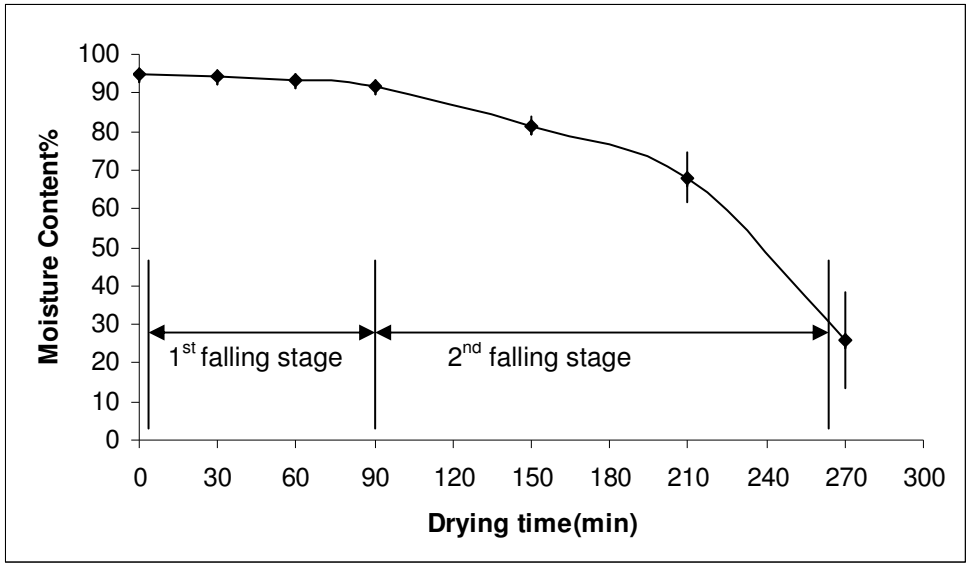

Figure 5-3 Moisture content percent variation during drying.
Error bars represents the standard deviations.

5.3.2 Impedance Variations

5.3.2.1 Magnitude of Impedance

The impedance curve displays a semi-circular arc with a depressed centre below the X-Axis in the Nyquist Plot. A mathematical fitting of the semi-circular arc was conducted by the Z-view software. Data of a typical sample at 0 minute drying is given as an example in Figure 5-4 to illustrate the fitting results. The red line represents raw data line and the green line represents the fitted circle. The individual frequency responses of the nine samples are detailed in the three dimensional perspective plots in Figure 5-5. X-axis represents frequency, Y-axis represents resistance, Z-axis represents reactance. By observing projections of the 3-D curve of the response in the Y-Z plane of the plot, it can be seen that all the nine samples have the consistent semicircular curve shape. Impedance at various frequencies, such as 100Hz, 1kHz, 10kHz, 100kHz and 1MHz, were chosen to observe impedance changes during the drying process (Figure 5-6).

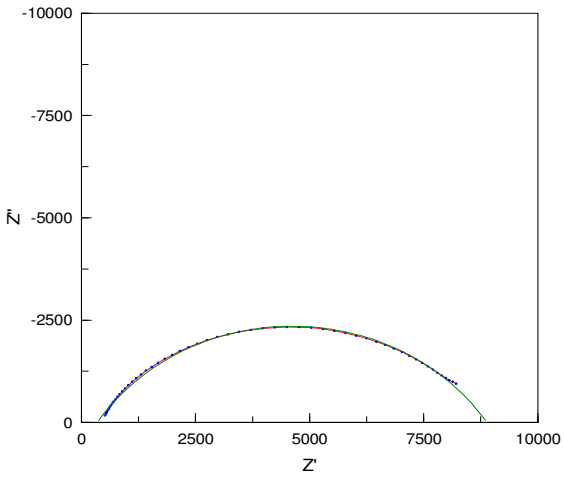

Figure 5-4 An example of the circular fitting of one typical sample. The red line is the raw data and the green line is the fitted circle. The sweeping frequency range is from 100 Hz to 1 MHz.

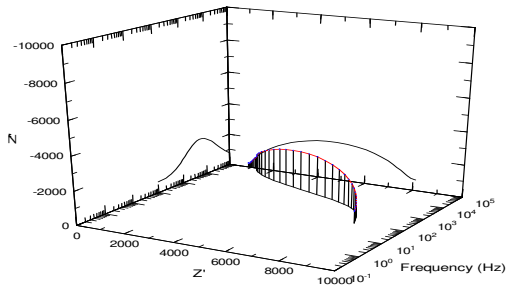

Sample 1

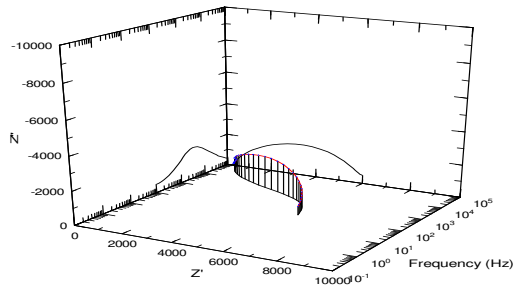

Sample 2

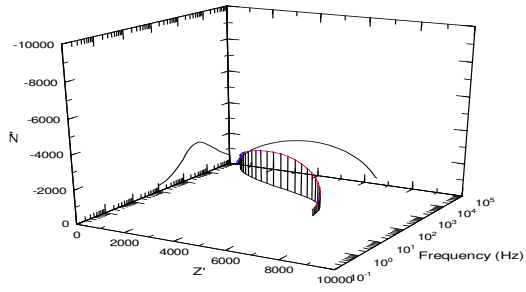

Sample 3

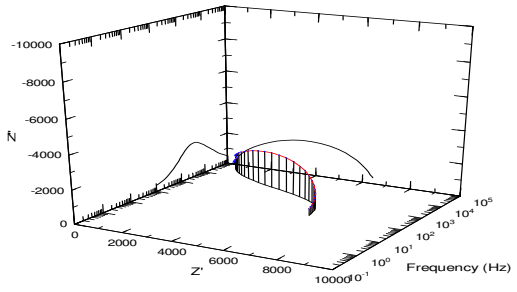

Sample 4

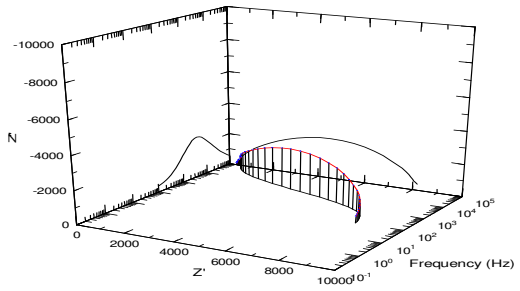

Sample 5

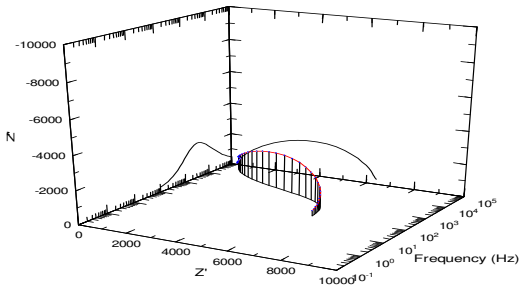

Sample 6

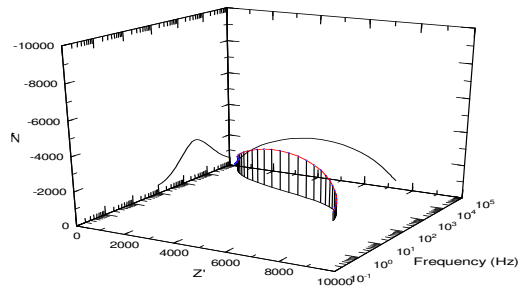

Sample 7

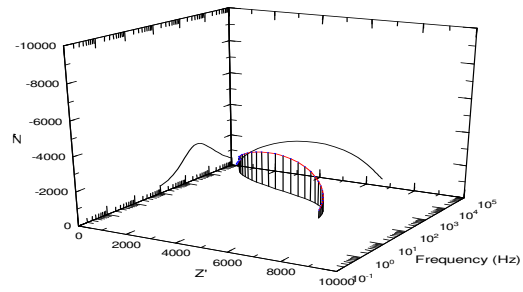

Sample 8

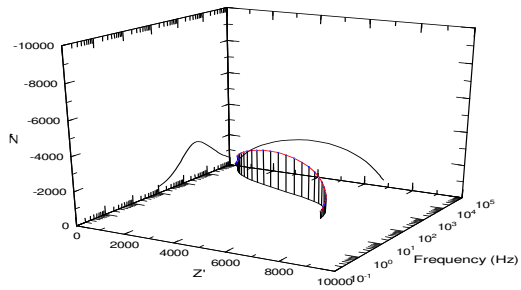

Sample 9

Figure 5-5 Individual 3-D Plots of the nine samples before drying. The sweeping frequency range is from 100 Hz to 1 MHz.

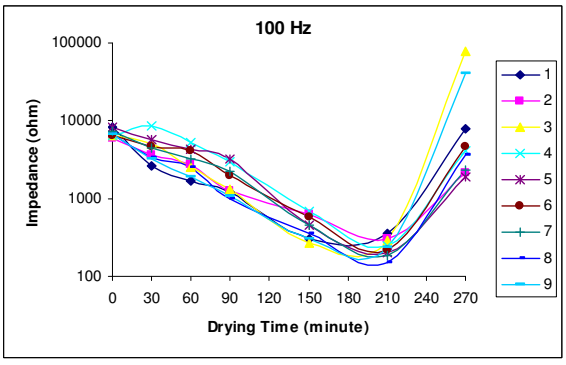

A

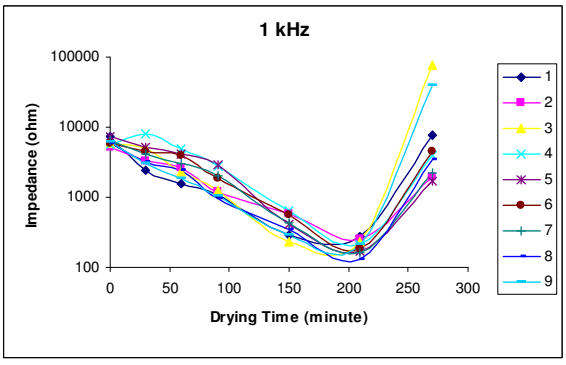

B

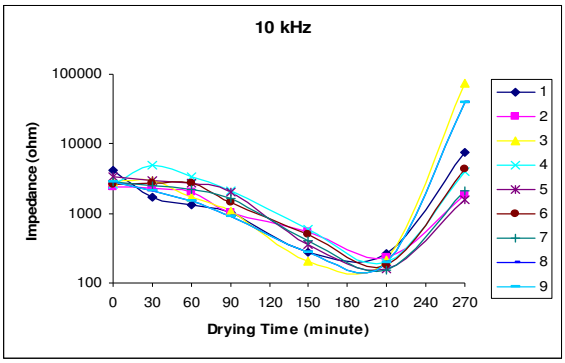

C

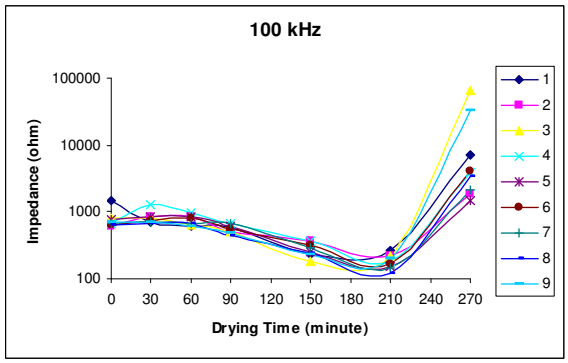

D

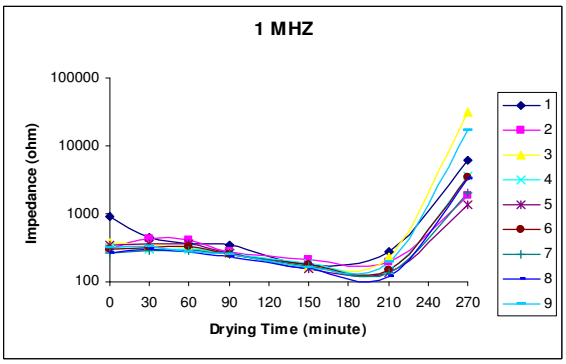

E

Figure 5-6 Impedance variations during the 270 minutes drying for 9 samples at the selected frequencies.

It is apparent that impedances of all 9 samples followed a similar trend during drying process at the selected frequencies. Impedance declined from the beginning of drying to 210 minutes drying. There is a dramatic increase from 210 minutes to 270 minutes. This sharp increase is typically visible in Sample 3 and Sample 9 above. At 100 Hz, the impedance of Sample 3 jumped from 285 ohms to 78184 ohms and impedance of Sample 9 jumped from 234 ohms to 39940 ohms during the last 60 minutes drying.

5.3.2.2 Diameter of Impedance Arc

The relationships between the diameter of impedance arc and moisture content for the 9 samples were plotted as Figure 5-7. Upon observation of the impedance arc variations, the curved shape of the last measurement at 270 minute is no longer a semicircular arc; it consists of two straight lines instead (refer Figure 5-8). Consequently, the circular fitting could not be applied for the data measured at 270 minutes. Figure 5-7 shows that the diameter of impedance arc decreases with the loss of the moisture content for all cucumber slices except Sample 4. The decreasing of impedance diameter can also be separated into two stages. The

first falling stage is from 0 minute to 90 minutes, the second falling stage is from 90 minutes to 210 minutes. The diameter decreased faster at the first falling stage, while the moisture content dropped more slowly during the same drying period. In contrast, the diameter decreased slower at the second falling stage, while the moisture content dropped faster at the same time. However, the impedance arc diameter does not reflect the sharp rise of the impedance at the last dehydration stage.

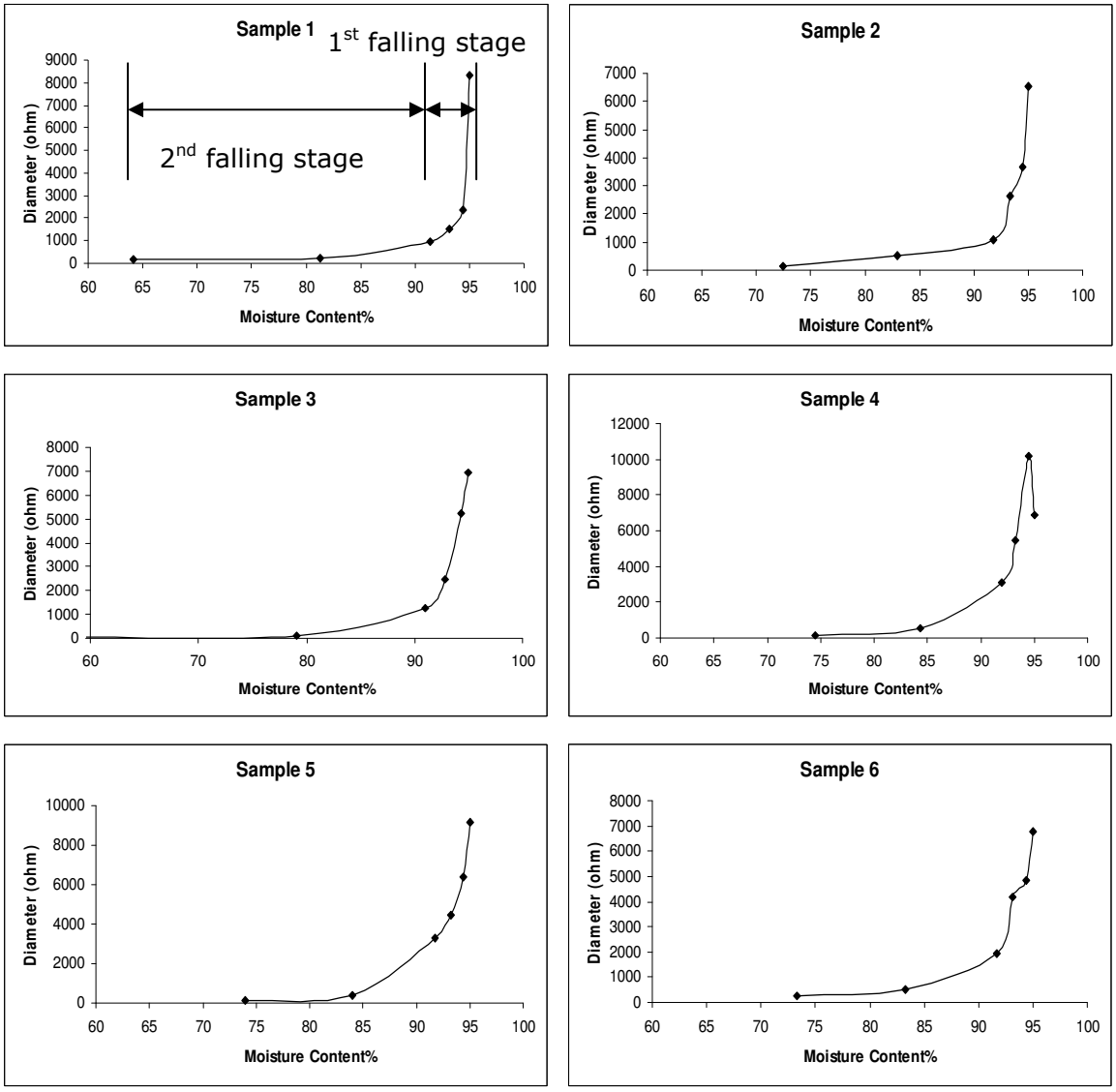

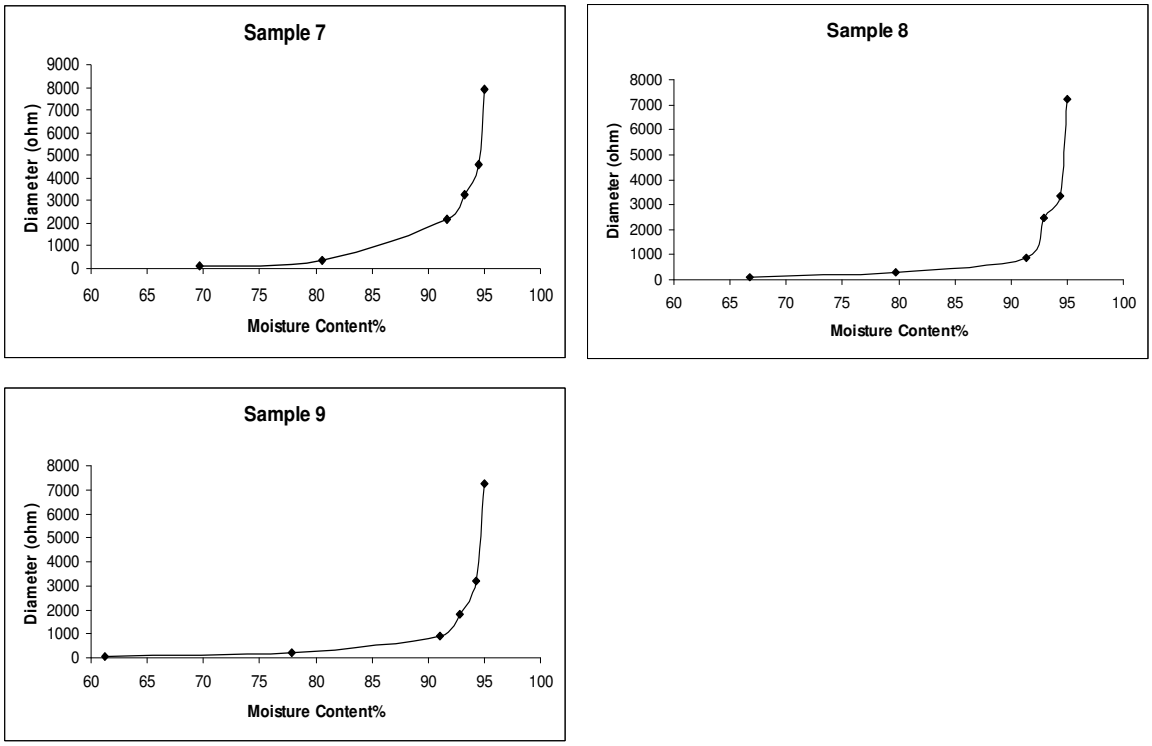

Figure 5-7 Diameter of impedance arc changes with moisture content for 9 samples. The two falling stages are detailed in Sample 1.

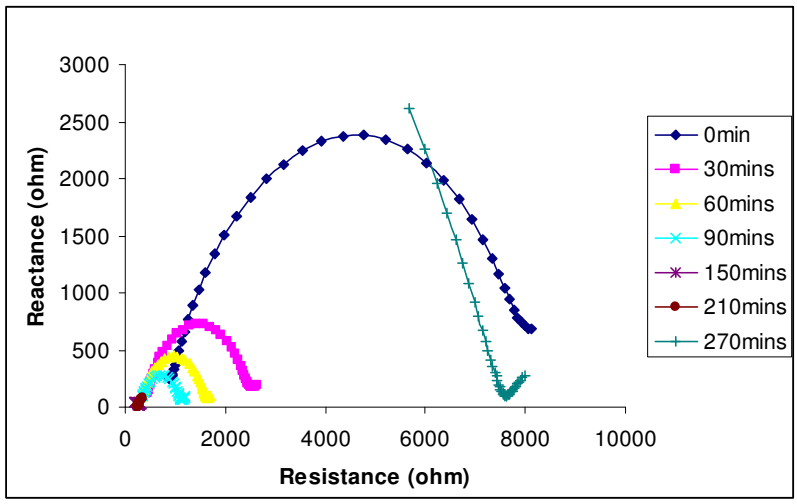

Figure 5-8 Impedance changes during the 270 minutes dehydration progress (Sample 1)

5.3.3 Relationship between the Impedance Property and Moisture Content

Upon the observations from the above sections, it was found that the impedance properties changed with the different moisture content. The magnitude of impedance decreased when moisture dropped from 95% to 68.05% after 210 minutes drying. Cucumbers are rich in fibre,

minerals silica, potassium and magnesium ion (Kotsiras et al., 2002). The loss of moisture content contributes to the increase in electrolyte concentration. As a result, the equivalent electrical conductivity increases and the impedance decreases. However, the magnitude of impedance increased during the last 60 minutes drying. The rapid increase in impedance magnitude can be explained that the further moisture loss reduces the total amount of current paths. As a result, the activities of free ions are limited and impedance increases. Alternatively, the influence of fibre becomes apparent when the moisture content is reduced to a certain level (i.e. 25.85% in this case). Cucumber slices represent dielectric characteristic owing to the woody characteristic of fibre. Therefore, the tested electrical signal mainly comes from the fibre. Thus the overall impedance magnitude jumped to a relatively high value.

The diameter of the impedance arc as shown in the Nyquist Plot also reflects the moisture content variations. The diameter decreases with the loss of moisture in cucumbers over the 210 minutes drying. The trend is opposite with the previous dehydration investigation on apples and carrots (Meszaros et al., 2004; Toyoda et al., 1997). However, the semicircular arc was replaced by two straight lines when moisture was reduced to a relatively low level. The disappearance of the impedance arc in the Nyquist Plot indicates that the sample is no longer a good electrical conductor.

5.3.4 Equivalent Electrical Modelling

Both the Hayden model and the double-shell model were fitted to the impedance data of cucumber samples. The parameters of the equivalent electrical circuits were estimated by the Z-view software based on the CNLS curve fitting principle.

The Chi-Squared value and the weighted SS for the two electrical models are summarised in Table 5-2 below. It can be seen from the table that the average of Chi-Squared value and the average of SS value for the double-shell model are approximately 11-fold smaller than the corresponding values for the Hayden model. It is considered that the smaller the goodness-of-fit value, the more accurate the model. It is also shown that the error percentages for individual circuit component in the double-shell model are below 6%. In contrast, the error percentages for the Hayden model are around several 10^{8} %. Thus, the Hayden model fits the

cucumber data fairly poor. In comparison, the double-shell model is a better equivalent electrical model for cucumbers.

Table 5-2 Summary of the goodness-of-fit values for the fitting of the Hayden model and the double-shell model

Electrical Model	Chi-Squared Value		Weighted Sum of Squares	
	Mean	SD*	Mean	SD*
Hayden Model	0.115472	0.006796	9.006489	0.529716
Double-Shell Model	0.010868	0.002018	0.836847	0.155339

*SD-standard deviation

In addition, the fit of the electrical model can be improved by using a distributed model. The distributed model consists of a resistor in series with a distributed element (DCE). The DCE contains a Constant Phase Element (CPE) in parallel with a resistor (Figure 5-9). CPE reveals a frequency dispersion of the impedance response for the electrochemical system (Jorcin et al., 2006). The impedance of the CPE is given as (Lasia, 1999):

$$\boldsymbol{Z} = \frac{1}{\boldsymbol{T}(j\omega)^{\phi}} \qquad \text{Eq. 5-2}$$

where T is a constant in $\mathrm{F}\boldsymbol{cm}^{-2}\boldsymbol{s}^{\phi-1}$. j is the imaginary number, $\boldsymbol{j} = \sqrt{-1}$. ω is the angular frequency, $\omega = 2\pi\boldsymbol{f}$. ϕ is related to the angle of rotation of a purely capacitive line on the complex plane plots. ϕ is ranged from 0 to 1. CPE represents the behaviour of a capacitor for ϕ=1, a resistor for ϕ=0, and an inductor for ϕ=-1. Therefore, CPE is an extremely flexible fitting parameter.

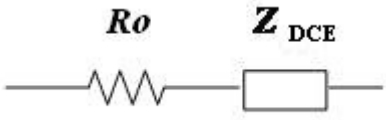

Figure 5-9 The distributed element consists of a resistor R_o in parallel with a DCE

The impedance of the distributed model is given as:

$$Z = R_0 + \frac{R}{1 + RT(j\omega)^{\phi}} \qquad \text{Eq. 5-3}$$

The Chi-Squared value and the weighted SS for the distributed model are 0.00156 ± 0.0012, 0.11871 ± 0.09633 respectively. It is observed that the weighted SS of the distributed mode is the smallest compared with the two models in Table 5-2. Therefore, the distributed model is the best model fits cucumbers.

It has been reported that the distributed model is ideal for highly non-uniform woody plant tissue (Repo et al., 1993). The cucumber slices present woody characteristic gradually due to the loss of moisture content. This makes the distributed model suitable for the fitting of cucumber. The advantage of the distributed model is the small number of circuit elements. Only four parameters can determine a system in the distributed model compared with five parameters in the double-shell model. However, its disadvantage is the lacking of reasonable response to a specific cellular structure. Only the resistance of the extracellular and intracellular compartments can be estimated from the DCE model. But it is not possible to associate the parameters of T and ϕ to specific cellular structures.

5.4 Conclusion

This chapter outlines preliminary research in the application of electrical impedance measurement for monitoring cucumber dehydration progress. The magnitude of impedance was useful to monitor the drying progress. Impedance spectroscopy is sensitive towards the moisture content changes. For instance, the moisture content decreased by 2% from 93% to 91%, accordingly, its impedance at 100 Hz decreased by 26.5% from 1880 ohms to 1382 ohms in one of the samples. Moreover, the impedance arc of pure cucumber pulp represents a tendency to fall when moisture content dropped from 95% to 65%. The semicircular arc of impedance in the Nyquist Plot disappeared when further drying continued until the moisture content was relatively low. The conductivity of experimental specimen was poor after 270 minutes drying owing to the woody characteristic of fibre inside cucumber.

Furthermore, the distributed model fits the cucumber data well compared with the Hayden model and the double-shell model, due to the woody characteristic of the dried cucumbers. However, this empirical electrical model (the distributed model) cannot be connected to a specific cellular structure.

Since only few investigations have been performed to monitor the moisture content changes during hot-air drying process using impedance measurement, this study pave the way for understanding electrical impedance properties change during drying process. It is recommended that future investigation can take real-time impedance measurement into account to observe instant electrical properties variations during drying.

Hot-air drying is widely used in processing fruits, vegetables, herbs etc. The classifications of dried herbs with high commercial value (i.e. Ginseng) mainly rely on the manufacturer's experience. Therefore, the electrical impedance method can be used as an alternative objective measurement to assess dried herbs qualities and monitor quality changes during dehydration.

Chapter 6 Conclusions and Future Research

6.1 Conclusions

This thesis outlines a study on electrical impedance spectroscopy on specific fruit and vegetables for quality assessment, i.e. apples, bananas and cucumbers. The taste quality of apples, ripening of bananas, and dehydration of cucumbers were explored.

The main findings are summarised below:

- The relationship between impedance and chemical compositions was explored for apples in Chapter 3. The plots of resistance against reactance of all the fruit chosen in this study were verified by the relevant literatures. The four apple varieties were separated into three groups by the ratio of ºBrix to TA, and pH value, namely low-acid variety (Fuji, Red Delicious), medium-acid variety (Pink Lady), and high-acid variety (Granny Smith).

- The predictors chosen for the four apple varieties were based on the results from the Best Subsets Regression. It was found that each variety displays different characteristics at various frequencies. From the results of the Multiple Regression tests, it was found that the Impedance Square Root (ISR) had linear relationship with the total soluble solids content for the low-acid variety, and a linear relationship with TA for the high-acid variety. In contrast, ISR has a linear relationship with both the total soluble solids content and TA for medium-acid variety. The frequencies used to represent these relationships were different. It is deemed that TA plays an important role in these relationships. The threshold value for TA to be involved into the relationships is 0.47%.

- Chapter 4 outlines a series of experiments to investigate the application of EIS in banana ripening. Fruit peel colour was used to determine the ripening stages. The impedance results were further applied to two other plant cell electrical models, the Hayden model and the double-shell model. It was found the double-shell model gives better description of the electrical properties of bananas. The accuracy of each model was determined by comparing the weighted of sum of squares for the two electrical models. The determination of the electrical properties of the cellular elements was achieved by using the Complex Nonlinear Least Squares fitting approach based on the double-shell model.

- Electrical impedance had a linear relationship with banana peel colour grade for the Cavendish banana and a fourth polynomial relationship for the Lady Finger banana. Impedance increased with the colour grade during ripening, particularly from colour grade 3.5 to 7. However, the impedance varied after colour grade 7 for the two varieties. Impedance of the Cavendish banana decreased, whilst the impedance of the Lady Finger rose. Therefore, the banana ripening process can be divided into three stages according to the observed trend: physiological self-development, the eating-ripe stage and the overripe stage respectively.

- Additionally, based on the double-shell electrical model, it has been found that the resistances of the cell wall and vacuole have positive linear correlations with banana peel colour changes in the ripening process. But the resistance of cytoplasm, the capacitors of plasma membrane and tonoplast did not show any regular variations in accordance with peel colour grade. Moreover, with electrical modelling, it has been found that the accuracy of any model depends on the number of circuit components and the starting value of each component. The electrical model can be used to therefore help understand the changes of the plant electrical properties.

- Chapter 5 outlines the application of EIS in the food dehydration progress monitoring. Changes in the moisture content take place as drying progresses. Dehydration was conducted on cucumber slices without peel for total 270 minutes. The magnitude of impedance is a good indicator of the cucumber drying process. The impedance decreased when moisture content was reduced from 95% to 68.05%. However, it increased sharply when the moisture dropped to 25.83% (CV= 48.82%). The large dispersion of data at the 270 minutes drying was caused by two typically low dried samples. The diameter of the

impedance arc also decreased with the loss of moisture content. It disappeared when moisture dropped to 25.83%.

- It is suggested that the decrease in impedance magnitude from 0 minute drying to 210 minutes drying is caused by the increase in electrolyte concentration. Further moisture loss limited the activity of free ions and reduced the current paths inside cucumber. As a result, the overall impedance was very high. A distributed model fits the cucumber data very well compared with the Hayden model and the double-shell model.

6.2 Future Research

Electrical impedance spectroscopy provides a helpful and effective method to determine fruit and vegetables quality. It can be performed in both invasive and non-invasive channels. It has shown the merits in exploring the associations with food taste, colour, and moisture content. However, there are still some research questions that need to be further investigated.

Experiments to detect the relationships between electrical impedance characteristics and the biochemical properties of food were conducted on a small number of groups. It is suggested that future research should involve an increase in the number of groups and samples. A database could then be established based on this information. It could be also used for different fruits, such as grapes, as the wine industry has strict requirements for wine. This method could be applied to classify fruit ripening stages based on sugar level and/or acid content.

This study also provides a preliminary insight into vegetable thermal dehydration. It is proposed that there may be ion leakage during the drying progress. Therefore, ion leakage measurement is suggested for future investigation. Furthermore, EIS in cellular structure analysis may contribute to the modelling of dehydration.

Additionally, the quality of fruit and vegetables during ripening and storage will be affected by temperature and humidity. All the experiments in this investigation were performed at room temperature. It is suggested that further studies may include observation of fruits and vegetables quality with different temperature and humidity variations. It may help to examine

experimental error caused by these factors, and thus expand the applications of impedance measurement in food quality assessment.

Reference

1. Ackmann, J.J., Seitz, M.A. 1984. Methods of Complex Impedance Measurements in Biological Tissues. CRC Crit. Rev. Biomed. Eng. 11, 281-311.

2. Aked, J. 2002. Maintaining the Post-harvest Quality of Fruits and Vegetables. In: Jongen, W., (Ed.), Fruit and Vegetable Processing- Improving Quality. William Andrew Publishing. pp. 119-149.

3. Alexander, C.K., Sadiku, M.N.O. 2004. Fundamentals of Electric Circuits. 2nd ed. McGraw-Hill, Boston, New York, San Francisco.

4. Alters, S., Alters, B. 2006. Biology: Understanding Life John Wiler & Sons, INC., Hoboken.

5. Bao, J.Z., Davis, C.C., Schmukler, R.E. 1992. Frequency Domain Impedance Measurements of Erythrocytes. Biophys. J. 61, 1427-1434.

6. Barbosa-Canovas, V.G., Vega-Mercado, H. 1996. Dehydration of Foods. 1st ed. International Thomson Publishing, New York.

7. Barnell, H.R. 1940. Studies in Tropical Fruits. VIII. Carbohydrate Metabolism of the Banana Fruit during Development. Ann. Botany 4, 39-71.

8. Barringer, S.A. 2004. Vegetables: Tomato Processing. In: Smith, J.S., Hui, Y.H., (Eds.), Food Processing:Principles and Applications. Blackwell Publishing Professional, Iowa. pp. 473-490.

9. Bauchot, A.D., Harker, F.R., Arnold, W.M. 2000. The Use of Electrical Impedance Spectroscopy to Assess the Physiological Condition of Kiwifruit. Postharvest Biology and Technology 18, 9-18.

10. Berdanier, C.D. 1994. Advanced Nutrition: Micronutrients CRC Press LLC, USA.

11. Berdanier, C.D. 2000. Advanced Nutrition: Macronutrients. 2nd ed. CRC Press LLC, USA.

12. Bethea, R.M., Duran, B.S., Boullion, T.L. 1995. Statistical Methods for Engineers and Scientists. 3rd ed. Marcel Dekker, Inc., New York, Basel, Hong Kong.

13. Bower, J.H., Biasi, W.V., Mitcham, E.J. 2003. Effect of Ethylene in the Storage Environment on Quality of 'Bartlett Pears'. Postharvest Biology and Technology 28, 371-379.

14. Cabre, E., De Leon, R., Planas, R., Bertran, X., Domenech, E., Gassull, A.M. 1995. Reliability of Bioelectric Impedance Analysis as a Method of Nutritional Monitoring in Cirrhosis with Ascites. Gastroenterol Hepatol 18, 359-365.

15. Cherepenin, V.A., Karpov, A.Y., Korjenevsky, A.V., Kornienko, V.N., Kultiasov, Y.S., Ochapkin, M.B., Trochanova, O.V., Meister, J.D. 2002. Three-dimensional EIT Imaging of Breast Tissues Systems Design and Clinical Testing. IEEE Transactions on Medical Imaging 21, 662-667.

16. Clarkson, D.T. 1974. Ion Transport and Cell Structure in Plants McGraw-HILL Book Company (UK) Limited, London.

17. Cole, K.S. 1940. Permeability and Imperneability of Cell Membranes for Ions. Cold Spring Harbor Symp. Quant. Biol. 8, 110-122.

18. Cole, K.S., Curtis, H.J. 1950. Bioelectricity: Electric Physiology. In: Glasser, O., (Ed.), Medical Physics, Vol. 2. the Year Book Publisher INC., Chicago. pp. 82-90.

19. Cornish, B.H., Thomas, B.J., Ward, L.C. 1993. Improved Prediction of Extracellular and Total Body Water Using Impedance Loci Generated by Multiple Frequency Bioelectrical Impedance Analysis. Phys. Med. Biol. 38, 337-346.

20. Cornish, B.H., Jacobs, A., Thomas, B.J., Ward, L.C. 1999. Optimizing Electrode Sites for Segmental Bioimpedance Measurements. Physiol. Meas. 20, 241-250.

21. Cox, M.A., Zhang, M.I.N., Willison, J.H.M. 1993. Apple Bruise Assessment Through Electrical Impedance Measurements. Hournal of Horticultural Science 68, 393-398.

22. De Lorenzo, A., Andreoli, A. 2003. Segmental Bioelectrical Impedance Analysis. Curr Opin Clin Nutr Metab Care 6, 551-555.

23. DeBaerdemaeker, J., Sansen, W., Jancsok, P., Schotte, S., Varlan, A.R. 1997. Electrical and Mechanical Impedance in Fruit Quality Assessment, Sensores for Nondestructive Testing Measuring the Quality of Fresh Fruit and Vegetables. Northeast Regional Agricultural Engineering Service, Cooperative Extension, Orlando FLA. pp. 13-26.

24. DeLong, D. 1979. How to Dry Foods Fisher Publishing, Inc., Tucson, U.S.A.

25. Deurenberg, P., Andreoli, A., De Lorenzo, A. 1996. Multi-frequency Bioelectrical Impedance:a Comparison between the Cole-Cole Modeling and Hanai Equations with the Classical Impedance Index Approach. Ann. Hum. Biol. 6, 31-40.

26. Driscoll, R. 2004. Food Dehydration. In: Smith, J.S., Hui, Y.H., (Eds.), Food Precessing:Principles and Applications. Blackwell Publishing Professional, Iowa. pp. 31-44.

27. Fellers, P.J. 1991. The Relationship Between the Ratio of Degrees Brix to Percent Acid and Sensory Flavor in Grapefruit Juice. Food Technology 45, 68-75.

28. Ferris, C.D. 1974. Introduction to Bioelectrodes Plenum Press, New York.

29. Freywald, K.H., Pliquett, F., Schoberlein, L., Pliquett, U. 1995. Passive Electrical Properties of Meat as a Characteristic of its Quality, the IX. International Conference on Electrical Bio-impedance, Heidelberg, Germany. pp. 366-369.

30. Fukushima, T., Yamazaki, M. 1978. Chilling-Injury in Cucumbers. V. Polysaccharide Changes in Cell Walls. Scientia Horticulturae 8, 219-227.

31. Furmanski, R.J., Buescher, R.W. 1979. Influence of Chilling on Electrolyte Leakage and Internal Conducitivity of Peach Fruits. HortScience 14, 167-168.

32. Gabrielli, C. 1993. Use and Applications of Electrochemical Impedance Techniques. Schlumberger Technical Report, England.

33. Garner, D., Crisosto, C.H., Wiley, P., Crisosto, G.M. 2005. Measurement of pH and Titratable Acidity [Online]. Available by Kearney Agricultural Center http://www.uckac.edu/postharv/PDF%20files/Guidelines/quality.pdf (verified November, 27, 2006).

34. Glerum, C. 1973. Annual Trends in Frost Hardiness and Electrical Impedance for Seven Coniferous Species. Can. J. Plant Sci. 53, 881-889.

35. Goovaerts, H.G., Faes, T.J.C., de Valk-de Roo, G.W., ten Bolscher, M., Netelenbosch, J.C., van der Vijgh, W.J.F., Heethaar, R.M. 1998. Extra-cellular Volume Estimation by Electrical Impedance-Phase Measurement or Curve Fitting: A Comparative Study. Physiol. Meas. 19, 517-526.

36. Greco, T.G., Rickard, L.H., Weiss, G.S. 2002. Experiments in General Chemistry:Principles and Modern Applications. Eighth ed. Prentice-Hall Inc., Millersville.

37. Grimnes, S., Martinsen, Q.G. 2000. Bioimpedance and Bioelectricity Basics Academic Press, London.

38. Gunasekaran, S. 2001. Nondestructive Food Evaluation: Techniques to Analyze Properties and Quality MerceL Dekker, Inc., New York.

39. Hall, J.L., Flowers, T.J., Robert, R.M. 1974. Plant Cell Structure and Metabolism. 1st ed. Longman Group Limited, London.

40. Harker, F.R., Maindonald, J.H. 1994a. Ripening of Nectarine Fruit. Plant Physiol. 106, 165-171.

41. Harker, F.R., Dunlop, J. 1994b. Electrical Impedance Studies of Nectraines During Coolstage and Fruit Ripening. Postharvest Biology and Technology 4, 125-134.

42. Harker, F.R., Forbes, S.K. 1997. Ripening and Development of Chilling Injury in Persimmon Fruit: an Electrical Impedance Study. New Zealand Journal of Crop and Horticultual Science 25, 149-157.

43. Harker, F.R., Marsh, K.B., Young, H., Murray, S.H., Gunson, F.A., Walker, S.B. 2002a. Sensory Interpretation of Instrumental Measurement 2: Sweet and Acid Taste of Apple Fruit. Postharvest Biology and Technology 24, 241-250.

44. Harker, F.R., Maindonald, J., Murray, S.H., Gunson, F.A., Hallett, I.C., Walker, S.B. 2002b. Sensory Interpretation of Instrumental Measurements 1: Texture of Apple Fruit. Postharvest Biology and Technology 24, 225-239.

45. Hayden, R.I., Moyse, C.A., Calder, F.W., Carwford, D.P., Fensom, D.S. 1969. Electrical Impedance Studies on Potato and Alfalfa Tissue. Journal of Experimental Botany 20, 177-200.

46. Hills, A.P., Byrne, N.M. 1998. Bioelectrical Impedance and Body Composition Assessment. Mal. J. Nutr. 4, 107-112.

47. Hinton, A.J., Sayers, B. 1998. Advanced Instrumentation for Bioimpedance Measurements. Solartron Analytical, UK.

48. Hoehn, E., Gasser, F., Guggenbuhl, B., Kunsch, U. 2003. Efficacy of Instrumental Measurements for Determination of Minimum Requirements of Firmness, Soluble Solids, and Acidity of Several Apple Varieties in Comparison to Consumer Expectations. Postharvest Biology and Technology 27, 27-37.

49. Hua, P., Woo, E.J., Webster, J.G., Tompkins, W.J. 1993. Using Compound Electrodes in Electrical Impedance Tomography. IEEE Transactions on Medical Imaging 40, 29-34.

50. Hung, Y.-C., Prussia, S.E., Ezeike, G.O.I. 1999. Nondestructive Maturity Sensing using a Laser Airpuff Detector. Postharvest Biology and Technology 16, 15-25.

51. Jackson, M. 2001. Growing to Retailing, a Global Perspective – Australia's Position. Australian Nuffield Farming Scholars Association, NSW.

52. Jackson, P.J., Harker, F.R. 2000. Apple Bruise Detection by Electrical Impedance Measurement. HortScience 35, 104-107.

53. Jayaraman, K.S., Das Gupta, D.K. 1992. Dehydration of Fruits and Vegetables-Recent Developments in Principles and Techniques. Drying Technology 10, 1-50.

54. John, P., Marchal, J. 1995. Bananas and Plantains Publ. Chapman and Hall, London.

55. Johnson, I.T. 2004. New Approaches to the Role of Diet in the Prevention of Cancers of the Alimentary Tract. Mutation Research 551, 9-28.

56. Jorcin, J.B., Orazem, M.E., Pebere, N., Tribollet, B. 2006. CPE Analysis by Local Electrochemical Impedance Spectroscopy. Electrochimica Acta 51, 1473-1479.

57. Kende, H., Zeevaart, J.A.D. 1997. The Five "Classical" Plant Hormones. American Society of Plant Physiologists 9, 1197-1210.

58. King, G.L., Henderson, K.J., Lill, R.E. 1989. Ultrastructural Changes in Nectarine Cell Wall Accompanying Ripening and Storage in a Chilling-resistant and Chilling-sensitive Cultivar. New Zealand Journal of Crop and Horticultual Science 17, 337-344.

59. Kotsiras, A., Olympios, C.M., Drosopoulos, J., Passam, H.C. 2002. Effects of Nitrigen Form and Concentration on the Distribution of Ions Within Cucumber Fruits. Scientia Horticulturae 95, 175-183.

60. Kyle, U.G., Bosaeus, I., De Lorenzo, A.D., Deurenberg, P., Elia, M., Gomez, J.M., Heitmann, B.L., Kent-Smith, L., Melchior, J., Pirlich, M., Scharfetter, H., Schols, A.M.W.J., Pochard, C. 2004a. Bioelectrical Impedance Anlysis-part I: Review of Principles and Methods. Clinical Nutrition 23, 1226-1243.

61. Kyle, U.G., Bosaeus, I., De Lorenzo, A.D., Deurenberg, P., Elia, M., Gomez, J.M., Heitmann, B.L., Kent-Smith, L., Melchior, J., Pirlich, M., Scharfetter, H., Schols, A.M.W.J., Pochard, C. 2004b. Bioelectrical Impedance Analysis-part ii:Utilization in Clinical Practice. Clinical Nutrition 23, 1430-1453.

62. Labavitch, J.M., Greve, L.C., Mitcham, E. 1998. Fruit Bruising: It's More than Skin Deep, Perishables Handling Quarterly Issue. pp. 7-9.

63. Lammertyn, J., Verlinden, B.E., Nicolai, B.M. 2002. Applying Advanced Instrumental Method: Mealiness in Fruit. In: Jongen, W., (Ed.), Fruit and Vegetable Processing - Improving Quality. William Andrew Publishing. pp. 170-187.

64. Lasia, A. 1999. Electrochemical Impedance Spectroscopy and its Applications in Modern Aspects of Electrochemistry Kluwer Academic/Plenum Publishers, New York.

65. Lehnert, E.M., Clarke, D.D., Gibbons, J.G., Ward, L.C., Golding, S.M., Shepherd, R.W., Cornish, B.H., Crawford, D.H.G. 2001. Estimation of Body Water Compartments in Cirrhosis by Multiple-Frequency Bioelectrical Impedance Analysis. Nutrition 17, 31-34.

66. Li, M., Slaughter, D.C., Thompson, J.F. 1997. Optical Chlorophyll Sensing System for Banana Ripening. Postharvest Biology and Technology 12, 273-283.

67. Lin, Y.C. 1980. Study of the Compositional Difference of Apples, Pears, Liu-Cheng and Banana. Chinese Nutrition Society 5, 67-74.

68. Lurie, S., Crisosto, C.H. 2005. Chilling Injury in Peach and Nectarine. Postharvest Biology and Technology 37, 195-208.

69. Macdonald, J.R., (Ed.) 1987. Impedance Spectroscopy-Emphasizing Solid Materials and Systems. Wiley-Interscience, New York.

70. Macdonald, J.R. 1992. Impedance Spectroscopy. Annals of Biomedical Engineering 20, 289-305.

71. Macdonald, J.R., Garber, J.A. 1977. Analysis of Impedance and Admittance Data for Solids and Liquds. Journal of the Electrochemical Society 124, 1022-1030.

72. Macdonald, J.R., Potter, L.D. 1987. A Flexible Procedure for Analyzing Impedance Spectroscopy Results:Description and Illustrations. Solid State Ionics 23, 61-79.

73. Madamba, L.S.P., Base, A.U., Jr, D.B.M. 1977. Effect of Maturity on Some Biochemical Changes during Ripening of Banana. Fd. Chem. 2, 177-183.

74. Malcolm, C.B. 1982. Food Texture and Viscosity: Concept and Measurement Academic Press, INC., San Siego.

75. Marchand, L.L., Murphy, S.P., Hankin, J.H., Wilkens, L.R., Kolonel, L.N. 2000. Intake of Flavonoids and Lung Cancer. Journal of the National Cancer Institute 92, 154-160.

76. Marshall, D.L., Wiese-Lehigh, P.L. 1997. Comparison of Impedance, Microbial, Sensory, and pH Methods to Determine Shrimp Quality. J. Aquatic Food Product Technology 6, 17-31.

77. Matthie, J., Zarowitz, B., De Lorenzo, A., Andreoli, A., Katzarski, K., Pan, G., Withers, P. 1998. Analytic Assessment of the Various Bioimpedance Methods Used to Estimate Body Water. The American Physiological Society, 1801-1816.

78. Meszaros, P., Vozary, E., D.B., F. 2004. Electrical Impedance of Apple Slices During Drying. In: Nowakowski, A., Wtorek, J., Bujnowski, A., Janczulewicz, A., (Eds.), International Conference on Electrical Bioimpedance and Electrical Impedance Tomography, Vol. 1. Gdansk University of Technology Publishing Office, Poland. pp. 61-64.

79. Mortan, J. 1987. Banana, Fruits of Warm Climates. Creative Resource Systems, Inc., Miami, FL.

80. Mushnick, R., Fein, P.A., Mittman, N., Goel, N., Chattopadhyay, J., Avram, M.M. 2003. Relationship of Bioelectrical Impedance Parameters to Nutrition and Survival in Peritoneal Dialysis Patients. Kidney International 64, 53-56.

81. Niu, J., Lee, J.Y. 2000. A New Approach for the Determination of Fish Freshness by Electrochemical Impedance Spectroscopy. Journal of Food Science 65, 780-785.

82. Omoaka, P., De Proft, M., Sansen, W. 1997. The Use of Electrical Impedance Measurements to Assess the Ripening Stage of Bananas, Crop Protection & Food Quality: Meeting Customer Needs, Canterbury. pp. 412-419.

83. Otto, G. 1950. Bioelectricity: Electric Physiology. In: Cole, K.S., Curtis, H.J., (Eds.), Medical Physics Year Book, Vol. 2. The Year Book Publishers, Chicago. pp. 82-90.

84. Palko, T. 2004. Impedance-Cardiography as a Method of Cardiac Electrotherapy Monitoring. In: Nowakowski, A., Wtorek, J., Bujnowski, A., Janczulewicz, A., (Eds.), International Conference on Electrical Bioimpedance and Electrical Impedance Tomography, Vol. 1. Gdansk University of Technology Publishing Office, Gdansk, Poland. pp. 189-192.

85. Pathange, L.P., Mallikarjunan, P., Marini, R.P., O'Keefe, S., Vaughan, D. 2006. Non-destructive Evaluation of Apple Maturity using an Electronic Nose System. Journal of Food Engineering 77, 1018-1023.

86. Patterson, R. 1989. Body Fluid Determinations Using Multiple Impedance Measurements. IEEE Engineering in Medicine and Biology Magazine 8, 16-18.

87. Pecoraro, P., Guida, B., Caroli, M., Trio, R., Falconi, C., Principato, S., Pietrobelli, A. 2003. Body Mass Index and Skinfold Thickness Versus Bioimpedance Analysis: Fat Mass Prediction in Children. Acta Diabeetol 40, 278-281.

88. Pencharz, B.P., Azcue, M. 1996. Use of Bioelectrical Impedance Analysis Measurements in the Clinical Management of Malnutrition. American Journal of Clinical Nutrition 64, 485-488.

89. Peneau, S., Hoehn, E., Roth, H.R., Escher, F., Nuessli, J. 2006. Importance and Consumer Perception of Freshness of Apples. Food Quality and Perference 17, 9-19.

90. Pirlich, M., Schutz, T., Ockenga, J., Beiering, H., Gerl, H., Schmidt, B., Ertl, S., Plauth, M., Lochs, H. 2003. Improved Assessment of Body Cell Mass by Segmental Bioimpedance Analysis in Malnourished Subjects and Acromegaly. Clinical Nutrition 22, 167-174.

91. Poll, L., Flink, J.M. 1984. Aroma Analysis of Apple Juice: Influence of Salt Addition on Headspace Volation Composition as Measured by Gas Chromatography and Corresponding Sensory Evaluations. Food Chemistry 13, 193-207.

92. Reddy, L., Odhav, B., Bhoola, K.D. 2003. Natural Products for Cancer Prevention: a Global Perspective. Pharmacology & Therapeutics 99, 1-13.

93. Redgwell, R.J., MacRae, E., Hallett, I., Fischer, M., Perry, J., Harker, R. 1997. In vivo and In vitro Swelling of Cell Walls During Fruit Ripening. Planta 204, 162-173.

94. Repo, T. 1992. Seasonal Changes of Frost Hardiness in *Pices abies* (L.) Karst. and *Pinus sylvestris* (L.) in Finland. Can. J. Forest Res. 22, 1949-1957.

95. Repo, T. 1994. Influence of Different Electrodes and Tissues on the Impedance Spectra of Scots Pine Shoots. Electro- and Magnetobiology 13, 1-14.

96. Repo, T. 2004. The Electrical Impedance of Plant Tissues. In: Nowakowski, A., Wtorek, J., Bujnowski, A., Janczulewicz, A., (Eds.), International Conference on Electrical Bioimpedance and Electrical Impedance Tomography, Vol. 1, Poland. pp. 37-40.

97. Repo, T., Zhang, M.I.N. 1993. Modelling Woody Plant Tissue Using a Distributed Electrical Circuit. Journal of Experimental Botany 44, 977-982.

98. Repo, T., Zhang, G., Ryyppo, A., Rikala, R. 2000. The Electrical Impedance Spectroscopy of Scots Pine (*Pinus Sylvestris L.*) Shoots in Relation to Cold Acclimation. Journal of Experimental Botany 51, 2095-2107.

99. Robert, L.S., Bernhard, B. 2000. Food Supply Chains: from Productivity toward Quality, Fruit & Vegetable Quality: An Integrated View. Technomic Publishing Company, Inc., U.S.A. pp. 3-20.

100. Rodriguez-Saona, L.E., Fry, F.S., McLaughlin, M.A., Calvey, E.M. 2001. Rapid Analysis of Sugars in Fruit Juices by FT-NIR Spectroscopy. Carbohydrate Research 336, 63-74.

101. Rogers, E.J., Milhalik, S., Ortizz, D., Shea, T.B. 2003. Apple Juice Prevents Oxidative Stress and Impaired Cognitive Performance Caused by Genetic and Dietary Deficiencies in Mice. The Journal of Nutrition, Health & Aging 7, 92-97.

102. Ruan, R.R., Chen, P.L. 2001. Nuclear Magnetic Resonance Techniques and Their Application in Food Quality Analysis. In: Gunasekaran, S., (Ed.), Nondestructive Food Evaluation-Techniques to Analyze Properties and Quality. Marcel Dekker, INC., Basel. pp. 165-216.

103. Saltveit, M.E. 2002. The Rate of Ion Leakage from Chilling-Sensitive Tissue Does Not Immediately Increase upon Exposure to Chilling Temperatures. Post. Biol. Technol. 26, 295-304.

104. Schloerb, R.P., Forster, J., Delcore, R., Kindscher, D.J. 1996. Bioelectrical Impedance in the Clinical Evaluation of Liver Disease. *Am J Clin Nutr* 64, 510-514.

105. Schoeller, D.A. 2000. Bioelectrical Impedance Analysis: What Does it Measure? Annals of the New York Academy of Sciences 904, 159-162.

106. Schoeller, D.A., Kushner, R.F. 1989. Determination of Body Fluids by the Impedance Technique. IEEE Engineering in Medicine and Biology Magazine, 19-21.

107. Schwan, H.P. 1963. Determination of Biological Impedances. In: Nastuk, W.L., (Ed.), Physical Techniques in Biological Research, Vol. 323. Academic Press, New York.

108. Shedlovsky, T. 1930. J. Am. Chem. Soc. 52, 1806.

109. Steinmetz, K.A., Potter, J.D. 1996. Vegetabls, Fruit, and Cancer Prevention: A Review. Journal of the American Dietetic Association 96, 1027-1039.

110. Szczesniak, A.S. 1963. Classification of textural characteristics. Journal of Food Science 28, 385-389.

111. Thompson, C.M., Kong, C.H., Lewist, C.A., Hill, P.D., Thompson, F.D. 1993. Can Bio-electrical Impedance Be Used to Measure Total Body Water in Dialysis Patients? Physiol. Meas. 14, 455-461.

112. Torrey, M. 1974. Dehydration of Fruits and Vegetables Noyes Data Corporation, London.

113. Toyoda, K., Tsenkova, R.N., Nakamura, M. 2001. Characterization of Osmotic Dehydration and Swelling of Apple Tissues by Bioelectrical Impedance Spectroscopy. Drying Technology 19, 1683-1695.

114. Toyoda, K., Kojima, H., Miyomoto, S., Takeuchi, R. 1997. Measurement and Analysis of Moisture Changes in Agricultural Products Using FFT Noise Impedance Spectroscopy. Drying Technology 15, 2025-2035.

115. Varlan, A.R., Sansen, W. 1995. Multifrequency Impedance Measurement for Fruit Quality Evaluation. Innovation and Technology in Biology and Medicine 16, 727-735.

116. Varlan, A.R., Sansen, W. 1996. Nondestructive Electrical Impedance Analysis in Fruit: Normal Ripening and Injuries Characterization. Electro- and Magnetobiology 15, 213-227.

117. Vozary, E., Laszlo, P., Zsivanovits, G. 1999. Impedance Parameter Characterizing Apple Bruise. Annals New York Academy of Sciences 873, 421-429.

118. Wang, Y.M. 1994. The Chemistry and Biochemistry of Melon Fruit Development and Quality, University of Western Sydney, Sydney.

119. Whiting, G.C. 1970. Sugars. 2ed ed. Academic Press INC. (London) LTD, Norwich.

120. WHO. 2002. The World Health Report 2002. Reducing Risks, Promoting Healthy Life. World Health Organization, Geneva.

121. WHO/FAO. 2003. Diet, Nutrition and the Prevention of Chronic Diseases. World Health Organisation, Food and Agriculture Organization of the United Nations, Geneva.

122. Woodrow, G., Oldroyd, B., Turney, J.H., Smith, M.A. 1996. Segmental Bioelectrical Impedance in Patients with Chronic Renal Failure. Clinical Nutrition 15, 275-279.

123. Wu, X.L., Beecher, G.R., Holden, J.M., Haytowitz, D.B., Gebhardt, S.E., Prior, R.L. 2004. Lipophilic and Hydrophilic Antioxidant Capacities of Common Foods in the United States. J. Agric. Food Chem. 52, 4026-4037.

124. Zhang, M.I.N., Willison, J.H.M. 1991. Electrical Impedance Analysis in Plant Tissues: A Double Shell Model. Journal of Experimental Botany 42, 1465-1475.

125. Zhang, M.I.N., Willison, J.H.M. 1993. Electrical Impedance Analysis in Plant Tissues: Impedance Measurement in Leaves. Journal of Experimental Botany 44, 1369-1375.

126. Zhang, M.I.N., Stout, D.G., Willison, J.H.M. 1990. Electrical Impedance Analysis in Plant Tissue: Symplastic Resistance and Membrane Capacitance In the Hayden Model. J. Exp. Bot. 41, 371-380.

127. Zillikens, C.M., Van Den Berg, W.J., Wilson, H.J., Rietveld, T., Swart, R.G. 1992. The Validity of Bioelectrical Impedance Analysis in Estimating Total Body Water in Patients with Cirrhosis. *J Hepatol* 16, 59-65.

128. Zywica, R., Pierzynowska-Korniak, G., Wojcik, J. 2005. Application of Food Products Electrical Model Parameters for Evaluation of Apple Puree Dilution. Journal of Food Engineering 67, 413-418.

Appendix Raw Data and MATLAB Scripts

The raw data of the investigations of apples, bananas and cucumber are attached in the enclosed CD.